



**PROCEEDINGS OF THE 24TH
INTERNATIONAL APPLIED GEOCHEMISTRY SYMPOSIUM
FREDERICTON, NEW BRUNSWICK, CANADA**



JUNE 1ST-4TH, 2009

EDITED BY

DAVID R. LENTZ, KATHLEEN G. THORNE, & KRISTY-LEE BEAL



VOLUME II



All rights reserved.

This publication may not be reproduced in whole or in part, stored in a retrieval system or transmitted in any form or by any means without permission from the publisher.

ISBN 978-1-55131-137-1 (Volume 2)

©2009 AAG

**PROCEEDINGS OF THE 24TH
INTERNATIONAL APPLIED GEOCHEMISTRY SYMPOSIUM
FREDERICTON, NEW BRUNSWICK
CANADA
JUNE 1ST-4TH, 2009**

EDITED BY

**DAVID R. LENTZ
KATHLEEN G. THORNE
KRISTY-LEE BEAL**

VOLUME II

Land use/land cover influences on the estimated time to recovery of inland lakes from mercury enrichment	815
<i>Matthew J. Parsons¹ & David T. Long¹</i>	815
Potential for contamination of deep aquifers in Bangladesh by pumping-induced migration of higher arsenic waters	819
<i>Kenneth G. Stollenwerk</i>	819
CURRENT CAPABILITIES AND FUTURE PROSPECTS OF REAL-TIME, IN-FIELD GEOCHEMICAL ANALYSIS	823
LIBS-based geochemical fingerprinting for the rapid analysis and discrimination of minerals – the example of garnet	825
<i>Daniel C. Alvey¹, Jeremiah J. Remus², Russell S. Harmon³, Jennifer L. Gottfried⁴, & Kenneth Morton²</i>	825
The U-tube sampling methodology and real-time analysis of geofluids	829
<i>Bary Freifeld¹, Ernie Perkins², James Underschultz³, & Chris Boreham⁴</i>	829
LIBS as an archaeological tool – example from Coso Volcanic Field, CA	833
<i>Jennifer L. Gottfried¹, Russell S. Harmon², Anne Draucker³, Dirk Baron³, & Robert M. Yohe³</i> ..	833
The application of visible/infrared spectrometry (VIRS) in economic geology research: Potential, pitfalls and practical procedures	837
<i>Andrew Kerr, Heather Rafuse, Greg Sparkes, John Hinchey, & Hamish Sandeman</i>	837
Analysis of gem treatments: comparison of nano-second and pico-second laser-induced breakdown spectroscopy	841
<i>Nancy J. McMillan¹, Patrick Montoya, Carlos Montoya, & Lawrence Bothern</i>	841
Laser ablation chemical analysis LIBS and LA-ICP-MS for geochemical and mining applications	843
<i>R.E. Russo^{1,2,3}, J. Yoo², J. Plumer¹, J. Gonzalez², & X. Mao³</i>	843
In-situ Mössbauer spectroscopy on Earth, Mars, and beyond	847
<i>Christian Schröder¹, Göstar Klingelhöfer¹, Richard V. Morris², Bodo Bernhardt³, Mathias Blumers¹, Iris Fleischer¹, Daniel S. Rodionov^{1,4}, & Jordi Gironés López¹</i>	847
Archaeometry in the House of the Vestals: analyzing construction mortar with portable infrared spectroscopy	851
<i>Jennifer Wehby¹ & Samuel E. Swanson¹</i>	851
Fluorescence analysis of dissolved organic matter (DOM) in landfill leachates	853
<i>Caixiang Zhang¹, Yanxin Wang¹, & Zhaonian Zhang²</i>	853
Innovation for the CHIM method	857
<i>Liu Zhanyuan, Sun Binbin, Wei Hualing, Zeng Daoming, & Zhou Guohua</i>	857
GEOCHEMICAL ASPECTS OF MINE WASTES	861
Geochemistry of the Lake George Antimony mine tailings, Lake George, New Brunswick, Canada: Understanding antimony mobility in a tailings environment	863
<i>Pride T. Abongwa¹ & Tom A. Al¹</i>	863
Contribution of <i>Cistus ladanifer</i> L. to natural attenuation of Cu and Zn in some mine areas of the Iberian Pyrite Belt	867
<i>Maria J. Batista¹ & Maria M. Abreu²</i>	867
The Diavik Waste Rock Project: Design, construction and preliminary results	871
<i>D. W. Blowes¹, L. Smith², D. Segó³, L.D. Smith^{1,4}, M. Neuner², M. Gup-ton², B.L. Bailey¹, N. Pham³, R.T. Amos¹, & W.D. Gould¹</i>	871

Prediction of acid mine generating potential: Validation using mineralogy	875
<i>Hassan Bouzahzah^{1,2}, Mostafa Benzaazoua¹, Benoît Plante¹, Bruno Bussière¹, & Eric Pirard²</i>	
Preliminary investigation into tailings-ground water interactions at the former Steep Rock iron mines, Ontario, Canada	879
<i>Andrew G. Conly¹, Peter F. Lee², & Chris Perusse¹</i>	
Long-term fate of ferrihydrite in uranium mine tailings	883
<i>Soumya Das¹ & M. Jim Hendry¹</i>	
Methods for obtaining a national-scale overview of groundwater quality in New Zealand	887
<i>Christopher J. Daughney, Uwe Morgenstern, Rob van der Raaij, Robert Reeves, Matthias Raiber, & Mark Randall</i>	
Mineralogical characterization of arsenic, selenium, and molybdenum in uranium mine tailings	891
<i>Joseph Essilfie – Dughan¹, M. Jim Hendry¹, Ingrid Pickering¹, Graham George¹, Jeff Warner², & Tom Kotzer³</i>	
Spatial and temporal evolution of Cu-Zn mine tailings while dewatering	895
<i>D. Jared Etcheverry¹, Barbara L. Sherriff¹, Nikolay Sidenko^{1,2}, & Jamie VanGulck³</i>	
Adding value to Kinetic Testing Data II – Interpretation of waste rock humidity cell data from an exploration perspective at the Adanac Molybdenum Corporation, Ruby Creek Molybdenum Project, BC, Canada	899
<i>David R. Gladwell¹ & Catherine T. Ziten¹</i>	
Alteration of sulfides within an open air waste-rock dump: Application of synchrotron μ -XRD, μ -XRF, and μ -XANES analyses	903
<i>Pietro Marescotti¹, Cristina Carbone¹, Gabriella Lucchetti¹, & Emilie Chalmin²</i>	
Arsenic speciation in wastes resulting from pressure oxidation, roasting and smelting	907
<i>Dogan Paktunc</i>	
Importance of sorption in the geochemistry of nickel in waste rock	911
<i>Benoît Plante¹, Mostafa Benzaazoua¹, Bruno Bussière¹, & Donald Laflamme²</i>	
Distribution of elements of concern in uranium mine tailings, Key Lake, Saskatchewan, Canada	915
<i>Sean A. Shaw¹, M. Jim Hendry¹, Joseph Esselie-Dughan¹, Tom Kotzer², & Harm Maathuis²</i> ..	
Source, attenuation and potential mobility of arsenic at New Britannia Mine, Snow Lake, Manitoba	919
<i>Stephanie Simpson¹, Barbara L. Sherriff¹, Nikolay Sidenko^{1,2}, & Jamie Van Gulck³</i>	
Geochemistry and mineralogy of ochre precipitates formed as waste products of passive mine water treatment	923
<i>Teresa M. Valente¹, Marcel D. Antunes, Maria Amália S. Braga, & Jorge M. Pamplona</i>	
Instability of AMD samples and evolution of ochre-precipitates in laboratory conditions	927
<i>Teresa M. Valente¹ Lúcia M. Guise, & Carlos A. Leal Gomes</i>	
Arsenic mineralogy and potential for bioaccessibility in weathered gold mine tailings from Nova Scotia	931
<i>Stephen R. Walker¹, Michael B. Parsons², & Heather E. Jamieson¹</i>	
GEOCHEMICAL SURVEYS IN GOVERNMENT - NEW DEVELOPMENTS AND USES	935
Presentation of regional geochemical data via Internet Earth browsers	937
<i>Stephen W. Adcock¹, Wendy A. Spirito¹, & Eric C. Grunsky¹</i>	
The National Geochemical Survey of Australia: 2009 update on progress	941

TECHNICAL EDITORS
(Listed in alphabetical order)

Mark Arundell
U. Aswathanarayana
Roger Beckie
Chris Benn
Robert Howell
Charles Butt
Bill Coker
Hugh deSouza
Sara Fortner
David Gladwell
Wayne Goodfellow
Eric Grunsky
William Gunter
Gwendy Hall
Jacob Hanley
Russell Harmon
David Heberlein
Brian Hitchon
Andrew Kerr
Dan Kontak
Kurt Kyser

David Lentz
Ray Lett
Matthew Leybourne
Steven McCutcheon
Beth McClenaghan
Nancy McMillan
Paul Morris
Lee Ann Munk
Dogan Paktunc
Roger Paulen
Ernie Perkins
David Quirt
Andy Rencz
David Smith
Cliff Stanley
Gerry Stanley
Nick Susak
Bruce Taylor
Ed Van Hees
James Walker
Lawrence Winter

GEOCHEMICAL ASPECTS OF MINE WASTES

EDITED BY:

DOGAN PAKTUNC
U. ASWATHANARAYANA

Geochemistry of the Lake George Antimony mine tailings, Lake George, New Brunswick, Canada: Understanding antimony mobility in a tailings environment

Pride T. Abongwa¹ & Tom A. Al¹

¹Department of Geology, P.O. Box 4400, University of New Brunswick, NB, E3B 5A3 Canada
(e-mail: z4v08@unb.ca)

ABSTRACT: Sulfide minerals in the Lake George Antimony deposit included stibnite (Sb_2S_3), arsenopyrite (FeAsS), boumonite (PbCuSbS_3), chalcopyrite (CuFeS_2), cubanite (CuFe_2S_3), kermesite ($\text{Sb}_2\text{S}_2\text{O}$), pyrite (FeS_2), pyrrhotite ($\text{Fe}_{(1-x)}\text{S}$), senarmontite (Sb_2O_3), sphalerite ($(\text{Zn,Fe})\text{S}$), stibivanite (Sb_2VO_5) and tetrahedrite ($(\text{Cu,Fe})_{12}\text{Sb}_4\text{S}_{13}$). Native antimony (Sb) was also found. The major gangue minerals are calcite and quartz, with minor amounts of plagioclase and muscovite, and accessory rutile and zircon (Abbot & Watson 1975). The pore-water geochemistry of the Lake George Antimony Mine tailings was characterized by collecting and analyzing samples at discrete depths throughout the vadose zone. As a consequence of sulfide oxidation and associated mineral-water reactions, the pore water in the near surface tailings is characterized by elevated SO_4 , Fe, Mn, Ca, Na, Al, K, and Si concentrations. The pH is near neutral throughout the tailings because of acid-neutralization reactions involving carbonate minerals. Relatively low Sb concentrations were recorded in the near-surface tailings pore-water compared to pore-water at greater depth. The results of SEM/EDS analyses indicate the presence of secondary Sb and Fe oxyhydroxide minerals in the near surface tailings. Precipitation of secondary Sb oxide phases presents limitations on Sb mobility, as does adsorption of Sb on the surfaces of Fe oxyhydroxides.

KEYWORDS: Tailings, antimony, Fe-oxyhydroxides, oxidation, sorption

INTRODUCTION

The Lake George Antimony Mine is located 39 kilometers west-southwest of Fredericton, New Brunswick, Canada. Stibnite (Sb_2S_3) and native antimony (Sb) were the main sources of antimony in the 100 year history of the mine (1880-1996).

Many hydrochemical studies of tailings systems have focused on tailings derived from copper, nickel, lead, zinc, and gold deposits (e.g., Dubrovsky *et al.* 1985, Al *et al.* 1994; Jambor & Blowes 1994; McGregor *et al.* 1998a; Johnson *et al.* 2000). Extensive research has been conducted on these types of tailings, which has led to a solid understanding of the geochemical processes that occur. The oxidation of sulfide minerals in tailings piles will lead to significant changes in pore-water geochemistry over time. The tailings from the Lake George Antimony Mine contain abundant arsenopyrite and stibnite which have reached an advanced state of weathering. The weathering of

stibnite and associated antimony minerals in tailings has not been studied previously.

METHODS

Geochemical data were obtained from vertical cores retrieved using aluminum casing (7.5 cm diameter, 3 m long) that were driven through the unsaturated and saturated zones of the tailings. After collection, the cores were cut into 25 cm lengths and centrifuged to extract pore water. During centrifugation, the pore-water was collected in a N_2 -purged reservoir and then extracted directly into syringes to prevent contact with the atmosphere. Anion analysis was performed using Ion Chromatography and analysis of cations was performed by both Inductively-Coupled Plasma Mass Spectroscopy (ICP-MS) and Inductively-Coupled Plasma Optical-Emission Spectroscopy (ICP-OES).

Aqueous geochemical modeling was performed using the program PHREEQC

Interactive Version 2.15.0 (Parkhurst & Appelo 1999). The Inl.dat database distributed with PHREEQC was used for all calculations. Geochemical modeling was used to speciate the components of the tailings pore-water at discrete depths and to investigate the thermodynamic stability of mineral phases through out the tailings.

Additional cores were collected in 5 cm diameter aluminum casings for mineralogical analysis. The cores were cut into 50 cm lengths and sealed in the field. They were then frozen upon arrival in the laboratory and analyzed on a later date. The cores were dried in a N₂ atmosphere for three weeks. The cores were then impregnated with low-viscosity epoxy for thin section preparation. The primary mineralogy of the tailings was determined using optical microscopy, X-ray Diffraction (XRD) and Scanning Electron Microscopy/Energy Dispersive Spectroscopy (SEM/EDS).

RESULTS & DISCUSSION

In the near-surface tailings, aqueous concentrations of SO₄, Fe, Mn, Ca, Na, Al, K, Si, and As were elevated with respect to the respective concentrations in the deeper tailings (Fig. 1). The E_h is relatively high in the near-surface tailings and the pH is near neutral throughout the tailings (Fig. 1). The elevated SO₄ and metal concentrations in the near surface tailings are a result of silicate and sulfide mineral weathering under oxidizing conditions. Acid generated by sulfide oxidation is buffered by neutralization reactions involving carbonate mineral dissolution. The distribution of Ca and alkalinity concentrations versus depth, as well as total C analyses (Fig. 2) with depth are consistent with carbonate consumption in the near-surface oxidation zone. Saturation indices (Fig. 3) indicate that the tailings pore-water is near equilibrium with respect to gypsum, with gypsum expected to precipitate in response to the release of Ca and SO₄ from carbonate dissolution and sulfide-oxidation reactions respectively.

Although elevated Sb concentrations

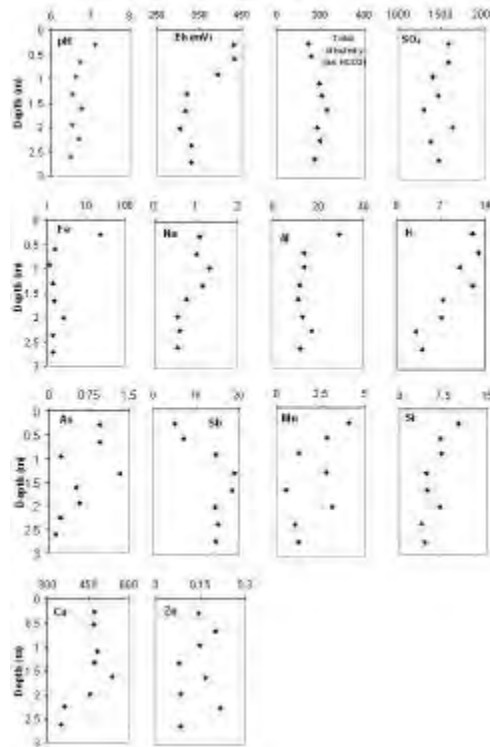
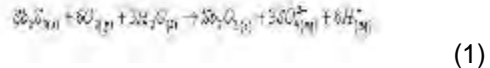


Fig. 1. Aqueous geochemical data from the Lake George Antimony Mine tailings. The x-axis represents concentrations in mg/L unless otherwise stated.

might be expected in the near-surface pore-water due to greater stibnite oxidation in contact with oxygen in the unsaturated zone, Sb concentrations are relatively low in the near surface pore-water and increase with depth (Fig. 1).

Geochemical speciation calculations suggest that Sb occurs predominantly as Sb(III) throughout the tailings pore-waters and that Sb concentrations are limited by the precipitation of common Sb(III) minerals, such as sernamontite (Sb₂O₃, reaction 1).



The pore-water in the near-surface tailings is supersaturated with respect to stibnite oxidation products sernamontite, Sb₂O₅, and Sb(OH)₃ (Fig. 3). Iron concentrations as high as 23.49 mg/L were recorded in the near-surface pore-water with lower concentrations at depth (Fig. 1).

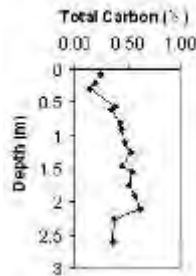


Fig. 2. Total inorganic C vs. depth (expressed as wt.% calcite).

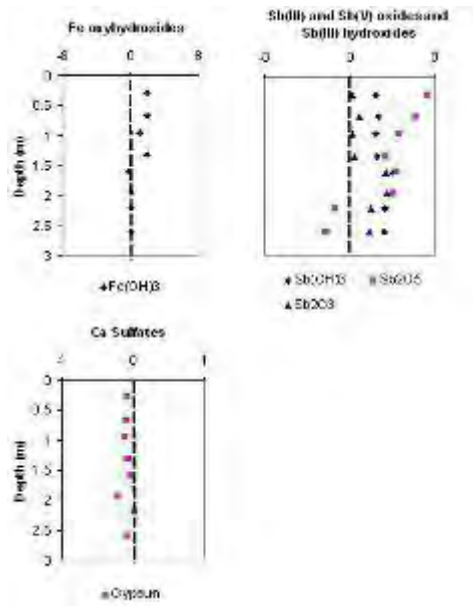


Fig. 3. Pore-water mineral saturation indices calculated with PHREEQC (Parkhurst & Appelo 1999) using the Iln.dat database.

The pore-water is undersaturated with respect to siderite but supersaturated with respect to Fe (III) hydroxides such as goethite and amorphous $\text{Fe}(\text{OH})_3$ (Fig. 3). These results, consistent with SEM/EDS analyses showing Fe oxyhydroxide mineral precipitates in the near-surface tailings (Figs. 4 & 5), suggest that adsorption reactions involving Fe oxyhydroxides may play a role in controlling Sb mobility in the tailings environment. A series of laboratory experiments by Leuz *et al.* (2006), showed that the Fe oxyhydroxide, goethite, (FeOOH) is an important sorbent for Sb(III) and Sb(V) species in the near-neutral pH range.

However, their results indicate that

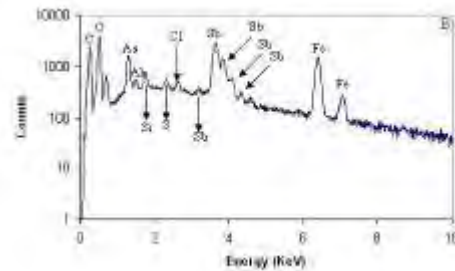
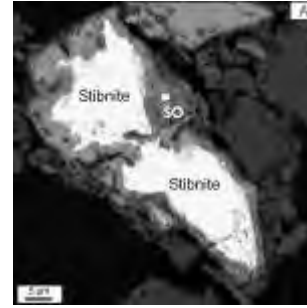


Fig. 4. (A) Backscattered electron image (BSEI) showing oxidation of stibnite. (B) SEM/EDS spectra obtained within a secondary oxide (mixture of Fe and Sb oxide). White square is the location of the EDS analysis shown in (B) and SO means secondary oxide.

elevated aqueous Sb concentrations are expected at pH above 7 or 8 because Sb(III) may be oxidized to Sb(V) by reaction with Fe-oxyhydroxides (Belzile *et al.* 2001), and adsorption of the product Sb(V), decreases above this pH range.

CONCLUSIONS

Trends in pore-water geochemistry in the near surface tailings of the Lake George Antimony Mine reflect the effects of sulfide-mineral oxidation. The SO_4 , and most metal concentrations are relatively high in the surficial (oxidation) zone of the tailings. The presence of carbonates in the tailings neutralizes the acidity produced by sulfide oxidation, resulting in near-neutral pH. The relatively low Sb concentration in the near-surface tailings compared to concentrations at depth are thought to result from the combination of secondary Sb-oxide mineral precipitation and adsorption of Sb on secondary Fe oxyhydroxides. Identification of secondary minerals important for controlling Sb mobility will commence in the future with

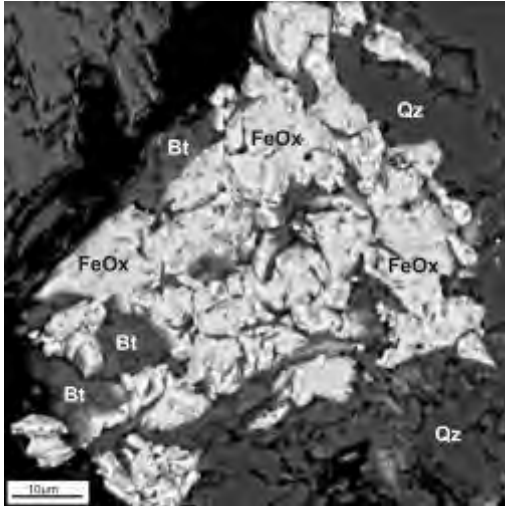


Fig. 5. BSEI showing secondary Fe oxyhydroxide minerals. Qz = Quartz, Bt = Biotite and FeOx = Fe oxyhydroxides

detailed, nano-scale mineralogical studies.

ACKNOWLEDGMENTS

Funding for this research was provided by an NSERC Discovery grant to Dr. T. Al. The first author would also like to thank the Geological Society of America (GSA) and Dr. J.S Little (J.S Little International Fellowship, administered via the University of New Brunswick) through a student research grant that contributed to this research. The authors would also like to thank members of the Geochemistry research group at the University of New Brunswick for assistance with field and laboratory work.

REFERENCES

ABBOT, D. & WATSON, D. 1975. Mineralogy of

- the Lake George Antimony deposit, New Brunswick. *CIM Bulletin*, **68** (July), 111-113.
- AL T.A., BLOWES D.W., JAMBOR J.L., & SCOTT J.D. 1994. The geochemistry of mine-waste pore water affected by the combined disposal of natrojarosite and base-metal sulfide tailings at Kidd Creek, Timmins, Ontario. *Canadian Geotechnical Journal*, **31**, 502-512.
- BELZILE, N., CHEN, Y.W., & WANG, Z.J., 2001. Oxidation of antimony (III) by amorphous iron and manganese oxyhydroxides. *Chemical Geology*, **174**, 379-389.
- DUBROVSKY N.M., CHERRY J.A., REARDON E.J., & VIVYURKA, A.J. 1985. Geochemical evolution of inactive pyritic tailings in the Elliot Lake uranium district. *Canadian Geotechnical Journal*, **22**, 110-128.
- JAMBOR, J.L. & BLOWES, D.W. 1994. Environmental Geochemistry of Sulfide Mine-Wastes. *Mineralogical Association of Canada Short Course* **22**, 438 p.
- LEUZ, A.C., MÖNCH, H., & JOHNSON, C.A. 2006. Sorption of Sb(III) and Sb(V) to goethite: Influence on Sb(III) oxidation and mobilization. *Environmental Science and Technology*, **40**, 7277-7282.
- MCGREGOR, R.G., BLOWES, D.W., JAMBOR J.L., & ROBERTSON W.D. 1998. Mobilization and attenuation of heavy metals within a nickel mine tailings impoundment near Sudbury, Ontario, Canada. *Environmental Geology*, **36**, 305-319.
- PARKHURST, D.L. & APPELO, C.A.J. 1999. User's Guide to PHREEQC (Version 2.15.0)-A Computer Program for Speciation, Batch-Reaction, One-Dimensional Transport and Inverse Geochemical Calculations. *U.S. Geological Survey, Water Resources Investigation Report* **99-4259**.

Contribution of *Cistus ladanifer* L. to natural attenuation of Cu and Zn in some mine areas of the Iberian Pyrite Belt

Maria J. Batista¹ & Maria M. Abreu²

¹INETI, Apartado 7586, 2721-866, Alfragide PORTUGAL (email: joao.batista@ineti.pt)

²Instituto Superior Agronomia-UTL, Tapada da Ajuda, Lisboa PORTUGAL

ABSTRACT: The comparison between four groups of soils and rock rose plants (*Cistus ladanifer* L.) developed on these soils was made using three mine areas of different ages (Neves Corvo, Brancanes, Monte dos Mestres) and a control area (Lombador). Copper and zinc soil-plant relationship was different in Neves Corvo, ongoing exploitation of copper and zinc, when compared with the control area of Lombador reflecting the actual influence of the present exploitation. The rock rose plants seem to have contributed to the natural attenuation of Cu in soils of Brancanes area where mining stopped more than a century ago.

KEYWORDS: *Cistus ladanifer* L., mining areas, control area, natural attenuation, copper mines

INTRODUCTION

The role of green plants in natural attenuation is an important way of phytostabilization of degraded areas, especially in the abandoned mine areas where well adapted and tolerant spontaneous plants grow. These plants contribute to decrease soil erosion, the mobility of contaminants in soil and to reduce or eliminate the risk to both human health and the environment.

The rock rose (*Cistus ladanifer* L.) is a typical Mediterranean plant well adapted to thin soils with low nutritional characteristics and water holding capacity as some of those found in the Iberian Pyrite Belt (IPB) (Carvalho Cardoso, 1965). This metallogenetic province is renowned by the existence of important polymetallic massive sulfide deposits and because was exploited for base metals since pre-Roman times.

The objective of this study was to evaluate the role of chemical elements uptake by rock rose (a well adapted plant to mine environments) in natural attenuation by phytostabilization of soils polluted during different periods of mining activity and abandon.

MATERIALS AND METHODS

The capacity of rock rose to contribute to the natural attenuation of contaminated areas was evaluated by comparison, among different mine areas, the chemical elements in soils and plants. These areas were selected because of the similar geological environment and, the different periods of mining and abandon. The mines are located in the Vulcano Sedimentary formations of Upper Devonian epoch (Carvalho & Ferreira 1993). Three different areas of sampling were chosen. NC area - correspond to the Neves Corvo still active Cu and Zn mine where 19 soils and plants samples were collected. MM area - represent the Monte dos Mestres area which includes the following subareas: Courela das Ferrarias (a mine exploited until 1987), Cerro da Cachaçuda, Herdade do Castelo and Cerro das Guaritas all exploited for Mn (abandoned before 1980) and Cerro do Algaré exploited for copper and pyrite. In MM area were collected 26 samples of soils and plants. The third area, named B – represent the Brancanes mine that was exploited until the end of the XIX century. In this area were collected 11 samples of soils and plants. For comparison, seven samples of soils and plants were collected

Table.1A. Mean and median (mg kg⁻¹) of soil pH and Cu, Zn, Fe, Mn, Ca, P, Mg, Al, K in soil samples (S) and plants (F-Leaves; R-roots) in Lombador (control area) and Monte dos Mestres.

	Lombador (L)		Monte dos Mestres (MM)	
	Mean	Median	Mean	Median
CuS	24	20	74	47
CuF	9	9	34	26
CuR	10	10	12	9
ZnS	49	42	56	49
ZnF	66	63	78	67
ZnR	17	16	23	23
MnS	685	543	1074	776
MnF	835	860	876	727
MnR	304	268	300	289
FeS	27429	23600	28342	29450
FeF	623	593	768	604
FeR	608	600	908	850
CaS	1957	2200	2308	1900
CaF	9600	10100	7692	7150
CaR	6571	5200	6427	6150
PS	437	410	612	590
PF	1530	1460	1455	1505
PR	350	360	386	375
MgS	5429	4500	4046	4500
MgF	2947	2613	2770	2750
MgR	655	699	745	756
AlS	62257	60300	65046	63500
AlF	1286	1200	1462	1350
AlR	1386	1400	1808	1850
KS	13114	11700	16542	15450
KF	5416	6400	5784	6000
KR	1984	2200	2295	2176
pH	6.0	6.2	6.0	6.1

the rock rose plants in Lombador, especially in low pH environment ($r=0.79$). These results showed the importance of Cu and Zn uptake by plants (Wenzel & Jockwer 1999; Kidd *et al.* 2004) as these elements are essential micronutrients. The soil-root relationship, possibly more related with plant uptake, is higher in Cu than in Zn. The relation soil-leaf (possibly more related with

Table 1B. Mean and median (mg kg⁻¹) of soil pH and Cu, Zn, Fe, Mn, Ca, P, Mg, Al, K in soil samples (S) and plants (F-Leaves; R-roots) in Neves Corvo and Brancanes areas.

	Neves Corvo		Brancanes	
	Mean	Median	Mean	Median
CuS	978	226	46	44
CuF	179	95	9	9
CuR	30	14	9	9
ZnS	165	83	52	54
ZnF	101	107	52	54
ZnR	28	23	20	19
MnS	1420	1017	966	1015
MnF	770	643	765	796
MnR	350	286	323	308
FeS	33479	30800	30945	29300
FeF	1538	1000	615	600
FeR	797	800	874	700
CaS	3000	2000	3418	2900
CaF	7377	7100	8107	8030
CaR	6109	5700	7139	6539
PS	700	600	827	800
PF	1406	1380	1548	1620
PR	387	354	374	330
MgS	5232	5400	4427	4900
MgF	2605	2600	2797	3003
MgR	758	789	695	666
AlS	63853	65000	68455	68500
AlF	1316	1226	1750	1550
AlR	1464	1498	1021	958
KS	15732	15000	18045	18100
KF	5311	5300	4816	6100
KR	2282	2200	2205	2186
pH	5.5	5.7	5.8	5.8

translocation mechanisms is higher in Zn (Alvarenga *et al.* 2004).

In contrast, in the Neves Corvo mining area the correlations between each element (Cu, Zn and Fe) in soil-root, soil-leaf and leaf-root samples, and low pH are high. Therefore, mobility of those elements in the soil-plant system seems to be facilitated in this nowadays mining area.

The Dunett test considers a control area (Lombador) for comparison. In this area,

phosphorus in soils is not comparable with the other mine areas groups which are in accordance with the Tucker test results. Phosphorous is an essential element in plant nutrition and its soil-plant relationship is different between the control area, where soils were developed on Visean age metasediments, and the mining areas whose substrata is composed of Volcano Sedimentary formations. The copper and zinc showed significant differences in the soil-plant system between the control area and Neves Corvo area. These differences indicate the obvious fact that those elements are nowadays mined in Neves Corvo, being present in the superficial environment of the area.

The comparable soil-plant copper relationship between Brancanes abandoned mine area and the Lombador control area, means that the period of more than a century of abandon may have contributed to some natural attenuation of this element in the mining area.

CONCLUSIONS

The comparison between Tuckey and Dunnett tests indicated that the reference area of Lombador presents significant differences with the ongoing exploitation of Neves Corvo Cu and Zn mine. On the contrary, Cu relationship of soil-plant is similar in the Lombador control area and in Brancanes which is abandoned over a century. This fact suggests that natural attenuation effects on Cu in the soil-plant system have already happened in Brancanes mining area. The rock rose species (*Cistus ladanifer*, L.) seems to play an important role in the natural

attenuation process.

The major elements Mg, Ca, Al, K does not presented significant differences between the areas showing some independency of mining effects in these soil-plant systems. Phosphorus presents a different behavior between control and mining areas what may be related with parent material differences or plant physiology.

REFERENCES

- ALVARENGA, P; ARAÚJO, M.F., & SILVA, J.A. 2004. Elemental uptake and root-leaves transfer in *Cistus ladanifer* L. Growing in a contaminated Pyrite Mining Area (Aljustrel-Portugal). *Water, Air and Soil Pollution*, **152**, 81-96.
- CARVALHO CARDOSO, J.V.J. 1965. Os solos de Portugal, sua classificação, caracterização e génese – 1- A sul do Rio Tejo-. *Direcção Geral dos Serviços Agrícolas, Lisboa*.
- CARVALHO, P. & FERREIRA, A. 1993. Geologia de Neves Corvo: Estado Actual do Conhecimento". *Simpósio de Sulfuretos Polimetálicos da Faixa Piritosa Ibérica, APIMINERAL, Évora, Portugal Mineral*, **33**, 11-1 to 1.11-21.
- KIDD, P.S; Díez, J., & MONTERROSO MARTINEZ, C. 2004. Tolerance and bioaccumulation of heavy metals in five populations of *Cistus ladanifer* L. subsp. *Ladanifer*. *Plant and Soil*, **258**, 189-205.
- SEAMAN, M.A., LEVIN, J.R., & SERLIN, R.C. 1991. New developments in pairwise multiple comparisons: Some powerful and practicable procedures. *Psychological Bulletin*, **110**, 577-586.
- WENZEL, W.W. & JOCKWER, F. 1999. Accumulation of heavy metals in plants grown on mineralised soils of the Austrian Alps. *Environmental Pollution*, **104**, 145-155.

The Diavik Waste Rock Project: Design, construction and preliminary results

D. W. Blowes¹, L. Smith², D. Segó³, L.D. Smith^{1,4}, M. Neuner², M. Gupton²,
B.L. Bailey¹, N. Pham³, R.T. Amos¹, & W.D. Gould¹

¹Department of Earth and Environmental Sciences, University of Waterloo CANADA
(email: blowes@uwaterloo.ca)

²Department of Earth and Ocean Sciences, University of British Columbia CANADA

³Department of Civil and Environmental Engineering, University of Alberta CANADA

⁴Diavik Diamond Mines Inc. CANADA

ABSTRACT: Predicting the effluent water quality from waste rock stockpiles at new mines is challenging because of the limited understanding of the subsurface geology and the small volumes of samples available. Testing protocols, based on laboratory tests conducted on small volumes of rock, have been developed to assess the acid generating potential of waste rock. Extending these small scale tests to provide quantitative estimates of the concentrations of dissolved constituents anticipated in effluent water of full-scale stockpiles, the scale up problem, is more challenging. The Diavik waste rock research program includes the measurement and comparison of waste rock characteristics across a wide range of scales, varying from samples of less than a kilogram to the construction of three large-scale waste rock piles (15 m in height × 60 m × 50 m) to assess the evolution of the hydrology, geochemistry, temperature, and biogeochemistry of the waste rock piles over time. The study also provides insight to the hydrologic, geochemical, and thermal behavior of waste rock piles located in areas with continuous permafrost.

KEYWORDS: *Diavik Diamond Mine, waste-rock management, scale-up, mine drainage*

INTRODUCTION

Development of open pits during mining at the Diavik Diamond Mine will result in the excavation of large volumes of country rock. The Diavik Country Rock Management Plan requires that country rock be segregated into three types during deposition: Type I (less than 0.04 wt % total sulfur); Type II (between 0.04 and 0.08 wt % total sulfur); and Type III (more than 0.08 wt % total sulfur). The Type III rock is considered to be potentially acid generating. The proposed reclamation covers for the country rock piles consist of Type I rock and till covers for Type III stockpile, and a Type I cover for Type II stockpile. The Diavik Waste Rock Research Program is designed to evaluate the benefits of the proposed reclamation strategies for the Diavik Country Rock Stockpiles, and to provide information to evaluate techniques used to scale the results of laboratory studies to predict the environmental impacts of full-

scale rock stockpiles. Understanding the relationship between these small-scale tests and full-scale waste rock piles is important to designing mine-waste disposal facilities and in developing management plans for new and operating mines that protect the environment.

SITE DESCRIPTION

Diavik Diamond Mine Inc. is located on an island in Lac de Gras, 300 km northeast of Yellowknife, NT (Fig. 1). Open pit mining will lead to the eventual development of two 200 Mt permanent stockpiles of waste rock. The country rock consists of granite averaging <0.04 wt.% S and biotite schist averaging >0.08 wt.% S. Both rock types contain low concentrations of carbonate minerals.

TEST PILE CONSTRUCTION AND INSTRUMENTATION

Three 15 m high test piles were constructed beginning in the spring of

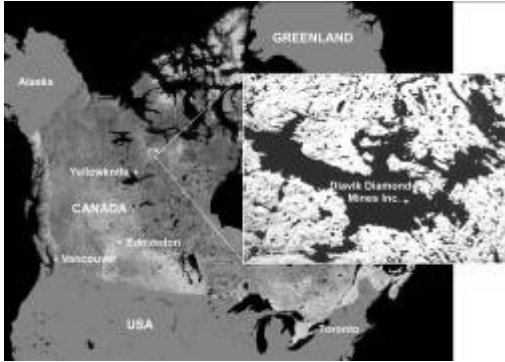


Fig. 1. Location of the Diavik Diamond Mine.

2005 and completed in the winter of 2007. These include the Type I pile, the Type III pile, and the Covered pile. The Covered pile consists of a Type III core, covered with a 1 m till layer and a 3 m Type I cap. Each pile was constructed with a basal drainage system for the collection and analysis of all water infiltrating through the piles, and a cluster of basal lysimeters for the collection of sub-samples of the infiltrating water to examine scale-up effects in flow variability and solute loadings.

The test piles were constructed with run-of-mine (ROM) material using standard mining equipment. Four tip faces spaced 5 m apart were instrumented with thermistors, soil water suction lysimeters (SWSS), tensiometers, gas sampling ports, time domain reflectometer (TDR) probes, air permeability probes, and access ports for thermal conductivity profiling and microbiological sampling. Stationary and portable data logging equipment is employed to collect data at frequent intervals. In addition to the three test piles, four continuously-draining collection lysimeters (two Type I and two Type II), each 2 m in diameter, were installed to monitor the flow and geochemistry of the active zone (Smith *et al.* 2009).

PRELIMINARY OBSERVATIONS

Physical Characterization

Physical characterization of the test piles has included grain size analysis, hydraulic properties, air permeability, and thermal



Fig. 2. Photo showing the basal drainage ditch excavated diagonally across the center of the Type I pad exiting through the SW corner (left side of picture).



Fig. 3. Basal drainage ditches excavated around the perimeter of the Type III pad exiting through the SW and NW corners (left side and bottom of picture, respectively). Basal lysimeters are visible in the centre of the photo.



Fig. 4. Waste rock sampling at the tip face.

conductivity. Grain size analyses indicate the test pile is representative of a "rock-

like” rather than a “soil-like” system, given the relatively small proportion of material less than 2 mm in diameter. The hydraulic properties of the waste rock have been measured at a number of different scales (Neuner *et al.* 2009). Porosity estimates are all on the order of 25%. Estimates of hydraulic conductivity vary greatly depending upon the scale of the measurement and the measurement technique, and range from 8×10^{-6} to $1 \times 10^{-2} \text{ m s}^{-1}$ (Neuner *et al.* 2009).

Water Flow and Transport

In the Type III pile, an apparent wetting front created by several artificial rainfall events conducted in late 2006 led to an elevated zone of moisture in the upper 3 m of the pile. Rainfall events late in the summer 2007, linked to two tracer tests, resulted in a wetting front that penetrated to a depth of approximately 8 m. This moisture was subsequently mobilized through the summer 2008 season as the pile warmed above 0°C (Neuner *et al.* 2009).

Outflow at the base of the Type III pile includes components originating as snowmelt on the batters of the pile, and infiltration of rainfall on the batters and, potentially, the top surface of the pile. The Type I test pile has only received natural rainfall events, resulting in cumulative outflow approximately one order of magnitude lower than the Type III pile. The Type I pile is apparently still accumulating water, with only the batters yielding flow at the base (Neuner *et al.* 2009).

Gas Transport

Measurements made in the Type I pile and the Type III pile show no depletion in oxygen or increase in carbon dioxide concentrations, indicating gas transport mechanisms are fast relative to the rate of the oxygen consumption and carbon dioxide production due to geochemical reactions. In the Covered pile, significant depletions in oxygen and increases in carbon dioxide concentration have been observed at some locations, suggesting gas transport rates are limited by the till

cover. Gas pressure measurements in the Type III pile show gas pressure gradients within the pile respond to changes in wind speed and wind direction. The calculated magnitude of oxygen transport due to wind driven pressure gradients is similar to oxygen transport due to diffusion and/or convection observed at other waste rock piles (Amos *et al.* 2009).

Thermal Regime

The air temperature fluctuations at the Diavik site results in ground surface temperatures that vary as much as 10°C during a month. The active layer in the bedrock at the site is about 4 m, as the surface temperatures vary between -28 and 16.5°C throughout the year. At 10 m depth into the bedrock, the temperature is stable at -5°C. In the Type I and Type III test piles, an active layer ranges from approximately 5 to 10 m depth under the influence of surface temperatures. Below a depth of 5 m, the cooling rate of waste rock varies from 2 to 3°C per year.

Test Pile Geochemistry

Geochemical results show that the degree of sulfide oxidation is dependent upon the temperature of the piles and the rock sulfide content. In the basal drain effluent of the Type III pile, a decrease in pH was observed throughout the summer as the pile warmed. Sulfate concentrations also increase with the warming of the pile and decrease as the pile cools. The decrease in pH is correlated with an increase in the concentrations of dissolved metals.

The pH of the effluent from the Type I pile remained near neutral during 2008 with elevated concentrations of sulfate. The pH of the basal drain effluent from the Covered pile was lower than observed at the Type I and Type III piles, potentially as a result of the higher sulfide content of the pile. The Covered pile effluent also had higher sulfate and conductivity (Bailey *et al.* 2009).

CONCLUSIONS

The objectives of the Diavik Waste Rock Research Program are to evaluate the benefits of the proposed reclamation

concepts for the Diavik Country Rock Stockpiles, and to evaluate techniques used to scale the results of laboratory studies to full-scale rock stockpiles. The data collection activities to date including hydrological, thermal, gas transport, and geochemical parameters address these objectives.

ACKNOWLEDGEMENTS

Funding for this research was provided by: Diavik Diamond Mines Inc. (DDMI); Canadian Foundation for Innovation (CFI) Innovation Fund Award, Natural Sciences and Engineering Research Council of Canada (NSERC); the International Network for Acid Prevention (INAP); and the Mine Environment Neutral Drainage (MEND) program. In-kind support provided by Environment Canada is greatly appreciated. We appreciate the support and assistance we have received from G. MacDonald, J. Reinson, L. Clark, and S. Wytrychowski, DDMI.

REFERENCES

AMOS, R.T., SMITH, L., NEUNER, M., GUPTON, M., BLOWES, D.W., SMITH, L., & SEGO, D.C. 2009. Diavik Waste Rock Project: Oxygen Transport in Covered and Uncovered Piles.

In: *Proceedings of the 2009, Securing the Future and 8th ICARD*, June 22-26, 2009, Skellefteå, Sweden.

BAILEY, B.L., SMITH, L., NEUNER, M., GUPTON, M., BLOWES, D.W., SMITH, L., & SEGO, D.C. 2009. Diavik Waste Rock Project: Early Stage Geochemistry and Microbiology. In: *Proceedings of the 2009, Securing the Future and 8th ICARD*, June 22-26, 2009, Skellefteå, Sweden.

NEUNER, M., GUPTON, M., SMITH, L., SMITH, L., BLOWES, D.W., & SEGO, D.C. 2009. Diavik Waste Rock Project: Unsaturated Water Flow. In: *Proceedings of the 2009, Securing the Future and 8th ICARD*, June 22-26, 2009, Skellefteå, Sweden.

PHAM, N., SEGO, D.C., ARENSON, L.U., SMITH, L., GUPTON, M., NEUNER, M., AMOS, R.T., BLOWES, D.W., & SMITH, L. 2009. Diavik Waste Rock Project: Heat Transfer in a Permafrost Region. In: *Proceedings of the 2009, Securing the Future and 8th ICARD*, June 22-26, 2009, Skellefteå, Sweden.

SMITH, L., NEUNER, M., GUPTON, M., MOORE, M., BAILEY, B.L., BLOWES, D.W., SMITH, L., & SEGO, D.C. 2009. Diavik Waste Rock Project: From the Laboratory to the Canadian Arctic. In: *Proceedings of the 2009, Securing the Future and 8th ICARD*, June 22-26, 2009, Skellefteå, Sweden.

Prediction of acid mine generating potential: Validation using mineralogy

Hassan Bouzahzah^{1,2}, Mostafa Benzaazoua¹, Benoît Plante¹,
Bruno Bussière¹, & Eric Pirard²

¹ Université du Québec en Abitibi-Témiscamingue (UQAT), 445 boul. de l'Université, Rouyn-Noranda, QC, J9X 5E4 CANADA (e-mail : Hassan.bouzahzah@uqat.ca)

² Université de Liège GeMME, B52 Sart Tilman, Liège 4000 BELGIUM.

ABSTRACT: Acid mine drainage (AMD) is a problem of major importance for the mining industry. Its prediction is very important for a proper management and rehabilitation of AMD generating sites. The Sobek test (1978) modified by Lawrence and Wang (1997) is the most used static test to predict the potential to generate AMD (particularly in North America). This method is compared in this work with mineralogy based static tests to evaluate the benefits of knowing the tailings mineralogy in AMD prediction. Three synthetic tailings composed of simple mixtures of well-characterized pure minerals are used. Although basically different in their principles and procedures, the modified Sobek test and mineralogy based static tests provide comparable results. The static prediction results are validated through the use of weathering cell kinetic tests.

KEYWORDS: *Tailings, Acid mine drainage, Static and kinetic tests, quantitative mineralogy,*

INTRODUCTION

Sulfidic mine tailings can generate acid mine drainage (AMD) under atmospheric water and oxygen action. Static tests (also called Acid base accounting ABA tests) are frequently used to predict AMD potential because they are fast and inexpensive. Reliable AMD prediction can help choosing proper mine waste management strategies during mining operation and selecting the appropriate mine closure plan. So, it is imperative to adequately estimate the acid generating potential of tailings especially. However, static tests have an important uncertain zone according to Ferguson and Morin (1991). Materials located in the uncertain zone are tested in this study. The Sobek test (1978) modified by Lawrence and Wang (1997), the most used static prediction test in North America, will be compared with three mineralogical static tests (Kwong 1993; Lawrence & Wang 1997; Paktunc 1999) to compare those different tests and to evaluate the benefits of tailings mineralogical composition knowledge in AMD prediction. For the mineralogy based prediction tests, it is absolutely essential to know the precise mineralogical composition of tailings. For

the relevance of this work, 3 "synthetic" tailings were made from a mixture of pure minerals. A combination of various chemical and mineralogical characterization techniques were used to estimate the mineralogy of the mixtures with sufficient accuracy to give relatively precise results when integrated into mineralogical prediction methods.

MATERIALS AND METHODS

In order to prepare standard mineral mixtures, pyrite (Py), pyrrhotite (Po), chalcopyrite (Cp), sphalerite (Sp), siderite (Sid), dolomite (Dol), calcite (Cal) and quartz (Qz) were acquired as pure mineral samples through a specialized distributor (Minerobec, Canada). These 8 pure minerals were further cleaned under a binocular microscope and separately crushed to reach 95% under 150µm (typical tailings grain size distribution; e.g. Aubertin *et al.* 2002). Each pure mineral powder was characterized thereafter with a series of chemical and mineralogical techniques. More details can be found in Bouzahzah *et al.* (2008). The relative density of each mineral specimen were measured with an He pycnometer and are

close to the theoretical density of the minerals except for Po ($D_r = 4.4$; theoretical average = 4.61) and Sid ($D_r = 3.8$, theoretical 3.96). The XRD was used to identify and quantify the mineral species present in each pure mineral powder and confirmed that the Py, Cp, Dol, Cal, and Qz samples are almost pure. The Sid and Sp powders respectively show a slight contamination with rhodocrosite and quartz. The most impure sample is Po with 24 wt% pyrite and 12 wt% calcite, which explains its relative density discrepancy. The optical and scanning electron microscope observations confirm the XRD results.

The Atomic emission spectrometry (ICP-AES) results on the solids confirm the chemical purity of Py, Cp, Qz, Cal and Dol samples. The Po sample contains calcium which, after conversion into calcite, gives approximately 10 wt% of this mineral. Sid sample contains 10.3 wt% Mn and 1.86 wt% Mg, in agreement with measurements using a Scanning Electron Microscopy coupled to Energy Dispersive X-Ray Spectroscopy (SEM-EDS) analysis; again this explains the difference between the measured and theoretical density of the Sid powder.

Once the pure mineral powders characterized, 3 mixtures were manually prepared and named ML1, ML2 and ML3. They contain each of the 8 minerals in different proportions reproducing 3 mine tailings falling in the uncertainty zone of the static test used. The 3 synthetic tailings were characterized with the same techniques as for the pure minerals. Cp and Sp weight fractions were evaluated from their chemical element tracers (respectively Cu and Zn) obtained from ICP-AES analysis. Qz, Dol, and Sid samples are considered pure and their percentages in the mixtures are not corrected. Table 1 presents the fraction of each mineral in the three mixtures before and after correction taking into consideration the contamination of Po sample by pyrite and calcite, as previously determined. The corrected mineral proportions are used for calculation of the static test parameters based on

Table. 1. Corrected mineral composition (corr) of the three standard mixtures as compared to the initial dosing.

	ML1		ML2		ML3	
	Initial %	% corr	Initial %	% corr	Initial %	% corr
Py	6,50	6,86	8,50	9,34	12,00	12,48
Po	1,50	0,92	3,50	2,14	2,00	1,22
Cp	0,80	0,84	0,60	0,62	1,50	1,45
Sp	1,50	1,40	0,90	0,88	0,70	0,64
Dol	8,50	8,50	3,50	3,50	2,00	2,00
Cal	1,00	1,18	14,00	14,43	21,50	21,74
Sid	7,00	7,00	3,00	3,00	20,00	20,00
Qz	73,20	73,20	66,00	66,00	40,30	40,30
Total	100,00	99,90	100,00	99,91	100,00	99,83

mineralogy.

RESULTS AND DISCUSSIONS

Static tests

According to the Sobek test (1978) modified by Lawrence and Wang (1997), the acid potential (AP) is calculated from the sulfur content of the sample, and the neutralization potential (NP) is determined by an acid-base titration. For mineralogy based static tests, the calculation methods of Kwong (1993), Lawrence & Wang (1997) and Paktunc (1999) were used. The Lawrence and Wang (1997) method uses the inorganic carbon content for NP calculation. The amount of inorganic carbon and sulfur in samples were deduced from the mineralogical compositions. The Kwong (1993) and Paktunc (1999) methods are based on the summation of individual contributions of the minerals that produce (AP) and neutralize (NP) acid. The net neutralization potential (NNP) of a given tailings is defined as the difference between its NP and AP ($NNP=NP-AP$). The results obtained by the different static tests are listed in table 2 and graphically plotted (Fig. 1) according to the Ferguson and Morin (1991) interpretation. All static tests used in this study classify the tailings in the uncertain zone except for ML1 classified as acid generating with the modified Sobek test.

Kinetic test

To validate the static tests results presented above, weathering cells (small-

Table 2. Compilation of results from chemical and mineralogical static tests used in this study. For the Kwong test, if $M > 0$, the sample is considered acid generating, otherwise it is considered non acid generating.

		AP (Kg CaCO ₃ /t)	NP (Kg CaCO ₃ /t)	PNN (Kg CaCO ₃ /t)
Modified Sobek	ML1	139,35	91,9	-47,45
	ML2	197,8	176,3	-21,5
	ML3	238,15	237	-1,15
Lawrence and Wang	ML1	148,63	104,08	-44,55
	ML2	196,11	182,3	-13,81
	ML3	244,6	239,11	-5,49
Kwong M=PA-PN	ML1	0,16	0,08	M=0,08
	ML2	0,22	0,23	M= - 0,01
	ML3	0,31	0,38	M= - 0,07
Paktunc	ML1	122,23	104,18	-18,05
	ML2	176,33	182,24	5,91
	ML3	217,4	239,08	21,68

scale humidity cell tests) were performed (see Cruz *et al.* 2001 for more details on the method). The measured pHs in flushing waters show a slight fluctuation around 8 indicating that the 3 samples did not become acidic during the kinetic tests. The measured oxydo-reduction potentials (Eh) reflect oxidizing conditions as a result of sulfide oxidation. The sulfur measured in leachates (mainly as sulfate) is the product of this sulfide oxidation. Iron was not detected in the leachates since the measured Eh-pH values are favourable for its precipitation as oxyhydroxides minerals in the weathering cells. Trace levels of Mn, Zn and Cu in leachates, and undersaturation of Mn, Zn and Cu secondary minerals (determined by geochemical modeling using VMINTEQ) reflect that Sid, Sp and Cp are not oxidized during the kinetic tests. For more geochemical details see Bouzazhah (2006).

Figure 2 shows that the cumulative sulfur (as SO₄²⁻), Ca and Mg concentrations increase during the weathering cell tests for all samples. The cumulative Ca and Mg leaching is indicative of calcite and dolomite dissolution (related to acid neutralisation). Figure 2 also shows that the sulfide oxidation rate slows down for all tailings after a few days, and that the stabilized oxidation rate is greater for the ML3 sample than for the others, which are

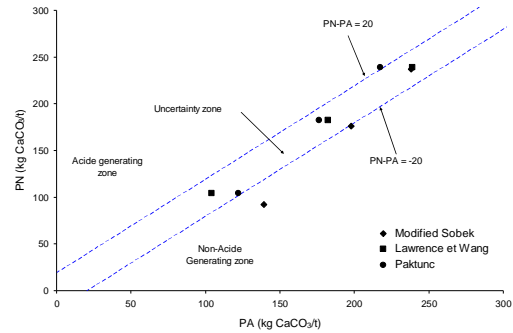


Fig. 1. Classification of the tree standard samples in terms of AP and NP according to Ferguson & Morin (1991).

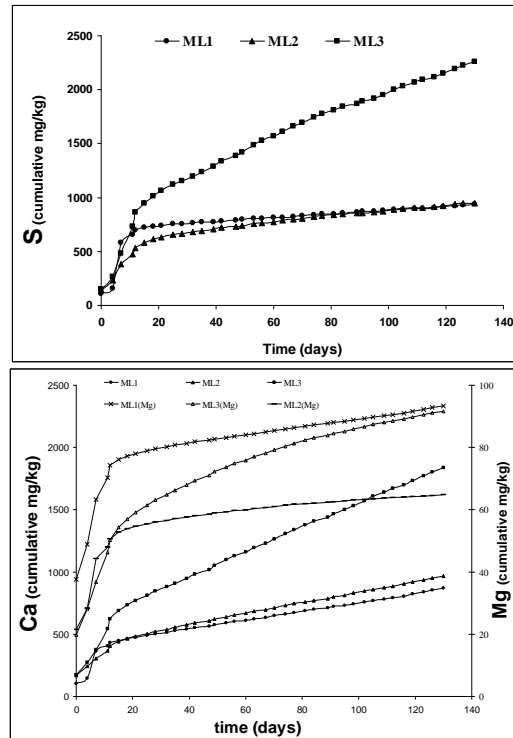


Fig. 2. Graphical representations of the evolution of cumulative concentrations of sulfur, calcium and magnesium collected throughout the kinetic test.

similar.

The oxidation-neutralization curve (Fig. 3) gives a long term prediction of AMD generation (see Benzaazoua *et al.* 2001 for more details). Assuming steady-state geochemical behaviour, the oxidation products (sulfates) would disappear before the neutralizing elements (Ca, Mg, and Mn).

CONCLUSIONS

Many chemical and mineralogical characterization techniques were used to precisely determine the mineralogy of 3 synthetic tailings. Mineralogy based static tests are useful when sample mineralogy is

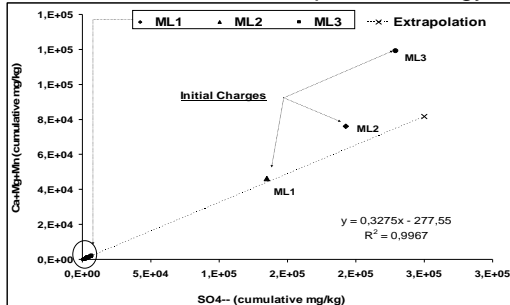


Fig. 3. Extrapolated oxidation-neutralization curve for the long-term prediction of acid mine drainage of the tree samples (Benzaazoua & Al 2001)

known with enough accuracy and give in our study comparable results to those of the modified Sobek test. The modified Sobek test seems to overestimate the AP prediction by taking into account the sulfur from sulfides that do not seem to oxidize in the conditions of the weathering cells.

REFERENCES

AUBERTIN, M. BUSSIERE, B., & BERNIER, L. 2002. Environnement et gestion des résidus miniers. CD, *Les Editions de l'Ecole Polytechnique de Montréal, CA.*

BENZAAZOUA, M., BUSSIERE, B., & DAGENAIS, A.M. 2001. *Comparison of kinetic tests for sulfide mine tailings.* In: *Tailings and Mine Waste "01"* Fort Collins, Colorado, January. Balkema, Rotterdam, 263-272.

BOUZHZA, H. 2006. *Prédiction du potentiel du drainage minier acide des résidus sulfurés.* Master thesis. University of Liege Belgium. 240p.

BOUZHZA, H., CALIFICE, A., BENZAAZOUA, M., MERMILLOD-BLONDIN, R., & PIRARD, E. 2008. Modal Analysis of Mineral Blends Using Optical Image Analysis Versus X-Ray Diffraction. *Ninth International Congress for Applied Mineralogy* Brisbane, QLD, 8-10 September 2008.

CRUZ R., BERTRAND, V., MONROY, M., & GONZÁLEZ, I. 2001. Effect of sulphide impurities on the reactivity of pyrite and pyritic concentrates: a multi-tool approach. *Applied Geochemistry*, **16**, 803-819.

FERGUSON, K.D. & MORIN, K.A. 1991. The prediction of acid rock drainage –Lessons from the data base. *Second International Conference on the Abatement of Acidic Drainage*, Montréal, Canada, **3**, 83-106.

KWONG, Y.T.J. 1993. Prediction and prevention of acid rock drainage from a geological and mineralogical perspective. *MEND Report 1.32.1* CANMET, Ottawa, 47 p.

LAWRENCE, R.W. & WANG, Y. 1997. Determination of neutralization potential in the prediction of acid rock drainage. *Proceedings of the 4th International Conference on Acid Rock Drainage, Vancouver*, **2**, 449-464.

PAKTUNC, A.D. 1999. Characterization of mine wastes for prediction of acid mine Drainage. In: *Environmental impacts of mining activities, emphasis on mitigation and remedial measures*, Springer Verlag, Berlin, Heidelberg, New York, Azcue, J.M., 19-40.

SOBEK, A.A., SCHULLER, W.A., FREEMAN, J.R., SMITH, R.M. 1978. Field and laboratory methods applicable to overburdens and mine soil. *EPA report no. EPA-600/2-78-054*, 47-50.

Preliminary investigation into tailings-ground water interactions at the former Steep Rock iron mines, Ontario, Canada

Andrew G. Conly¹, Peter F. Lee², & Chris Perusse¹

¹Department of Geology, Lakehead University, 955 Oliver Road, Thunder Bay, ON, P7B 5E1 CANADA
(e-mail: andrew.conly@lakeheadu.ca)

²Department of Biology, Lakehead University, 955 Oliver Road, Thunder Bay, ON, P7B 5E1 CANADA

ABSTRACT: Drainage impacts from mined waste materials on ground water at the former Steep Rock iron mines were investigated at two different sites. Site 1 consists of a goethite-hematite-quartz tailings impoundment that was constructed on top of a bog/wet land. Site 2 consists of a pyritic waste rock dump and a down gradient AMD affected zone, which overlies glaciolacustrine sediments. Ground water from site 1 is pH-neutral and contains moderate sulfate (<1000 mg/L) and low Fe (< 1 mg/L). In contrast, ground water from site 2 has a lower pH (<6) with elevated sulfate (>3000 mg/L) and Fe (>95 mg/L) concentrations. The primary control on ground water chemistry is mineralogy of the waste material. However, carbon and sulfur isotopes indicate that for site 1 ground water chemistry is influenced by waters and gases originating from organic-rich (bog) soils that underlie the tailings. The chemistry of water within catchment basins at both sites is largely controlled by the composition of ground water; however, dilution by surface run-off and precipitation has occurred.

KEYWORDS: ground water, tailings, sulfate, pit lake, acid mine drainage

INTRODUCTION

Flooding since 1979 of two open pits of the decommissioned Steep Rock iron mines near Atikokan, Ontario, has led to the formation of Hogarth and Caland pit lakes (Fig. 1). Distinct differences in water chemistry and quality exist between the two pit lakes: i) Hogarth is non-stratified, oxygenated and highly enriched in dissolved sulfate (1200-2000 mg/L), resulting in chronic sulfate toxicity (Goold 2008); and ii) Caland is not sulfate toxic and has an oxygenated fresh water lens that overlies an anoxic and moderately saline (200-500 mg/L sulfate) water column. The source of dissolved sulfate for both pit lakes is oxidization of pyrite within the buried ore zone; with the difference in sulfate levels reflecting differences in the pyrite content of the ore zones (Conly *et al.* 2008a,b). In addition, both pit lakes have near neutral pH due to reaction with carbonate wall rocks (Conly *et al.* 2008a,b).

However, the contributions of sulfate, acid and metals from ground and surface waters that interact with the numerous tailings and waste rock dumps located

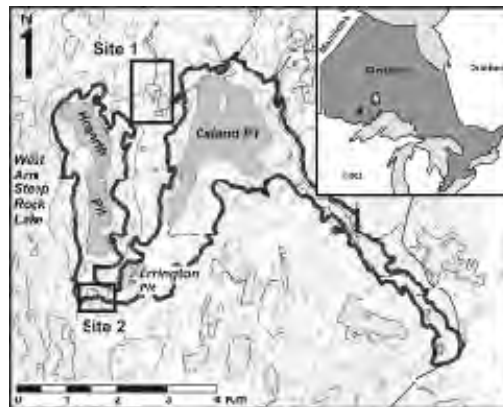


Fig. 1. Map showing location of the study sites relative to Hogarth and Caland pit lakes. Black outline represents original lake level (prior to draining for mining). Inset shows location of the Steep Rock iron deposit within Ontario.

throughout the Steep Rock site have not been extensively investigated.

Reconnaissance studies have shown that surface waters originating from waste rock and tailings dumps are typically characterized by low pH, high sulfate levels and variable metal contents. Consequently, the aim of this study is to investigate the nature of ground water interactions with

two different tailing materials, and examine how the products of these reactions interact with adjacent surface water bodies.

SITE DESCRIPTION

Site 1 (Figs. 1 & 2a) is tailings impoundment that was constructed on top of a bog/wet land. The tailings consist of goethite + hematite + quartz, with little to no pyrite. The tailings are largely contained behind a dam structure, which presently serves as an access road. There is a lateral variation in the grain size of the tailings material: i) on the western side of the bedrock knob the material consists of well-drained, sandy tailings; and, ii) along the northern and eastern side bedrock knob the material consists of water-laden clay-silt tailings. The area south of the dam (~14 m elevation drop) consists of marsh grasses growing in a mixed unit of organic-rich soil and silt-clay tailings. A stream (SW 12) flows along the northwestern margin of the tailings impoundment. Another stream flows southward through the clay-silt tailings into pond 2, and eventually into Caland pit lake.

Site 2 is situated on the south shore of Moore's pit (Figs. 1 & 2b). This site consists of: i) a pyritic waste rock pile, covered with a thin veneer of Fe-oxide tailings; and ii) a down stream acid drainage affected area that is characterized by a Fe oxide + sulfur-rich hard pan surface layer that overlies a stratified unit comprised of intensely altered (Fe-oxide stained) and unaltered Quaternary glaciolacustrine deposits. A small creek (product of beaver activities) flows along the eastern margin of the site into Moore's pond.

METHODS

Monitoring wells were installed to a depth of 3-4 m into soft tailings at sites 1 and 2. The wells are constructed of 1.5 inch-OD PVC pipe with the lower 1.2 m perforated for collection of ground water. Water was sampled using a LDPE tubing- foot valve assembly. Ground water and surface waters were sampled monthly from August to November 2008. Temperature, pH, and conductivity were measured in the field and

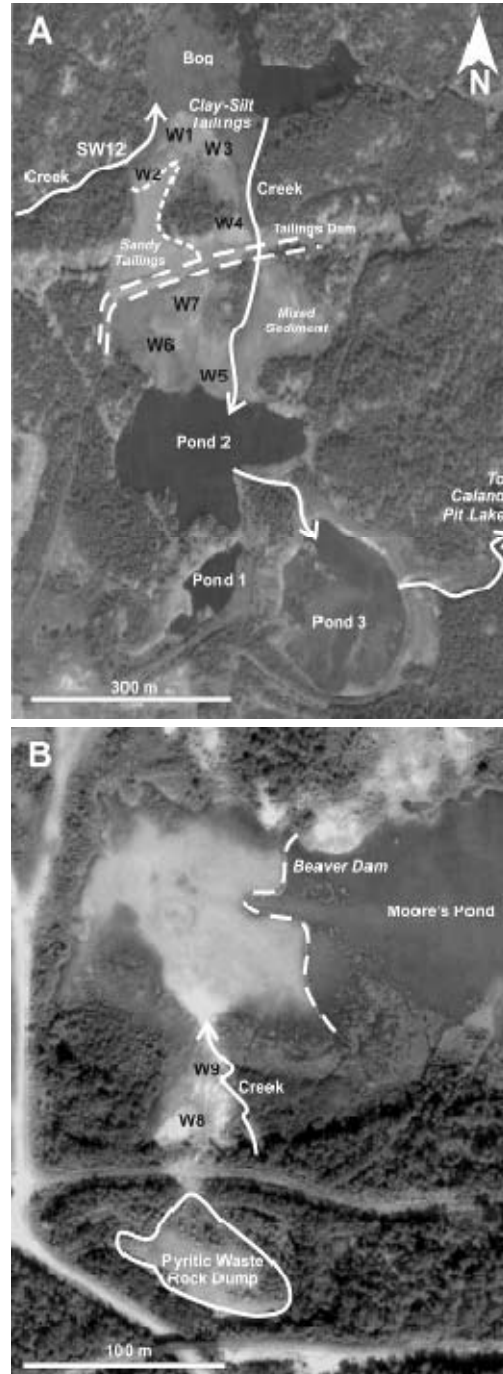


Fig. 2. Photo maps showing location of monitoring wells (W#), surface water bodies (flow directions of creeks indicated by arrows) and tailings/waste rock dumps for sites 1 (A) and 2 (B). Base images from Google™ Earth.

laboratory.

The chemical composition of the waters

was determined accordingly: 1) metals in filtered and acidified samples using a Varian ICP-AES; 2) Cl⁻ and SO₄²⁻ using a DIONEX ion chromatograph; and, 3) alkalinity by carbonate titration.

Stable isotope analyses were performed at the University of Calgary. The δ³⁴S ratio of dissolved sulfate (precipitated as BaSO₄) was determined by elemental analyzer-continuous flow-isotope ratio mass spectrometry (IRMS). δ¹³C_{DIC} of water was prepared by phosphoric acid digestion (McCrea1950) prior to IRMS. All isotopic compositions are expressed in per mil notation relative to international standards (δ³⁴S: CDT; δ¹³C_{DIC}: PDB). Analytical uncertainties are ±0.2‰ for δ¹³C_{DIC} and ±0.7‰ for δ³⁴S.

RESULTS AND DISCUSSION

Figure 3 shows the average composition of major anions and cations, Fe, Mn, total metals and pH for all ground water wells and selected surface waters. Both sites are characterized by sulfate-dominant ground waters, as opposed to the one regional ground water which is chlorine-dominant. Interactions with pyritic waste rock (site 2) produces ground waters with elevated sulfate (>3000 mg/L) low pH (<6) and high Fe (>95 mg/L). Fe-oxide + quartz tailings (site 1) produce pH-neutral ground waters with moderate to high concentrations of sulfate (200-1000 mg/L). The one major difference observed is that ground water from site 1 is highly Fe-depleted (<1 mg/L). The difference in pH, sulfate and Fe levels between the two sites reflects the following: i) the relatively insoluble behaviour of goethite and hematite in pH-neutral waters (site 1); ii) possible occurrence of soluble Fe-sulfates (site 1); and, iii) the relative abundance of pyrite and the rate at which it is oxidized (site 2).

Surface waters parallel the observed trends for ground waters. However, for both sites anion and cation abundances are typically lower, and likely reflect dilution from surface run-off and precipitation.

Figure 4 shows the variation in carbon and sulfur isotopes for Steep Rock ground water and surface water. δ³⁴S ratios for

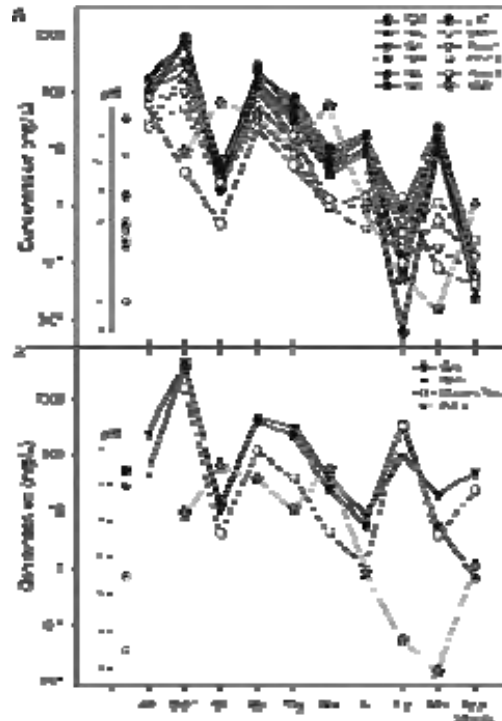


Fig. 3. Schoeller diagrams, with pH (inset), showing the average compositions for ground water and surface water from sites 1 (A) and 2 (B). Abbreviations: Alk – alkalinity; AGW – Atikokan ground water.

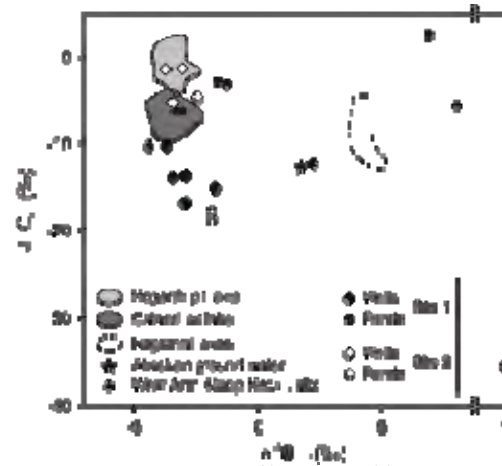


Fig. 4. Variation in δ¹³C and δ³⁴S of ground water and surface water from sites 1 and 2. Data for other waters (excluding regional water; unpublished) from Conly *et al.* (2008b).

ground water from both sites are within the reported range for the two pit lakes, and indicate that the dissolved sulfate is produced from the oxidation of pyrite

present in waste materials (*cf.* Conly *et al.* 2008b).

Ground water from site 2 displays a narrow range in $\delta^{13}\text{C}$, and is within the range reported for the two pit lakes. The $\delta^{13}\text{C}$ of ground waters from site 2 reflects exchange with atmospheric CO_2 and carbonate dissolution (*cf.* Conly *et al.* 2008b). In contrast, the $\delta^{13}\text{C}$ of ground water from site 1 is both more depleted and variable. Such values are interpreted to reflect isotopic exchange with CO_2 released from buried organic-rich (bog) soils.

The ground water from well 6 (site 1) yielded both the most depleted $\delta^{13}\text{C}$ and most enriched $\delta^{34}\text{S}$. Isotopic compositions of this dual nature are consistent with methanogenesis and bacterial sulfate reduction, arising from interaction with organic-rich (bog) soils from below.

CONCLUSIONS

The composition of ground water present in tailing impoundments and waste rock dumps is primarily controlled by the mineralogy of the mine waste: i) pyrite-bearing material produces in low pH, sulfate-rich and Fe-rich waters; and, ii) Fe-oxide-bearing material produces neutral pH, moderate sulfate and Fe-poor waters. The water chemistry of tailings catchment ponds is primarily controlled by the chemistry of the inflowing ground water, but has been diluted by run-off and direct precipitation inputs. Sulfur isotopes indicate that sulfate is derived from the oxidation of pyrite in waste materials. Although not reflected in anion, cation and metal concentrations, interactions between

ground water and deeper, bog-derived waters and gases can be inferred from depleted carbon and enriched sulfur isotope ratios. Both ground and surface waters arising from tailings/waste rock interactions contribute, to an unknown degree, to the water quality issues of the pit lakes.

ACKNOWLEDGEMENTS

We thank the Ontario Ministry of Natural Resources for their assistance with the project and allowing access to the site. Trow Engineering is thanked for their assistance with well installation. Funding for the project is provided through a NSERC Discovery grant awarded to AGC.

REFERENCES

- CONLY, A.G., LEE, P.F., GODWIN, A., & COCKERTON, S. 2008a. Experimental constraints for the source of sulfate toxicity and predictive water quality for the Hogarth and Caland pit lakes, Steep Rock Iron Mine, Northwestern Ontario, Canada. *Mine Water and the Environment Proceedings*, **10**, 551-554.
- CONLY, A.G., LEE, P.F., GOOLD, A., & GODWIN, A. 2008b. Geochemistry and stable isotope composition of Hogarth and Caland pit lakes, Steep Rock Iron Mine, Northwestern Ontario, Canada. *Mine Water and the Environment Proceedings*, **10**, 555-558.
- GOOLD, A.R. 2008. *Water quality and toxicity investigations of two pit lakes at the former Steep Rock iron mines, near Atikokan, Ontario*. MSc. thesis, Lakehead University, Thunder Bay, Ontario.
- MCCREA, J.M. 1950. On the isotopic chemistry of carbonates and a paleotemperature scale. *Journal of Chemistry and Physics*, **18**, 849-857.

Long-term fate of ferrihydrite in uranium mine tailings

Soumya Das¹ & M. Jim Hendry¹

¹ University of Saskatchewan, Department of Geological Sciences, 114 Science Place, Saskatoon, SK, S7N5E2
CANADA (e-mail: sod671@mail.usask.ca)

ABSTRACT: The kinetics and mechanisms of the phase transformation of 2-line ferrihydrite to goethite and hematite are being assessed as a function of pH, temperature and Fe/As, Fe/Se, Fe/Mo molar ratios using batch experiments, BET analyses, XRD, and XANES. Initial results from XRD analyses show that ferrihydrite is stable at high pH (~10) for up to seven days at 25°C, but considerable crystallization occurs at elevated temperatures. Specifically, XRD data show that ferrihydrite is transformed to a mixture of hematite and goethite at 50°C (~85% hematite and ~15% goethite) and 75°C (~95% hematite and ~5% goethite) after 24 hours and these ratios remain constant to the end of the experiments (seven days).

KEYWORDS: *ferrihydrite, goethite, hematite, phase transformation.*

INTRODUCTION

Ferrihydrite, a poorly crystalline iron (III) oxide (approximate formula: $5\text{Fe}_2\text{O}_3 \cdot 9\text{H}_2\text{O}$) is typically found in mine drainage environments with pH values >5 (Carlson *et al.* 2002). Ferrihydrite has a large specific surface area (>220 m²/g), and therefore can strongly adsorb many environmental pollutants (including As, Mo, and Se) in aquatic systems; consequently it can play a crucial role in the bioavailability and migration of trace metals (Carlson & Schwertmann 1981; Schwertmann & Taylor 1989). Ferrihydrite transforms to thermodynamically more stable and more crystalline products, such as goethite and hematite. This crystallization (phase transformation) is controlled by solution pH, temperature, and solutes present in the system (Johnston & Lewis 1983; Schwertmann & Murad 1983; Paige *et al.* 1997). During this phase transformation, sorbed metal cations desorb as a result of a rapid decrease in the reactive surface area (Ford *et al.* 1997; Arthur *et al.* 1999). In addition, this transformation can have a significant impact on the aqueous concentrations of sorbed ions. Although cation partitioning during phase transformation has been documented, few studies have addressed the impact of this phase change on oxy-anions such as As,

Mo, and Se, which are important elements of concern in uranium tailings.

The goal of this study is to determine the impact of ferrihydrite phase transformations on the long-term source terms for As, Mo, and Se in uranium mine tailings facilities. This is important as arsenic complexation in uranium mine tailings at Rabbit Lake minesite, northern Saskatchewan, Canada is predominantly 2-line ferrihydrite with sorbed arsenate (Moldovan *et al.* 2003). The specific objective of the current study was to investigate the transformation of both natural and synthetic 2-line ferrihydrite to goethite and hematite as a function of temperature. This objective is being met using batch experiments, X-ray Absorption Near Edge Spectroscopy (XANES), X-Ray diffraction (XRD), B.E.T surface analyses, and Surface Complexation Modeling (SCMs). Additional experiments, based on the findings of this study, are underway to elucidate the fate of sorbed As, Mo, and Se onto ferrihydrite during phase transformation as a function of pH, temperature, and the Fe/As,Mo,Se ratio.

MATERIALS AND METHODS

Initially, synthetic ferrihydrite, goethite and hematite were synthesized using the methods described by Cornell & Schwertmann (2003). These pure phases were analyzed using XRD, BET, and

XANES to ensure the quality of the synthates. Three batches of ferrihydrite were synthesized and precipitates were washed 5-6 times to ensure a chloride-free synthate. Ferrihydrite precipitates were re-dispersed in 200 mL of double deionized (DDI) water at (1) room temperature (25°C), as well as preheated in water baths to temperatures of (2) 50°C and (3) 75°C. For all of these slurries, pH was kept constant at 10 using 1M KOH. 40 mL samples were pipetted from each reaction vessel after 0, 1, 2, 3, and 7 days. Slurries were centrifuged, washed three times with DDI water and air dried for analyses (BET, XRD, and XANES). BET analyses were used to evaluate the decrease in surface areas with increasing crystallinity, and XRD and XANES were used to detail the structural and speciation changes in iron.

RESULTS AND DISCUSSION

Measured surface areas (11-point BET analyses) for pure phases such as ferrihydrite, goethite and hematite are in the range as proposed by Cornell & Schwertmann (2003) (Table 1). Preliminary XRD analyses showed that temperature impacts the kinetics of phase transformation of ferrihydrite. Data indicated that after seven days, the rate of transformation from ferrihydrite to more crystalline forms, if it was occurring, was too slow to be measured at 25°C (Fig. 1). In contrast to the 25°C experiment, significant, transformations were observed at 50 (Fig. 2) and 75°C (Fig. 3) after 24

Table 1. 11-point BET analyses of pure phases measured in this study. Expected values from Cornell & Schwertmann (2003) are also included to compare the results of present study.

Phase	Surface area (m ² /g)
Ferrihydrite	347* 200-400 [£]
Goethite	19* 20-30 [£]
Hematite	44* ~30 [£]

*This study [£]Cornell and Schwertmann (2003)

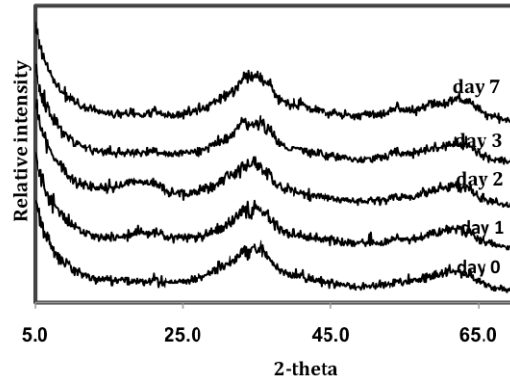


Fig. 1. XRD scans of solids at pH 10 and 25°C for day 0, 1, 2, 3, and 7 (from bottom to top). Scans show the dominance of ferrihydrite and lack of hematite and goethite.

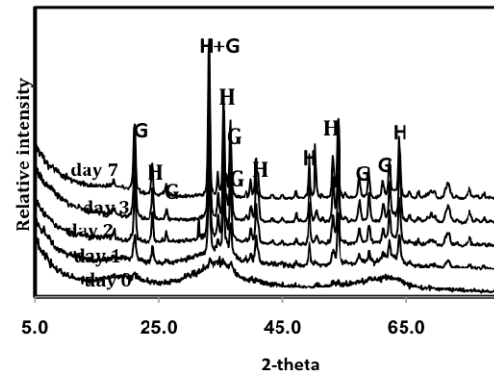


Fig. 2. XRD scans of solids at pH 10 and 50°C for day 0, 1, 2, 3, and 7 (from bottom to top). Scans show the dominance of ferrihydrite at day 0 but dominance of hematite and goethite in all subsequent scans.

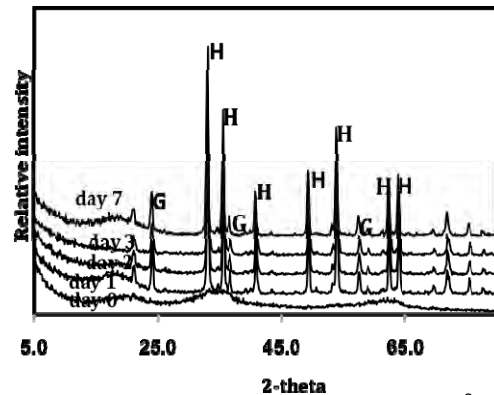


Fig. 3. XRD scans of solids at pH 10 and 75°C for day 0, 1, 2, 3, and 7 (from bottom to top). Scans show the dominance of ferrihydrite at day 0 but dominance of hematite and goethite in all subsequent scans.

hours. At both of these temperatures, ferrihydrite was transformed to a mixture of hematite and goethite (~85% hematite and 15% goethite at 50°C and ~95% hematite and 5% goethite at 75°C). These ratios of mixing of hematite and goethite remained constant for the remainder of the experiment (seven days). The transformation of ferrihydrite to hematite in these experiments is not inconsistent with a 2-stage crystallization process, as proposed by Vu *et al.* (2008). According to their findings, in the first stage, goethite is the stable product, but with extended heating, goethite transformed to hematite. These observations contradict with earlier workers (Schwertmann & Murad 1983; Shaw *et al.* 2005) who predicted goethite would be the final product instead of hematite. pH dependent experiments are in progress (pH 2 and 7). Results from these experiments will be of value to define the reaction kinetics of 2-line ferrihydrite in dilute solutions in nature over a wide range of pH and temperature.

PRELIMINARY CONCLUSIONS

Although additional analyses of the existing data and additional experiments are required to reach definitive conclusions on the phase changes of ferrihydrite in uranium mine tailings, preliminary XRD data suggest that in deionized water at elevated pH (pH=10) phase transformation of ferrihydrite can occur at elevated temperatures. In both elevated temperature experiments, hematite appeared to be the dominant transformation product. At room temperature, however, ferrihydrite remains stable after the duration of the experiment (seven days).

ONGOING WORK

Ongoing experiments are underway to determine:

- (1) pH dependence of crystallization by conducting experiments at pH 2 and 7 and at temperatures of 25, 50 and 75°C.
- (2) the effect of the Fe/As,Mo,Se molar ratio on adsorption and desorption kinetics during phase transformation

ACKNOWLEDGEMENTS

We would like to thank T. Bonli for assistance with the XRD and SEM analyses and J. Essilfie-Dughan for assistance with XANES analyses at the Canadian Light Source. This project was jointly funded by Cameco Corporation and NSERC through an IRC grant.

REFERENCES

- ARTHUR, S.E., BRADY, P.V., CYGAN, R.T., ANDERSON, H.L., & WESTRICH, H.R. 1999. Irreversible sorption of contaminants during ferrihydrite transformation. *WM'99 Conference*, February 28-March 4.
- CARLSON, L. & SCHWERTMANN, U. 1981. Natural ferrihydrites in surface deposits from Finland and their association with silica. *Geochimica et Cosmochimica Acta*, **45**, 421-429.
- CARLSON, L., BIGHAM, J.M., SCHWERTMANN, U., KYEK, A., & WAGNER, F. 2002. Scavenging of As from acid mine drainage by schwertmannite and ferrihydrite: a comparison with synthetic analogues. *Environmental Science and Technology*, **36**, 1712-1719.
- CORNELL, R.M. & SCHWERTMANN, U. 2003. The iron oxides: *Structure, properties, reactions, occurrences, and uses*. Wiley-VCH.
- FORD, R.G., BERTSCH, P.M., & FARLEY, K.J. 1997. Changes in transition and heavy metal partitioning during hydrous iron oxide aging. *Environmental Science and Technology*, **31**, 2028-2033.
- JOHNSTON, J. & LEWIS, D.G. 1983. A detailed study of the transformation of ferrihydrite to hematite in an aqueous medium at 92°C. *Geochimica et Cosmochimica Acta*, **47**, 1823-1831.
- MOLDOVAN, B.J., JIANG, D.-T., & HENDRY, M.J. 2003. Mineralogical characterization of arsenic in uranium mine tailings precipitated from iron-rich hydrometallurgical solutions. *Environmental Science and Technology*, **37**, 873-879.
- PAIGE, C.R., SNODGRASS, W.J., NICHOLSON, R.V., SCHARER, J.M., & HE, Q.H. 1997. The effect of phosphate on the transformation of ferrihydrite into crystalline products in alkaline media. *Water, Air, and Soil Pollution*, **97**, 397-412.
- SCHWERTMANN, U. & MURAD, E. 1983. Effect of pH on the formation of goethite and hematite from ferrihydrite. *Clays and Clay Minerals*, **31**(4), 277-284.
- SCHWERTMANN, U. & TAYLOR, R.M. 1989. Iron oxides. In: DIXON, J.B. AND WEED, S.B. (eds.) *Minerals in soil environments*, 2ed. Madison, Soil Science Society of America, 379-438.

SHAW, S., PEPPER, S.E., BRYAN, N.D., & LIVENS, F.R. 2005. The kinetics and mechanisms of goethite and hematite crystallization under alkaline conditions, and in the presence of phosphate. *American Mineralogist*, **90**, 1852-1860.

VU, H.P., SHAW, S., & BENNING, L.G. 2008. Transformation of ferrihydrite to hematite: an in situ investigation on the kinetics and mechanisms. *Mineralogical Magazine*, **72**, 217-220.

Methods for obtaining a national-scale overview of groundwater quality in New Zealand

Christopher J. Daughney, Uwe Morgenstern, Rob van der Raaij,
Robert Reeves, Matthias Raiber, & Mark Randall

GNS Science, 1 Fairway Drive, Avalon NEW ZEALAND (e-mail: c.daughney@gns.cri.nz)

ABSTRACT: This study presents methods developed to summarise groundwater quality in New Zealand, based on data collected since 1990 from over 100 monitoring sites comprising the National Groundwater Monitoring Programme (NGMP). Site-specific groundwater age determinations based on measured concentrations of tritium, CFCs and SF₆ range from less than one year to more than 100 years, with the 25th, 50th and 75th percentiles (across the entire NGMP) being approximately 10, 40 and 100 years, respectively. Hierarchical cluster analysis based on median concentrations of 15 major and minor constituents reveals three dominant water types across the NGMP. At 42% of the monitoring sites, groundwater quality shows some level of human influence, with nitrate, chloride and/or sulphate concentrations in excess of natural background levels. At 32% of the monitoring sites, groundwater quality shows little or no evidence of human influence, but due to high levels of oxygen in the aquifer, any introduced nitrate or sulphate will persist and accumulate. At the remaining 26% of the monitoring sites, the groundwater is oxygen-poor and is not likely to accumulate significant nitrate, but due to natural processes, it commonly accumulates concentrations of iron, manganese, arsenic and/or ammonia.

KEYWORDS: *hydrochemistry, groundwater age, multivariate statistics, New Zealand*

INTRODUCTION

The objective of this study is to provide an overview of groundwater quality across all of New Zealand (NZ). This is achieved by analysis of data collected through the NZ National Groundwater Monitoring Programme (NGMP). The NGMP, established in 1990, is a long-term research programme that aims to identify spatial and temporal trends in NZ groundwater quality and relate them to specific causes. The data analysis methods of interest in this study include hierarchical classification of monitoring sites from hydrochemistry (Daughney & Reeves 2005, 2006), and groundwater age determination based on measured concentrations of tritium, CFCs and SF₆ (Daughney *et al.* 2009).

Hierarchical Cluster Analysis (HCA) is a multivariate statistical method that can be used to assign groundwater samples or monitoring sites to distinct categories (hydrochemical facies). HCA offers several advantages over other methods of grouping or categorising groundwaters.

HCA does not require *a priori* assumptions about the number of groups or the criteria that control the groupings, such as aquifer lithology or confinement. HCA can be based on any number of variables, and these variables can be of any type (chemical, physical, biological; distributed or non-distributed). HCA can thus provide a more holistic approach to sample comparison than most other methods, which are limited in terms of the number of variables that can be simultaneously presented clearly. HCA produces a set of average parameter values (a centroid) for each cluster in the original units of the input variables, and hence the results of HCA can be more readily interpreted in the geological or hydrochemical context than multivariate methods based on transformation, e.g. Principal Components Analysis. The output of HCA can be displayed as a membership table, where each site or sample is unambiguously assigned to a single group. By contrast, for most graphical methods (e.g. Piper diagrams), it is difficult to determine

exactly where the boundaries of each group should be placed, how many groups there should be, or which samples should be assigned to each group.

Determination of groundwater age is valuable for a variety of reasons covering the spectrum from applied resource management to fundamental scientific research. Groundwater dating relies on measurement of one or more tracer substances, followed by fitting of the tracer concentration data with a lumped-parameter model (Zuber *et al.* 2005). Tritium, CFCs and SF₆ are the tracers most commonly used for dating young groundwater (less than about 100 years old).

It is often useful to estimate groundwater age independently of the tracer method in order to overcome ambiguities that can arise in age determinations based on limited tracer data at some sites and in some hydrogeological conditions. Ambiguity in groundwater age can be overcome by fitting the convolution integral to time series tracer data, but it may not be practical to make several measurements over perhaps several years, as might be necessary to permit detection of significant change in the tracer concentrations relative to analytical uncertainty. Major ion hydrochemistry and well construction can be used to estimate groundwater age independently from the direct method of measuring tracer concentrations.

Discriminant Analysis (DA) is a multivariate statistical method that generates a set of classification functions that can be used to predict into which of two or more categories an observation is most likely to fall, based on a certain combination of input variables. DA may be more effective than regression for relating groundwater age to major ion hydrochemistry and well construction because it can account for complex, non-continuous relationships between age and each individual variable used in the algorithm while inherently coping with uncertainty in the age values used for calibration, and there is no need to

assume that the sites involved are within the same aquifer or even within the same catchment.

METHODS

The NGMP includes 112 long-term monitoring sites across New Zealand; four sites that are no longer included in the NGMP were also considered as part of this study. NGMP sites are situated in discrete aquifers (or on discrete flow lines in large aquifer systems) and are selected to encompass a range of aquifer lithology, confinement and surrounding land use that is representative of New Zealand aquifers in general. Median well depth is 26 m below ground surface (b.g.s.), and the minimum, lower quartile, upper quartile and maximum well depths across all NGMP sites are 3, 10, 55, and 337 m b.g.s., respectively.

Samples are collected quarterly on an on-going basis from each NGMP site according to a standardized protocol. Electrical conductivity, pH and temperature are measured in the field using portable meters, and three different types of samples are collected for laboratory analysis of various parameters. An unfiltered, unpreserved sample is analysed in the laboratory for alkalinity, conductivity and pH using an autotitrator. A filtered (0.45 µm) unpreserved sample is analyzed for Cl, Br, F, SO₄, NO₃-N and PO₄-P by ion chromatography, and for NH₄-N by automated phenohypochlorite method. A filtered, acid-preserved (HNO₃) sample is analyzed for Na, K, Ca, Mg, Fe, Mn and SiO₂ by inductively coupled plasma optical emission spectrometry. The length of the historical record differs for each NGMP site but on average covers a period of seven years.

Groundwater age at each NGMP site has been assessed using multiple tracers. Tritium was analyzed in a 1 L unfiltered unpreserved sample using 70-fold electrolytic enrichment prior to ultra-low level liquid scintillation spectrometry (Morgenstern & Taylor 2005). Samples for analysis of CFCs and SF₆ (125 ml and 1 L, respectively) were collected in strict isolation from the atmosphere and

analysed by gas chromatography using an electron capture detector (Busenberg & Plummer 1992; van der Raaij 2003). Dissolved Ar and N₂ concentrations were used to estimate the temperature at the time of recharge and the excess air concentration, which allowed calculation of the atmospheric partial pressure of CFCs and SF₆ at the time of recharge.

The convolution integral and the Exponential Piston Flow Model (EPM) were used to relate measured tracer concentrations to historical tracer input. The tritium input function is based on tritium concentrations measured monthly since the 1960s near Wellington, New Zealand. CFC and SF₆ input functions are based on measured and reconstructed data from southern hemisphere sites. The EPM was applied consistently in this study because statistical justification for selection of some other response function requires a substantial record of time-series tracer data which is not yet available for the majority of NGMP sites, and for those NGMP sites with the required time-series data, the EPM and other response functions yield similar results for groundwater age.

HCA and DA were conducted using log-transformed site-specific median concentrations of various parameters as described by Daughney & Reeves (2005) and Daughney *et al.* (2009). HCA was conducted with median concentrations of Br, Ca, Cl, F, Fe, HCO₃, K, Mg, Mn, Na, NH₄-N, NO₃-N, PO₄-P, SiO₂ and SO₄ using the Nearest-Neighbour and Wards linkage rules. DA was conducted using electrical conductivity, well depth, and the median concentrations of Ca, Mg, Na, K, HCO₃, Cl and SO₄.

CONCLUSIONS

The range of hydrochemistry encountered across the NGMP can be summarized by assigning each site to one of three categories (hydrochemical facies) defined via HCA. 32% of the NGMP monitoring sites are assigned to the *natural-fresh* category and are typified by oxic groundwater showing little or no evidence of human or agricultural impact. 42% of

the NGMP sites are assigned to the *impacted* category, and are also typified by oxic groundwater, but with evidence of some degree of human or agricultural impact in the form of above-background concentrations of NO₃-N, often co-occurring with elevated concentrations of Cl and/or SO₄. The level of impact observed at these sites is variable, with 15% of sites having median NO₃-N concentration above the guideline for safe human consumption (11.3 mg/L). The remaining 26% of the NGMP sites are assigned to the *natural-evolved* category and are typified by reduced (anoxic) groundwater, often with measurable concentrations of NH₄-N, dissolved Fe and/or dissolved Mn, and relatively high total dissolved solids concentrations.

Site-specific groundwater age values ranged from less than one year to more than 100 years, with the 25th, 50th and 75th percentiles being approximately 10, 40 and 100 years, respectively, across the entire NGMP. Classification functions derived from DA allowed assignment of 71% of the sites to the correct of four age categories (mean residence time ten years or less, 11 to 40 years, 41 to 100 years, or more than 100 years).

Groundwater age displays a generally expected relationship to well depth, but the age category cannot be predicted from well depth alone. In line with expectation, over all NGMP sites, well depth has a weak positive correlation to groundwater age, with the youngest and oldest age categories generally being associated with shallow and deep bores, respectively. However, shallow wells do not always tap young groundwater: there were a small number of NGMP sites at which groundwater from the oldest age category was found in a well less than 10 m deep. This situation occurred in both confined and unconfined aquifers, corresponding to upward-moving groundwater at the discharge end of a flow system.

Likewise, despite certain expected relationships between groundwater age and hydrochemistry, a particular site's groundwater age category cannot be predicted from its hydrochemistry alone.

For example, the older the groundwater is, the more likely it is to be assigned to the natural-evolved hydrochemical category. This is expected because the longer the groundwater is in the aquifer and isolated from the atmosphere, the more likely it is to become anoxic and to accumulate dissolved substances through water-rock interaction. However, only 85% of the NGMP sites assigned to the oldest age category display the natural-evolved hydrochemical signature, indicating that groundwater can remain oxic in some New Zealand aquifers for more than 100 years. Conversely, the natural-evolved hydrochemical signature is found at a small proportion (5%) of NGMP sites in the youngest age category, indicating that in some situations groundwater can become anoxic in less than a decade. Not surprisingly, this confirms that the rates of hydrochemical reactions are variable, as would be expected for aquifers with varied or mixed lithologies.

There is no significant partitioning of the different age categories between the natural-fresh and impacted hydrochemical categories. In other words, the number of sites having oxic impacted groundwater is always roughly equal to the number of sites with oxic unimpacted groundwater, regardless of groundwater age category. This implies that the impact of human and agricultural activity on New Zealand's groundwater quality is of similar extent over the last ten years as over the previous century.

ACKNOWLEDGEMENTS

The authors thank personnel from New

Zealand regional councils for assistance with sample collection. This research was funded by the New Zealand Foundation for Research, Science and Technology (Contract C05X0706).

REFERENCES

- BUSENBERG, E. & PLUMMER, L.N. 1992. Use of chlorofluorocarbons (CCl₃F and CCl₂F₂) as hydrologic tracers and age dating tools: the alluvium and terrace system of Central Oklahoma. *Water Resources Research*, **28**, 2257-2283.
- DAUGHNEY, C.J., MORGENSTERN, U., VAN DER RAAIJ, R., & REEVES, R.R. 2009. Groundwater age in New Zealand aquifers: Tracer measurements and age estimation from hydrochemistry. *Journal of Hydrology*, in press.
- DAUGHNEY, C.J. & REEVES, R.R. 2005. Definition of hydrochemical facies in the New Zealand National Groundwater Monitoring Programme. *Journal of Hydrology NZ*, **44**, 105-130.
- MORGENSTERN, U. & TAYLOR, C.B. 2005. Low-level tritium measurement using electrolytic enrichment and LSC. *Proc. Int. Symp. Quality Assurance for Analytical Methods in Isotope Hydrology. International Atomic Energy Agency*.
- VAN DER RAAIJ, R.W. 2003. *Age dating of New Zealand groundwaters using sulphur hexafluoride*. M.Sc. thesis, School of Earth Sciences, Victoria University of Wellington, New Zealand.
- Zuber, A., Witczak, S., Rózański, K., Śliwka, I., Opoka, M., Mochalski, P., Kuc, T., Karlikowska, J., Kania, J., Jackowicz-Korczyński, M., & Duliński, M. 2005. Groundwater dating with ³H and SF₆ in relation to mixing patterns, transport modelling and hydrochemistry. *Hydrological Processes*, **19**, 2247-2275.

Mineralogical characterization of arsenic, selenium, and molybdenum in uranium mine tailings

Joseph Essilfie – Dughan¹, M. Jim Hendry¹, Ingrid Pickering¹, Graham George¹,
Jeff Warner², & Tom Kotzer³

¹Department of Geological Sciences, University of Saskatchewan, 114 Science Place, Saskatoon, SK, S7N 5E2
CANADA (e-mail: jim.hendry@usask.ca)

²Canadian Light Source Inc. University of Saskatchewan 101 Perimeter Road Saskatoon, SK, S7N 0X4 CANADA

³ Cameco Corporation, 2121-11th Street West, Saskatoon, SK, S7M 1J3 CANADA,

ABSTRACT: High-grade uranium ores from northern Saskatchewan can contain high levels of arsenic (As), selenium (Se) and molybdenum (Mo). A critical environmental issue around the uranium mining industry is the long-term mobilization of As, Se and Mo from its tailings facilities to the nearby groundwater systems. Our goal is to identify and characterize the mineralogical compositions of these elements, and ultimately determine their long-term stability in the environment. In order to meet the objectives we are using synchrotron radiation based X-ray absorption spectroscopy (XAS) techniques along with electron microprobe analysis (EMPA). Bulk XAS is being used to study the oxidation state of these elements as well as their coordination environment, which will allow us to identify their speciation. Electron microprobe analysis (EMPA) and synchrotron-based micro-X-ray fluorescence mapping and absorption spectroscopy (μ XRF; μ XAS) are being employed to study the spatial distribution and speciation of the elements of concern (EOC) at the micron scale. Understanding of their speciation as well as their distribution will help determine the long-term stability of As, Mo and Se in the aqueous environment in the mine tailings.

KEYWORDS: *Mine tailings, Arsenic, Molybdenum, Selenium, XAS, EMPA*

INTRODUCTION

Uranium mill tailings in northern Saskatchewan can contain elevated levels of arsenic (As), molybdenum (Mo), and selenium (Se). Arsenic is a carcinogen, with exposure via drinking water shown to cause cancer of the bladder, lungs, skin, kidney, and liver in humans (USEPA 1998). Mo and Se are essential trace elements, but with potentially toxic effects at elevated concentrations (Barceloux 1999; Frankenberger & Benson 1994). A critical environmental issue in the U mining industry is preventing mobilization of these elements from tailings facilities and contamination of regional ground water systems. The toxicity and bioavailability of As, Mo, and Se are functions of their chemical form or speciation. Thus, identification of the speciation of these elements in the mine tailings is necessary to determine their mobility, transformation and complexation in the solid and aqueous state.

The objectives of this study are to use synchrotron-based spectroscopic techniques, as well as EMPA, to identify and characterize the mineralogical compositions of As, Mo, and Se in mine tailings, and ultimately assist in determining their long-term stability in tailings containment facilities.

XAS provides a powerful probe of both physical and electronic structure of an element within a sample, and has the ability to determine the molecular level speciation of As, Mo and Se over the concentration range of 50 μ g/g to several weight percent (typical of mine tailings solids) (Brown *et al.* 1998) at the micron to mm scale.

EPMA is a technique for chemically analysing small selected areas of solid samples, in which X-rays are excited by a focused electron beam. Spatial distribution of specific elements can be recorded as two-dimensional X-ray "maps" using either energy dispersive spectroscopy (EDS) or

wavelength-dispersive spectroscopy (WDS). The spatial scale of analysis, combined with the ability to create detailed images of the sample, allows analyses of fine-grained geological materials such as mine tailings. (Reed 1996).

The accurate identification of As-, Mo-, and Se-bearing minerals in the tailings, as well as their distribution will help elucidate the source chemistry for these potential contaminants. This will facilitate characterization and quantification of the long-term migration of metals, oxyanions and metalloids from mine tailings facilities to adjacent groundwater systems. The information will also ultimately aid in the design of facilities aimed at minimizing migration of these elements into groundwater long after decommissioning.

METHODS AND RESULTS

Methods

Four uranium mine tailing samples (collected during the DTMF 2004/2005 drilling program) were selected based on the concentrations of EOC (As, Mo, and Se) as well as redox potential. Standard reference compounds to aid in the identification of the speciation of As, Mo and Se in the mine tailings were also selected based on previous studies in literature and potential mineral phases identified during diagnostic equilibrium modelling (using PHREEQC; Parkhurst & Appelo 1999; Charlton & Parkhurst 2002) using pore water chemical data from the tailings. Both samples and standard reference compounds were prepared using Kapton® tape over a Teflon® sample holder. Arsenic, Mo and Se K-edge X-ray Absorption Near Edge Spectroscopic (XANES) data was collected on both samples and standards using a hard x-ray beamline (HXMA - 06ID-1) at the Canadian Light Source, University of Saskatchewan (CLS) and solid state Germanium and Vortex detectors. Extended x-ray absorption fine structure (EXAFS) was collected where possible, depending on elemental concentrations. Data collected are currently being analysed using EXAFSPAK (George & Pickering 1995)

and IFFEFIT (Ravel & Newville 2005)

Four samples were similarly selected for the EPMA experiments. The samples were dried and embedded in polished epoxy cylindrical plugs. Backscattered electron (BSE) images as well as elemental maps of As, Fe and Ni (EDS/WDS) were collected using a JEOL 8600 Superprobe electron microprobe analyzer (Dept. of Geological Sciences, University of Saskatchewan).

Results

For As, Mo, and Se all samples displayed well-defined absorption edges, identified by the sharp increase in absorption over a 10 eV interval. The position of the absorption edge is sensitive to the oxidation state of the absorbing atom and thus has been used to determine the oxidation state of As, Mo, and Se in the mine tailings.

Comparison of As K edge absorption spectra for tailings and reference compounds of known oxidation states shows that arsenate (As^{5+}) is the dominant

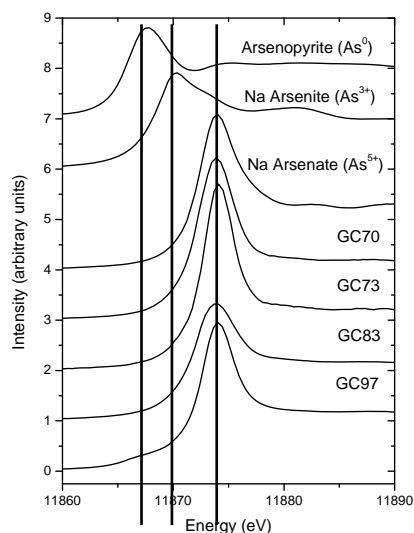


Fig. 1. X-ray absorption near-edge structure (XANES) of reference compounds with various As valence states and mine tailings samples. The As K-edge excitation potential for arsenic in the ground state (As^0) is at 11868 eV. The As K-edge excitation potential increases with increasing valence state.

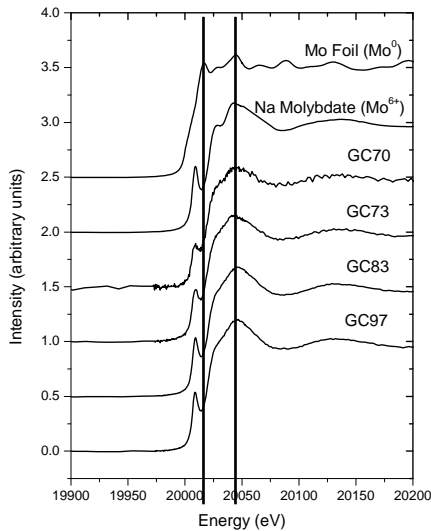


Fig. 2. X-ray absorption near-edge structure (XANES) of reference compounds with various molybdenum valence states and mine tailings samples. The Mo K-edge excitation potential for molybdenum in the ground state (Mo^0) is at 20000 eV. The Mo K-edge excitation potential increases with increasing valence state.

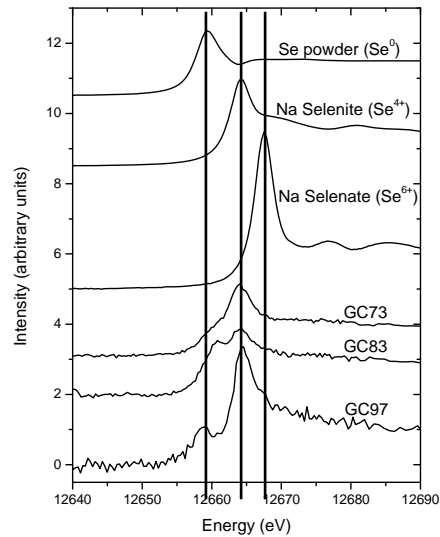


Fig. 3. X-ray absorption near-edge structure (XANES) of reference compounds with various Se valence states and mine tailings samples. The Se K-edge excitation potential for Se in the ground state (Se^0) is at 12658 eV. The selenium K-edge excitation potential increases with increasing valence state.

form of arsenic in the mine tailings (Fig. 1).

Similarly, comparison of the Mo K edge absorption spectra for tailings and reference compounds of known oxidation states (Fig. 2), shows that Mo^{6+} is the dominant form of molybdenum in the mine tailings. The characteristic pre-edge feature in the near edge spectra indicates that Mo in the tailings occurs mostly as a molybdate.

For Se (Fig. 3), comparison of the Se K edge absorption spectra for tailings relative to reference compounds of known oxidation states shows that selenite (Se^{4+}) was the dominant form of selenium in the mine tailings, along with a considerable amount of reduced Se species (selenide: S^0). These analyses are continuing to further determine the complexation mechanism for selenide and selenite present in the tailings.

Least squares fitting of the near edge spectra of the tailings to that of the standard reference spectra is currently underway to establish the chemical

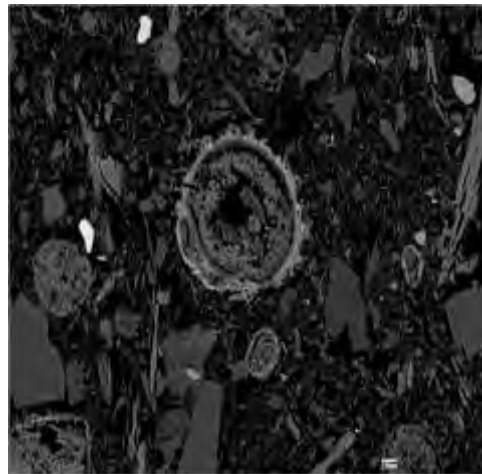


Fig. 4. BSE image of mine tailings showing the presence of gypsum nodules with bright rims around them.

complexation or mineralogy of the tailings with respect to As, Mo, and Se.

Electron microprobe analyses of the mine tailings samples (BSE image –Fig. 4) show the presence of notable nodule-like features with bright rims around them.

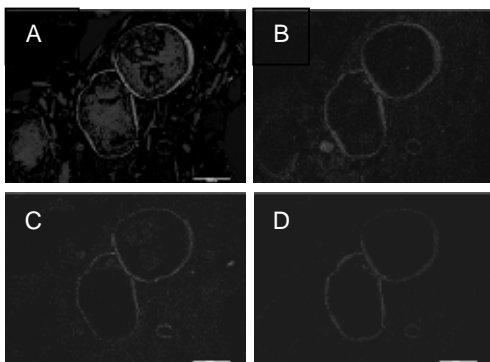


Fig. 5. BSE image of gypsum node (A) and elemental maps of As (B), Fe (C), and Ni (D).

Elemental x-ray maps (EDS) indicate the nodules are mainly Ca and S (i.e. gypsum) whereas surrounding rims mainly consist of As, Fe, and Ni (Fig. 5).

Concentration levels of Mo and Se in the tailings were below the detection limit (~ 100 ppm) of the instrument.

Although the EMPA technique provides spatial distribution information on elements of concern, it does not provide any information with regards to their chemical speciation and detailed complexation. The use of synchrotron focused-beam spectroscopy (μ XAS) and elemental mapping (μ XRF) is currently being explored at the CLS using VESPERS (07B2-1) and HXMA (06ID-1) hard x-ray beamlines. This technique will not only provide information spatial distribution of the elements of concern but their chemical form (speciation/complexation) as well, which is essential in predicting their solubility, mobility and toxicity.

ACKNOWLEDGEMENTS

The authors acknowledge the Cameco Corporation and the Cameco-NSERC Industrial Research Chair for financial

support. The authors also thank Tom Bonli Industrial Research Chair for financial support. The authors also thank Tom Bonli for his assistance in the EMPA work.

REFERENCES

- BARCELOUX, D.G. 1999. Molybdenum. *Journal of Toxicology- Clinical Toxicology*, **37**, 231-237.
- BROWN, G.E., FOSTER, A.L., & OSTERGREN, J.D. 1998. Mineral surfaces and bioavailability of heavy metals: A molecular-scale perspective. *Proceedings of the National Academy of Sciences of the United States of America*, **96**, 3388-3395.
- CHARLTON, S.R. & PARKHURST, D.L. 2002. PHREEQC-A computer program for speciation, reaction-path, advective transport, and inverse geochemical reactions. *U.S. Geological Surveys Water-Resources Investigations*, **95-4227**.
- FRANKENBERGER, W.T. JR. & BENSON, S.M. (eds.). 1994. *Selenium in the Environment*, Marcel Dekker, Inc., New York.
- GEORGE, G.N. & PICKERING, I.J. 1995. EXAFSPAK: a Suite of Computer Programs for Analysis of X-ray Absorption Spectra. *Stanford Synchrotron Radiation Laboratory*, Stanford, CA, USA.
- PARKHURST, D.L. & APPELO, C.A.J. 1999. *User's guide to PHREEQC (Version 2)—A computer program for speciation, batch-reaction, one-dimensional transport, and inverse modeling*.
- RAVEL, B. & NEWBILLE M. 2005. ATHENA, ARTEMIS, HEPHAESTUS: data analysis for X-ray absorption spectroscopy using IFEFFIT *Journal of Synchrotron Radiation*, **12**, 537-541.
- REED, S.J.B. 1996. *Electron Microprobe Analysis and Scanning Electron Microscopy in Geology*. Cambridge University Press.
- USEPA (UNITED STATES ENVIRONMENTAL PROTECTION AGENCY) 1998. *Arsenic in drinking water: Arsenic Research Plan*; Office of Water.

Spatial and temporal evolution of Cu-Zn mine tailings while dewatering

D. Jared Etcheverry¹, Barbara L. Sherriff¹,
Nikolay Sidenko^{1,2}, & Jamie VanGulck³

¹ Department of Geological Sciences, University of Manitoba, Winnipeg, MB, R3T 2N2 CANADA
(email: jared.etccheverry@gmail.com)

² TetreES Consultants Inc., Winnipeg, MB, R3C3R6 CANADA

³ Arktis Solutions Inc. 186 Steepleridge St., Kitchener, ON, N2P2V1 CANADA

ABSTRACT: The Ruttan Cu-Zn mine produced ~30 mT of fine-grained tailings over 30 years. Since the closure of the mine in 2002, the tailings have been systematically dewatered through trenches draining into the open pit and underground workings. This study evaluated the evolution of the reduced tailings, which were underwater until 2002, and also tailings that had been exposed to oxidizing conditions for more than 20 years. The mining process removed most of the sphalerite and chalcopyrite leaving the tailings dominated by pyrite and pyrrhotite. In oxidized tailings, there was extensive alteration of pyrrhotite, and sphalerite but only slight alteration of pyrite. There is very little carbonate to buffer the acidity.

Dewatering the submerged tailings resulted in changes in acidity of pore and shallow groundwater from rapid oxidation of fine grained sulfides. Depth profiles of metal concentrations in dissolved and solid fractions suggest that the tailings are in an early stage of oxidation and that these tailings will produce low pH, metal-laden water for years to come. Hydrated sulphate evaporite minerals formed during dry periods on the surface of the tailings providing a temporary storage for metals that are released during spring runoff and rain events.

KEYWORDS: Cu-Zn tailings, acidification, oxidation, dewatering, geochemistry

INTRODUCTION

From 1973 until 2002, Sherritt Gordon Mines Ltd. and later Hudson Bay Mining and Smelting, extracted copper and zinc ore from volcaniclastic and siliciclastic sequences of the Rusty Lake Greenstone Belt at the Ruttan Mine near Leaf Rapids, Manitoba, Canada.

Flotation refinement of the ore at the Ruttan Mine produced over 30 million tons of fine-grained sulfide rich tailings, some of which were submerged in retention ponds (Fig. 1). Since mine closure, there has been a systematic dewatering of the tailings ponds to allow for more geotechnically stable tailings pile dams. At the time of this study, 2004 and 2005, much of the surface tailings remained in a reduced state due to relatively wet conditions. However, parts of the tailings have been exposed to the atmosphere and oxidizing for many years.

Dewatering of the Ruttan tailings offered the opportunity to observe potentially acid generating tailings as they enter oxidizing



Fig. 1. Map of Ruttan mine site showing the drainage trenches in the tailings and flow direction of drainage water.

conditions in a natural setting. The subarctic climate of this region, coupled with the exposure of reduced tailings to oxidizing conditions set this project apart from similar studies.

METHODOLOGY

Samples of pore water, ground water, surface water and solid tailings were

obtained from similar locations in 2004 and 2005.

Samples of groundwater were obtained from piezometers installed at various locations throughout the tailings. Groundwater was retrieved using a baler. Pore water was squeezed from samples of solid tailings. All water samples were analysed for cations, anions, Eh and pH.

The piezometers were also used to estimate the hydraulic conductivities of the tailings. The Seep/WTM software package, was used to model the flow from the tailings into the drainage trenches.

Solid tailings were collected from test-pits and auger cuttings from boreholes in both the oxidized and reduced tailings. The tailings were analyzed for total metals. Sequential extraction of the tailings allowed the mobility of the metals to be assessed. Evaporites were also collected from the surface of the tailings.

The minerals of the solid tailings and evaporites were assessed qualitatively with X-ray diffraction, optical, and scanning electron microscopy.

RESULTS

Field Observations

Despite excessively wet conditions encountered in 2005, increases in the level of oxidation in the reduced tailings were observed since 2003. Visible changes were observed <15 cm depth.

In 2003 and 2004, oxidation was patchy as a change of colour from dark grey to orange-brown. The oxidation was usually restricted to one to two centimeter halos along vertical and horizontal cracks. Below 20 cm, the tailings were unoxidized. In 2005, the entire surface was oxidized and the halos of oxidation extended from the cracks, to almost completely oxidize the upper 15 cm. Below 20 cm, the tailings remained unoxidized.

Solid Tailings

The reduced tailings were found to be comprised of 20-30 % sulfides, and 70-80% gangue minerals and very fine-grained unidentifiable material. Sulfides were 50 -75 % pyrite, 30-40 % pyrrhotite, <5 % chalcopyrite, and <5 % sphalerite.

Gangue constituents included quartz, muscovite, biotite, chlorite, and pyroxene.

In the oxidized tailings, pyrrhotite and sphalerite (Fig. 2) show the most alteration with both minerals being surrounded by iron oxyhydroxides. Pyrite is relatively unaltered.

Chalcopyrite is also unaltered but by virtue of being armored within quartz.

Total metal concentrations in the reduced tailings varied for Fe (18-25 wt. %), Zn (0.2-0.5 wt. %), and Cu (0.03-0.09 wt. %). Similar concentrations were also measured in the oxidized tailings: 17-28 wt. % Fe, 0.04-0.44 wt. % Zn, and 0.03-0.10 wt. % Cu.

White and yellow evaporite minerals form thin crusts on the surface of and within fissures in the tailings. XRD analyses identified the hydrated iron sulphates, melanterite ($\text{FeSO}_4 \cdot 7\text{H}_2\text{O}$), Zn-melanterite ($(\text{Zn,Fe})\text{SO}_4 \cdot 7\text{H}_2\text{O}$), halotrichite ($\text{FeAl}_2(\text{SO}_4)_4 \cdot 22(\text{H}_2\text{O})$) and rozenite ($\text{FeSO}_4 \cdot 4\text{H}_2\text{O}$) (Alpers *et al.* 2000).

Sequential extraction showed that, for both reduced and oxidized tailings, most of the total Fe (75-85%) is in the residual phase with most of the remainder in the iron-hydroxide phase. Less than 1% Fe is in the mobile adsorbed-exchangeable-carbonate and water soluble phases in both reduced and oxidized tailings.

Zinc is primarily split between the residual (30-50%), water soluble (24-30%) and iron-hydroxide (20-28%) phases with

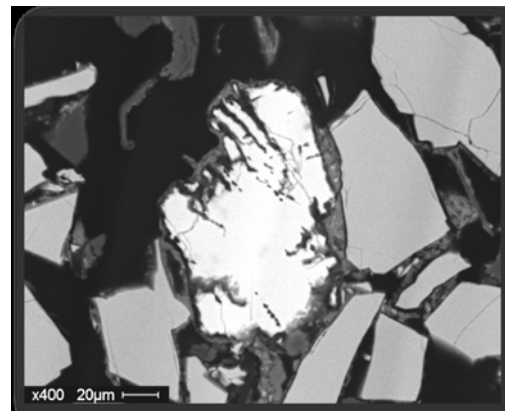


Fig. 2. SEM images of oxidized tailings showing altered sphalerite (white) with unaltered pyrite (light grey).

4-8% mobile in adsorbed-exchangeable-carbonate phases. There were higher percentages in the residual and iron hydroxide phases for the reduced than the oxidized tailings.

Copper was shown to be much more mobile with about 28% total Cu being water soluble or easily extractable: 40-50% in iron hydroxide phases and only about 20-30% in the residual.

There was no significant difference in sequential extraction results between 2004 and 2005. The only significant difference with depth was an increase in Fe-hydroxides near the surface.

Pore Water

The composition of pore water was similar in reduced and oxidized tailings with low pH (>1.8) and high total dissolved solids (~300 g/L) at the surface, and neutral pH and lower dissolved solids with depth. In general, pH values were lower and dissolved metal concentrations higher in 2005 than 2004.

In 2004, the pH of pore water in the reduced tailings was 4.4 at <10 cm depth, increasing to ~7 by 30 cm. Dissolved constituents follow pH, with concentrations of 36,000 ppm SO₄²⁻, 18,000 ppm Fe, and 9,600 ppm Zn at <10 cm depth. These concentrations decrease steadily with depth. Below 30 cm, most metals drop to below detection limits.

In 2005, concentrations of metals increased, with the highest concentrations between 10 and 20 cm depth: 47,000 ppm Fe, 290,000 ppm SO₄²⁻ and 1.9 ppm Cu.

Ground Water

There was a drastic change in groundwater composition from 2004 to 2005. Water within the reduced tailings went from 1 to 800 ppm Fe and 0.2 to 1.3 ppm Zn. The pH values decreased over the same time period from 6.9 to 3.5.

Surface Water

All mine surface water in direct contact with the tailings is characterized by low pH (2.0-3.5) and a large amount of dissolved solids (1,400-17,000 ppm TDS). Average concentrations of elements in solution

include 7,100 ppm SO₄²⁻, 1,200 ppm Fe, 11 ppm Cu and 180 ppm Zn. The highest TDS were measured in standing pools associated with the least oxidized tailings.

Water Flow Modeling

A flow model, created with the Seep/WTM software, indicated that the trench influences groundwater movement within an area of approximately 25 m, with the fastest flows closest to the trench. Flow rates within the tailings increase towards the trench with maximum flow of 1.2x10⁻⁷ m/s across the tailings/trench interface. Over a 10 m section this flow rate relates to about 10⁻⁵ m³/s of groundwater, entering the trench.

DISCUSSION

The objective of this study was to document changes in Cu-Zn tailings during one year of exposure to oxidizing conditions. The primary factor affecting the rate of tailings acidification is the primary mineralogy.

The tailings comprise 5-10 wt. % pyrrhotite; a highly reactive sulfide mineral that releases protons and Fe³⁺ into adjacent pore waters on oxidation. Further, the concentration of carbonate minerals in the tailings is low providing little buffering capacity above pH 5. Therefore, the tailings continued to acidify until they reach the pH of Al(OH)₃ (pH 4-4.5) and Fe(OH)₃ (pH 2.5-3.5) buffering.

As the reduced tailings continue to de-water and the water table drops, it is expected that oxygen will continue to diffuse deeper into the tailings creating a deepening zone of oxidation. Modeling shows that sulfide-rich tailings with a deep water table can oxidize for centuries (Blowes & Jambor 1990).

The conditions at Ruttan can be compared with Blowes *et al.* (2003) model of the geochemical evolution of tailings as the tailings oxidize. This suggests that much of Ruttan tailings are still in the early to moderate stage of oxidation. In both the reduced and oxidized tailings, there is at least a minor depletion in solid metal concentrations at the surface and a peak in dissolved metal concentrations just

below the top of the tailings. Pore water metal concentrations do not increase with depth; rather, they peak within the first meter of the tailings, further suggesting a juvenile oxidation stage.

Modeling the water flow through the tailings shows that the majority of the metal leaving the tailings is presently coming from surface runoff and dissolved evaporites rather than from the body of the tailings as seepage to the trenches.

CONCLUSIONS

The purpose of this study was to record the state of the Ruttan tailings during its early stages of oxidation and to observe changes in the tailings from one year to the next. Further, the presence of already oxidizing tailings at the site allowed a comparison between tailings at different stages of oxidation. Anomalous precipitation events in 2005 may have affected the data, however it is clear that the depth of oxidation in the reduced tailings increased and became more pervasive over the course of one year. A very fine grained fraction in the reduced tailings contributed to this rapid oxidation.

Respective weathering rates of sulfide minerals is pyrrhotite/sphalerite>pyrite. The buffering capacity of the tailings is low due to the lack of carbonates, allowing the rapid onset of low pH conditions.

Metals are temporarily attenuated as evaporite minerals on the surface or in secondary oxides and hydroxides in the tailings. The evaporites will re-dissolve in wet weather conditions and the secondary minerals become unstable with acidification of the tailings releasing these metals into the environment.

Large volumes of tailings and slow drainage conditions will lead to ARD conditions at this site for many years.

ACKNOWLEDGEMENTS

Funding for this project was provided by the Sustainable Development Initiatives Fund of Manitoba and the Natural Sciences and Engineering Research Council of Canada. Neil Ball, Sergio Mejia, and the late Gregg Morden provided assistance with geochemical and mineralogical analyses at the Department of Geological Sciences at the University of Manitoba. We thank Benjamin Edirmanasinghe and Ernie Armitt. Manitoba Mines Branch and Frank Bloodworth, Ruttan Mine for logistical support.

REFERENCES

- ALPERS, C.N., JAMBOR, J.L., & NORDSTROM, D.K. 2000. Sulfate Minerals: Crystallography, Geochemistry, and Environmental Significance. *Mineralogical Society of America, Geochemical Society: Reviews in Mineralogy and Geochemistry*, **40**, Washington, DC.
- BLOWES, D.W. & JAMBOR, J.L. 1990. The pore-water geochemistry and the mineralogy of the vadose zone of sulfide tailings, Waite Amulet, Quebec, Canada. *Applied Geochemistry*, **5**, 327-346.
- BLOWES, D.W., PTACEK, C.J., & JAMBOR, J.L. 2003. Mill Tailings: Hydrology and Geochemistry. Environmental aspects of Mine Waste. *Mineralogical Association of Canada Short Course series* **31**, 95-116.
- ETCHEVERRY, D.J. 2009. *Spatial and Temporal Variations in the Ruttan Mine Tailings, Leaf Rapids, Manitoba, Canada*. M.Sc. thesis, University of Manitoba, Winnipeg, Manitoba.

Adding value to Kinetic Testing Data II – Interpretation of waste rock humidity cell data from an exploration perspective at the Adanac Molybdenum Corporation, Ruby Creek Molybdenum Project, BC, Canada

David R. Gladwell¹ & Catherine T. Ziten¹

¹*Wardrop Engineering Inc., 900 – 330 Bay Street, Toronto, ON, M5H 2S8 CANADA
(david.gladwell@wardrop.com)*

ABSTRACT: Kinetic testing is usually applied in predicting the environmental impact of mining activities, however, this data may also be useful in geochemical exploration. Data is presented from kinetic testing of quartz monzonitic waste rock from the Adanac Molybdenum Corporation, Ruby Creek Project. XRD and petrological studies were used to define sample mineralogy, which includes mica, plagioclase, quartz, molybdenite, pyrite, chalcopyrite and minor clay minerals. PHREEQC computer software was used to compute the equilibrium concentrations of ionic species in leachate according to ion pair theory. Consideration of the sample mineralogy and aqueous geochemistry allowed delineation of periods of sulfide oxidation. The observed reaction products provide a suite of potentially anomalous elements which are confirmed by groundwater and surface water geochemistry in the vicinity of the mineralized monzonitic stock. Kinetic data are expensive to acquire; the case history data presented demonstrates that careful data interpretation maximizes return on this investment.

KEYWORDS: *Kinetic Testing, Waste Rock, Aqueous Speciation, PHREEQC, Molybdenum, Exploration*

INTRODUCTION

Geochemical exploration and environmental geochemistry are typically not carried out in tandem despite the fact that some data is common to both tasks. This paper examines the potential for using kinetic data collected for environmental purposes in combination with groundwater and surface water geochemistry to enhance the understanding of processes that may be exploited by the exploration geochemist. Kinetic tests are commonly used to predict whether waste rock or tailings will produce acid mine drainage (AMD) and are a precursor to environmental certification and are therefore a critical step in mine development. Kinetic tests are carried out using an elutriated cell or column that are typically operated over a period of about 1 year in carefully controlled laboratory conditions. Kinetic (or humidity cell) testing is a standard protocol (ASTM, 2001) involving periodic rinsing of tailings samples over time to remove all reaction

products that have accumulated following the previous rinsing. The results of kinetic tests provide indication of how waste rock (or tailings) will behave over time with the onset of oxidation, assist in calculating oxidation rates, mineral reaction rates, and with respect to prediction of acid generation facilitate estimation of the rate of NP depletion and the period when AMD is likely to commence (Richie 1994; Day *et al.* 1997; Price *et al.* 1997; Frostan *et al.* 2002; Howell & Parshley 2005; Ardaul *et al.* 2008).

This paper outlines a novel approach to maximising the value of kinetic data by combining mineralogy, aqueous geochemistry and kinetic test data to design ground and surface water exploration programs. The approach is tested on environmental data collected by Adanac Molybdenum Corporation at the Ruby Creek Molybdenum project, Atlin, BC, Canada.

RUBY CREEK MOLYBDENUM PROJECT

The Ruby Creek Molybdenum project is located east of Atlin, British Columbia, Canada. Molybdenum mineralization underlies the valley floor near the headwaters of Ruby Creek, (MacLeod 2007). The host plutonic rocks are generally classified as quartz monzonites although sufficient variation exists to distinguish three phases of magma intrusion. The host intrusion, which includes the contact phase between the Cretaceous Fourth of July and Surprise Lake batholiths consists of a highly variably textured unit that grades from “coarse-grained quartz monzonite” (CGQM) south of the Adera fault through a number of texturally transitional phases. North of the molybdenum deposit’s bounding fault (Adera fault) is a quartz monzonite with fewer quartz and feldspar phenocrysts (SQFP or “sparse quartz feldspar porphyry”), containing a higher proportion of pyrite leading to local gossan development at surface. The Mo mineralization is generally confined to fractures in quartz monzonite south of the Adera fault. Kinetic data from three lithologies were examined: an SQFP sample from north of the fault; a CGQM sample with low Mo content and; a sample of low grade molybdenite ore (LGO) from south of the fault. These lithologies were tested in humidity cells HC2, HC3 and HC6 respectively.

MINERALOGY/PETROGRAPHY

The mineral assemblages were determined using standard XRD (with Reitveld refinement) and petrographic procedures. Sample HC2 (SQFP) was found to contain quartz (35%), orthoclase (50%), anorthitic plagioclase (12%), muscovite/sericite (1.5%), kaolinite (0.3%) and pyrophyllite (0.9%) together with trace quantities of pyrite, chalcopyrite, marcasite and magnetite. Sample HC3 (CGQM) was found to contain quartz (45%), orthoclase (33%), Ca-rich plagioclase (15%), muscovite/sericite (6.6%) with minor kaolinite and limonite. Petrographic and XRD studies did not find any molybdenite in HC3 although three

repeat analyses yielded 180, 7.3 and 7.9 mg/kg Mo, illustrating a typical nugget effect. HC6 contained a sample of low grade Mo ore (<0.04 % Mo). Petrology for HC6 was not reported although carbonate minerals were found by acid digestion and ICP-MS analysis to be typically very low or absent in these lithologies.

KINETIC TEST DATA

Gladwell and Ziten (2009) have demonstrated that PHREEQC computer modelling of ion pairs in kinetic test leachate may be used to delineate periods of testing when sulfides are oxidizing. Figure 1 demonstrates this approach to kinetic test data from HC3 (CGQM) illustrating a period of sulfide oxidation from approximately weeks 37 to 54. $Al(OH)_2^+$ is also high during sulfide oxidation, probably reflecting reaction of Ca-rich plagioclase with the leachate.

This methodology allowed periods of sulfide oxidation to be identified in all three sets of kinetic test data.

Median leachate water chemistry during periods of sulfide oxidation was calculated for each parameter analyzed, by humidity cell. These data, for parameters that show distinct variation between cells, are presented as Table 1. HC2-SQFP, which contains more pyrite and very low carbonate content, rapidly generates acidic leachate causing its leachate to be higher in all parameters except Mo.

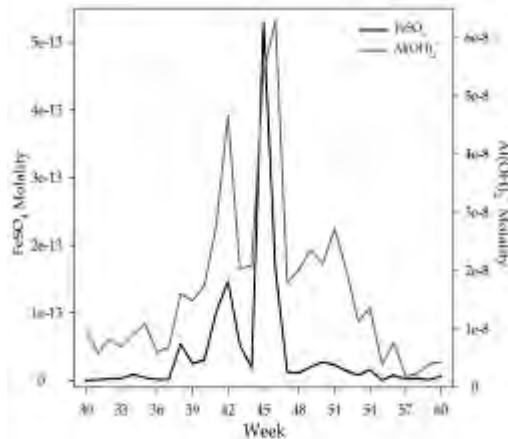


Fig. 1. Distribution of $FeSO_4$ and $Al(OH)_2^+$ for weeks 30 to 60 from humidity cell 3 (HC3-CGQM).

Table 1. Humidity cell data (mg/L) showing variation between periods of sulfide

oxidati	pH	Alkalinity	SO ₄	F	Al	Ba	Be	Cd	Ca	Co	Cu
HC2-SQFP	5.2	1.2	22	9.4	2.8	0.017	0.0036	6.E-04	6.8	0.0033	0.0082
HC3-CGQM	6.2	3.1	1	0.3	0.039	0.0004	0.0001	2.E-05	0.6	0.0001	0.0018
HC6-LGO	7.3	10	3	0.57	0.027	0.0077	4.1E-05	8.E-06	2.06	4.1E-05	0.00037
	Pb	Li	Mg	Mn	Mo	Ni	K	Si	Sr	U	Zn
HC2-SQFP	0.0011	0.0021	0.36	0.980	5.E-05	0.0007	0.98	4.2	0.015	0.14	0.098
HC3-CGQM	0.0004	0.0004	0.06	0.005	0.17	0.0001	0.55	1.3	0.0025	0.001	0.003
HC6-LGO	4.1E-05	0.001	0.01	0.004	4.E-03	4.1E-05	0.2	0.3	0.0084	0.002	0.00062

HC3-CGQM is slightly elevated in Mo and HC6-LGO shows much higher Mo in leachate from kinetic testing. Alkalinity and Mo are the only parameters which are higher in the molybdenite bearing (HC3-CGQM and HC6-LGO) samples

Since the SQFP sample outcrops for a significant portion of the Ruby Creek drainage area, it seems reasonable to expect elevated SO₄, Al, Ba, Cd, Ca, Co, Cu, Pb, Li, Mg, Mn, Ni, K, Si, Sr, U and Zn in ground and surface waters within the watershed. These high concentrations will not reflect the presence of ore, however, rather just the presence of natural acid rock drainage (Lett & Jackaman 1995). The kinetic testing shows that only the presence of elevated Mo in ground and surface waters within the watershed is likely to reflect the presence of molybdenum mineralization. Examination of the kinetic test data, collected for environmental purposes, thus allows prediction of useful parameters for an exploration survey sampling ground or surface water media.

GROUNDWATER SURVEY DATA

Groundwater samples were collected at a series of groundwater springs and artesian wells in the project area through 2004 and 2005 (MacLeod 2007). Groundwater data (Table 2) is grouped into two categories; one for background (BACK) sample sites (n=10); and the second are samples close to the area of molybdenum mineralization (MINER) (n=15). Median concentrations for parameters that were significantly (p=0.95) different between the two groups are presented in Table 2. Clearly, the predicted multi-element signature of HC2-SQFP is in fact observed in groundwater

data in the Ruby Creek watershed. In addition, the predicted elevated Mo levels reflecting the presence of molybdenum mineralization were also observed in groundwater data.

SURFACE WATER DATA

Surface water samples were also collected at a number of sites throughout the Ruby Creek watershed although only data collected from active stream flow were utilized here. The surface water data was also categorized into background areas (n=13) and sites downstream from mineralization area (n=21).

Median concentrations for parameters that were significantly (p=0.95) different between the background and mineralized surface water samples are presented in Table 2 under the surface water heading. There are fewer significant differences between surface water compared to ground water parameters. Be, Co, and Pb are anomalous in ground but not in surface water. This may simply be due to dilution by runoff. Both the SQFP multi-element suite associated with natural ARD and the high Mo concentrations associated with mineralization clearly persist into surface water.

CONCLUSIONS

Detailed interpretation of kinetic test data collected for environmental purposes has allowed criteria for ground and surface water geochemical exploration to be selected. Parameters predicted from kinetic testing to be anomalous in both ground and surface waters were observed to occur reflecting the presence of both molybdenum mineralization and natural acid rock drainage. Kinetic testing is very expensive and careful use of the acquired

Table 2. Significant differences between median (mg/L) background (BACK) and mineralized(MINER) area in ground and surface water in the Ruby Creek Watershed (p=0.95)

	Groundwater		Surface Water	
	BACK	MINER	BACK	MINER
pH	7.57	7.36	7.48	7.15
Alka	22	5.6	36.1	8.3
SO ₄	9.1	17.8	6.7	9.76
F	0.66	0.965	0.1	0.511
Al	0.012	0.1	0.014	0.048
Ba	0.00054	0.0097	0.0051	0.005
Be	0.00003	0.00025	-	-
Cd	0.00003	0.00012	0.00003	0.00012
Ca	6.6	9.12	6.89	4.84
Co	0.00005	0.0001	-	-
Cu	0.00073	0.00069	0.00099	0.001
Pb	0.00003	0.00005	-	-
Mg	2.29	0.79	6.67	1.49
Mn	0.00044	0.0019	0.00061	0.00096
Mo	0.0087	0.05	0.00034	0.024
Ni	-	-	0.0051	0.00094
Si	5.63	3.11	4.31	3.34
Sr	0.018	0.034	0.0152	0.0194
U	0.0013	0.0004	0.0001	0.0003
Zn	0.0013	0.005	0.0027	0.0055
As	0.0051	0.0016	0.002	0.0018

data in geochemical exploration adds considerable value to the investment.

ACKNOWLEDGEMENTS

The authors acknowledge the assistance and encouragement of Wardrop Engineering Inc. as they analysed the data and prepared this paper.

REFERENCES

ARDAU, C., BLOWES, D.W., & PTACEK, C.J. 2009. Comparison of laboratory testing protocols to field observations of the weathering of sulfide-bearing mine tailings. *Journal of Geochemical Exploration*, **100**, 182-191.
 BOWELL, R.J. & PARSHLEY, J.V. 2005.

Mineralogical controls on Pit Lake geochemistry, summer Camp Pit. Nevada. *Chemical Geology*, **215**, 373-385.
 DAY, S.J., HOPE, G., & KUIT, W. 1997. Waste rock management planning for the Kudz Ze Kayah project, Yukon Territory: 1. Predictive Static and Kinetic Test Work. *Proceedings of the 4th International Conference on Acid Rock Drainage*. Vancouver, I, 81-98.
 FROSTAD, S., KLEIN, B., & LAWRENCE, R.W. 2002. Evaluation of laboratory kinetic test methods for measuring rates of weathering. *Mine Water and the Environment*, **21**, 183-192.
 GLADWELL, D.R. & ZITEN, C.T. 2009. Adding Value to Kinetic Testing Data I-Interpretation of Tailings Humidity Cell Data from the Perspectives of Aqueous Geochemistry and Mineralogy at the Crowflight Minerals, Bucko Lake Nickel Project. In: *24th International Applied Geochemistry Symposium*, Fredericton (this volume).
 LETT, R.E. & JACKAMAN, W. 1995. Application of spring-water chemistry to exploration in the Driftpile Creek area, North-eastern British Columbia. *British Columbia Ministry of Energy, Mines and Petroleum Resources, Geological Fieldwork, 1994*, **1995-1**, 269-275.
 MACLEOD, M. 2007. Ruby Creek Molybdenum Project "Environmental Assessment Certification Application" http://a100.gov.bc.ca/appsdata/epic/html/deploy/epic_document_258_22610.html
 PRICE, W.A., MORIN, K.A., & HUTT, N.M. 1997. Guidelines for the prediction of acid rock drainage and metal leaching for mines in British Columbia: Part II. Recommended procedures for static and kinetic testing. In: *Proceedings of the 4th International Conference on Acid Rock Drainage*. Vancouver, I, 15-30.
 RITCHIE, A.I.K. 1994. Sulphide oxidation mechanisms—controls and rates of oxygen transport. In: ALPERS, C.N. & BLOWES, D.W. (eds.), *Environmental Geochemistry of Sulphide Oxidation*, ACS Symposium Series 550. Washington DC.

Alteration of sulfides within an open air waste-rock dump: Application of synchrotron μ -XRD, μ -XRF, and μ -XANES analyses

Pietro Marescotti¹, Cristina Carbone¹, Gabriella Lucchetti¹, & Emilie Chalmin²

¹DIP.TE.RIS. - Università di Genova, C.so Europa, 26, I-16132 Genova ITALY
(e-mail: marescot@dipeteris.unige.it)

²European Synchrotron Radiation Facility, Grenoble FRANCE

ABSTRACT: We have applied a combination of synchrotron-based techniques (μ -XRD, μ -XRF, and μ -XANES) to determine the mineralogy and the elemental distribution of metals in partially altered sulfide-mineralization fragments deposited within an open-air waste-rock dump (Libiola mine, eastern Liguria, Italy). In this dump AMD processes are active and intense and sulfide-mineralized clasts progressively undergo oxidation originating centimetric-thick hardpans cemented by secondary iron oxides and oxyhydroxides. Selected samples, containing the transition from unaltered sulfides to secondary oxidation products have been analyzed along several millimetric transects. The results evidenced that sulfides (pyrite + chalcopyrite \pm sphalerite) oxidation starts from the crystals rims or from intra-grain microfractures. Sulfide-S firstly oxidizes to sulfate and then is rapidly leached out from the system. The altered layers are composed almost exclusively of Fe-oxides (hematite) and -oxyhydroxides (goethite and minor bernalite) that replace sulfides and fill intra- and inter-grain interstices. Elemental maps and μ -XRF transects evidenced that these secondary minerals efficiently and selectively scavenge many of the elements released during sulfides (e.g. Cu, Zn, As) and gangue minerals (e.g. Ni, Cr, Al) alteration.

KEYWORDS: sulfide alteration, Acid Mine Drainage, micro-XRD, micro-XRF, micro-XANES.

INTRODUCTION

Supergenic interaction between sulfide mineralizations and atmospheric agents causes a series of mineralogical reactions that involve sulfides, gangue and host rock minerals, both in natural outcrops and mining sites. These reactions trigger several processes, known, on the whole, as AMD processes (Acid Mine Drainage; Jambor & Blowes 2003 and references therein). AMD processes determine: 1) the acidification of circulating water; 2) the release, the transport and the selective concentration of several ecotoxic elements; 3) the precipitation of secondary minerals within soils and in the stream sediments of the hydrographic basin.

In this case, the mineralogical studies on the mechanism of sulfide alteration and on the genesis and evolution of secondary oxidation products are of paramount environmental relevance because they allow a better understanding of the source and the mechanisms of release of the ecotoxic elements and the effective

scavenging capacity of the authigenic secondary minerals.

In recent years, several techniques based on synchrotron radiation have been applied to determine, with μ m-spatial resolution, the elemental distribution and speciation of metals in mine-contaminated soils (Manceau *et al.* 2003; Morin *et al.* 1999, 2001).

With this work we have applied a combination of synchrotron-based μ -XRD, μ -XRF, and μ -XANES analyses to determine the mineralogy and the elemental distribution of metals in partially altered sulfide-mineralization fragments deposited within an open-air waste-rock dump (Libiola mine, eastern Liguria, Italy).

GEOLOGICAL SETTING

The Libiola Fe-Cu sulfide mine is located 8 km behind Sestri Levante (eastern Liguria, Italy). It was exploited from 1864 until 1962 and produced over 1Mt of Fe-Cu sulfides. The mine covers a surface area of about 4 km² and comprises more than 30 km of underground tunnels and 3

major open pits. The sulfide ore has been classified as stratabound Volcanic-associated Massive Sulfide deposit (VMS) and occurs as massive lenses near the top of a pillow basalt sequence that overlies ophiolitic breccias and serpentinized ultramafites (Zaccarini & Garuti 2008). The ore assemblage consists of pyrite and chalcopyrite, with minor sphalerite and pyrrhotite.

Non-mineralized rocks (mainly basalts and serpentinites), non-valuable mineralizations, and tailings were dumped in five main open-air waste-rock dumps and in several small bodies close to the main mine adits.

The sampling site is the main waste-rock dump of the Libiola mine, which is about 100 m in height and covers a surface of over 3 ha. The deposited materials are highly heterogeneous in grain size and in lithology. In this dump AMD processes are active and intense with sulfide-mineralized clasts progressively undergoing oxidation originating centimetric-thick hardpans cemented by secondary iron oxides and oxyhydroxides (Marescotti *et al.* 2008).

METHODS AND RESULTS

Two samples, representative of different stages of sulfide oxidation have been analyzed: a) mineralized fragment containing the transition from unaltered sulfides to sulfide-free oxidation products (Fig. 1a); b) evolved hardpan characterized by rhythmic alternation of sub-millimetric red- and ochreous-layers (Fig. 1b).

ANALYTICAL METHODS

Two different experiments have been performed at ID18F (μ -XRD and μ -XRF) and ID21 (μ -XRF and μ -XANES) beamlines at the ESRF (European Synchrotron Radiation Facilities, Grenoble, France).

At ID18F beamline simultaneous μ -XRF (excitation energy of 28 keV; spectrum collection using a Si(Li) solid state detector with detection limits in the range 0.01 ppm for $30 < Z < 35$ and < 0.1 ppm for $Z > 25$) and μ -XRD (monochromatic X-rays

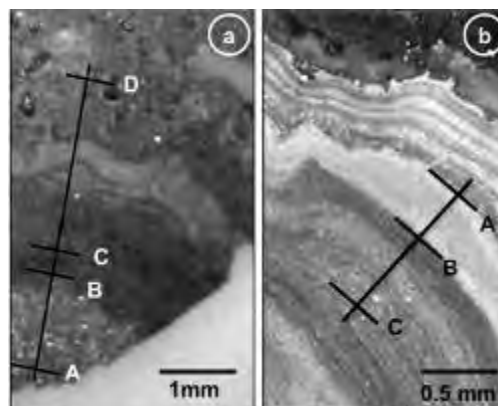


Fig. 1. Photomicrograph of the analyzed samples. a) transition from unaltered sulfides (segment AB) to sulfide-free oxidation products (segment CD). The segment BC corresponds to the transition zone. b) layered hardpan with rhythmic alternation of goethite-rich (segment AB) and hematite-rich (segment BC) layers.

of $\lambda = 0.44285 \text{ \AA}$; spectrum collection using a high resolution MAR CCD camera) analyses have been performed on both samples along millimetric transects with analytical steps of $2 \mu\text{m}$ (Fig. 1a, b).

At ID21 beamline μ -XANES and μ -XRF maps have been obtained along the same transects analyzed at ID18F. The maps were carried out in area of $100 \times 100 \mu\text{m}$ with a resolution of $1 \times 1 \mu\text{m}$. The sulfur oxidation state was determined by scanning the energy of the exciting beam across the sulfur absorption K-edge (total-S = 2.55 KeV; sulfide-S = 2.472 KeV; sulfate-S = 2.482 KeV).

RESULTS

Micro-XRD and micro-XANES analyses showed that the earliest stage of sulfide alteration is marked by the progressive oxidation of sulfide-S to sulfate-S that is then rapidly leached out from the system. Sulfide oxidation starts from particle rims or from intra-grain microfractures and is accompanied by a progressive loss of sulfur; sulfides are then pseudomorphically replaced by goethite and minor bernalite. In addition to sulfides, many gangue silicates are efficiently altered and only quartz is preserved within the altered layers.

Elemental maps and μ -XRF transects confirmed the high affinity of the secondary minerals to adsorb or incorporate many of the elements released by sulfides or gangue minerals (Fig. 2). In particular, we routinely observed significant concentrations of Ni, Cu, Zn, and As in the goethite-bernalite layers

The evolved hardpans (Fig. 1b) are composed by rhythmic alternation of submillimetric goethite-rich (ochreous) and hematite-rich (red) layers. This layering is the result of a complex evolution of the pristine authigenic Fe-oxides and -oxyhydroxides during which the mineral phases are cyclically involved in transformation processes including recrystallization, dissolution and reprecipitation (Carbone *et al.* 2005).

Micro-XRF transects evidenced a significant mineralogical control on the mobility of several elements released during sulfide and gangue minerals alteration (Fig. 3); in particular goethite-rich layers are enriched in Ni and Zn, whereas hematite-rich layers selectively concentrate As, Se, Mo, and Cu.

CONCLUSIONS

Synchrotron-based μ -XRD, μ -XRF, and μ -XANES techniques allowed us to determine, with μ m-spatial resolution, the mineralogical and chemical variations occurring during the alteration of sulfide mineralizations.

The main results can be summarized as follow:

(1) sulfides and gangue silicates (with the exception of quartz) are completely altered along oxidation fronts and are progressively replaced by secondary Fe-oxyhydroxides (mainly goethite with minor bernalite);

(2) the pristine oxidation products evolve toward well consolidated crusts (hardpans) that are composed by rhythmic alternation of submillimetric goethite-rich and hematite-rich layers;

(3) several ecotoxic elements released during sulfides and silicates alteration are efficiently scavenged by the newly formed Fe-oxide and -oxyhydroxides;

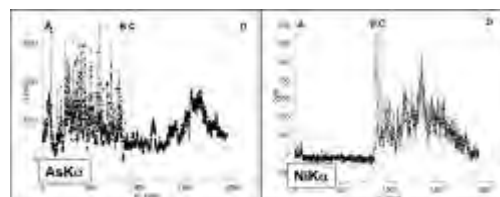


Fig. 2. μ -XRF line scans evidencing the chemical variations of As (left), and Ni (right), across the transect of Fig. 1a.

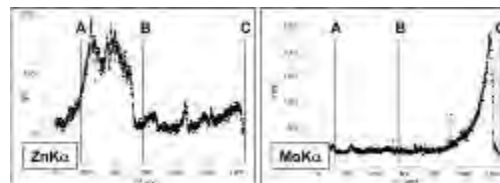


Fig. 3. μ -XRF line scans evidencing the chemical variations of Zn (left), and Mo (right), across the transect of Fig. 1b. Segment AB = goethite-rich layer; segment BC = hematite-rich layer.

(4) there is a significant mineralogical control on the mobility of these elements; in particular goethite appears to be an effective sink for Ni and Zn, whereas hematite can efficiently scavenge As, Se, Mo, and Cu.

ACKNOWLEDGEMENTS

The authors wish to acknowledge the financial support of MIUR (Italian Ministero dell'Istruzione, dell'Università e della Ricerca), PRIN-COFIN2006: "The role of mineral phases in the mobilization and storage of contaminant elements within mining sites of eastern Liguria".

REFERENCES

- CARBONE, C., DI BENEDETTO, F., MARESCOTTI, P., MARTINELLI, A., SANGREGORIO, C., CIPRIANI, C., LUCCHETTI, G., & ROMANELLI, M. 2005. Genetic evolution of nanocrystalline Fe oxide and oxyhydroxide assemblages from the Libiola Mine (eastern Liguria, Italy): structural and microstructural investigations. *European Journal of Mineralogy*, **17**, 785-795.
- JAMBOR, J.L., BLOWES, D.W., & RITCHIE, A.I.M. 2003. Environmental aspects of mine wastes. *Mineralogical Association of Canada, Short Course Series*, **31**, Vancouver, British Columbia.
- MANCEAU, A., TAMURA, N., CELESTRE, R.S., MACDOWELL, A.A., GEOFFROY, N., SPOSITO, G., & PADMORE, H.A. 2003. Molecular-scale

- speciation of Zn and Ni in soil ferromanganese nodules from loess soils of the Mississippi Basin. *Environmental Science Technology*, **37**, 75-80.
- MARESCOTTI, P., CARBONE, C., DE CAPITANI, L., GRIECO, G., LUCCHETTI, G., & SERVIDA, D. 2008. Mineralogical and geochemical characterisation of open pit tailing and waste rock dumps from the Libiola Fe-Cu sulphide mine (eastern Liguria, Italy). *Environmental Geology*, **53**, 1613-1626.
- MORIN, G., OSTERGREN, J.D., JUILLLOT, F., ILDEFONSE, P., CALAS, G., & BROWN, G.E. 1999. XAFS determination of the chemical form of lead in smelter-contaminated soils and mine tailings: importance of adsorption processes. *American Mineralogist*, **84**, 420-434.
- MORIN, G., JUILLLOT, F., ILDEFONSE, P., CALAS, G., SAMAMA, J.C., CHEVALLIER, P., & BROWN, G.E. 2001. Mineralogy of lead in a soil developed on a Pb-mineralized sandstone (Largentiere, France). *American Mineralogist*, **86**, 92-104.
- ZACCARINI, F. & GARUTI, G. 2008. Mineralogy and chemical composition of VMS deposits of northern Apennine ophiolites, Italy: evidence for the influence of country rock type on ore composition. *Mineralogy and Petrology*, **84**, 61-83.

Arsenic speciation in wastes resulting from pressure oxidation, roasting and smelting

Dogan Paktunc

Mining and Mineral Sciences Laboratories, CANMET, 555 Booth Street, Ottawa, ON, K1A 0G1 CANADA
(e-mail: dpaktunc@nrcan.gc.ca)

ABSTRACT: Arsenic commonly occurs in elevated concentrations in some gold and base-metal deposits. Mining and metallurgical processing of gold and base-metal ores results in solid wastes, effluents, and air emissions containing high concentrations of arsenic. Such wastes form an important source of anthropogenic arsenic in the environment. The nature and occurrence of arsenic in solid wastes are complex and highly variable. A combination of microanalytical tools and techniques including XAFS were used to determine the form and speciation of arsenic in wastes resulting from pressure oxidation, roasting and smelting, and impacted soil. As K-edge and Fe K-edge XAFS analyses of the pressure oxidation residues indicate that arsenic in tetrahedral coordination is corner-linked to 5 to 6 FeO₆ octahedra that are edge- and perhaps face-sharing. During roasting of refractory gold ores, oxidation of As to As₂O₅ species may be incomplete, which is detrimental to not only gold recovery but also the tailings management options. As K-edge XANES spectra indicate that more than one-third of the arsenic released from a copper smelter stack is composed of As³⁺ species. Most likely arsenic species in the smelter-impacted soil include arsenolite, goethite with adsorbed As⁵⁺, monomethylarsonic acid, and tetramethylarsonium iodide.

KEYWORDS: *Arsenic, speciation, mine wastes, impacted soil, XAFS*

INTRODUCTION

Arsenic is an abundant element in gold and base-metal ore deposits. Mining and metallurgical processing operations result in the accumulation of arsenic-bearing minerals in the tailings and waste rock. Arsenic can be readily released to the environment due to dissolution of the arsenic-bearing minerals under atmospheric conditions. Effluents resulting from mineral processing, refining and smelting operations can carry significant concentrations of As and the effluents have to be treated before they are discharged to the environment. Precipitates that form during processing and effluent treatment include ferric arsenates, ferric sulfoarsenates, ferrihydrite, hematite, and jarosite. These compounds end up in sludge and tailings ponds and their long term stabilities are important in terms of As releases from the wastes. Other sources of arsenic include air emissions in the form of dust and particulates originating from smelters and roasters.

Prediction of arsenic releases from the wastes and their bioavailability and toxicity assessments require solubility and stability tests, as well as speciation and molecular-scale characterization studies.

Several examples of arsenic speciation in wastes resulting from pressure oxidation, roasting and smelting, and impacted soil are given in this manuscript with the overall goal to promote further research in this area.

METHODOLOGY

Bulk and micro-XAFS analyses were performed at the PNC-CAT's bending magnet (20-BM) and undulator (20-ID) beamlines of the Advanced Photon Source (APS), Argonne, IL, USA. Other microanalytical and mineralogical characterization studies were conducted at CANMET. Details of the methodology can be found in Paktunc (2008) and other publications by the author.

RESULTS AND DISCUSSION

Arsenic in Refractory Gold Ores

Prior to gold extraction by cyanidation, refractory gold ores are either roasted or pressure oxidized to liberate the gold contained as submicroscopic particles or in solid solution in arsenopyrite and arsenic-rich pyrite. Gold extraction from such ores require roasting or pressure oxidation or bacterial oxidation prior to cyanidation to destroy the sulfide structure.

Pressure Oxidation

Arsenical compounds that can form during pressure-oxidation of refractory gold ores in the autoclaves include Phase-3, Phase-4, Type 2 and FeOH₂SO₄ (Fig. 1). In addition, scorodite can form in autoclave with sulfate substituting up to 20% arsenate. Jarosite is another phase with limited arsenate substituting for sulfate (Paktunc & Dutrizac 2003).

Phase-3 has a variable composition (Fe_{0.9-1.3}As_{0.3-0.6}S_{0.4-0.7}O₄(OH)_{0.3-3.3}). As K-edge and Fe K-edge XAFS results indicate that there are about 4 Fe atoms around the central As atom at a distance of approximately 3.33 Å and 2 Fe at ~3.5 Å. In return, there are between 1 and 2 Fe around the central Fe atom at ~2.9 Å, 1-2 As at ~3.3 Å, and 2 As at ~3.5 Å. It appears that two oxygen atoms around As are bridging edge- or face-sharing FeO₆ octahedra.

Phase-4 (Fe_{0.9-1.0}AsO₄(OH)_{0.0-0.6}) is identical to ferric orthoarsenate where the central As is coordinated to 5 Fe, three of which are forming edge-sharing FeO₆ octahedra (Fig. 3).

FeOH₂SO₄ contains minor As (i.e. up to 10% of the S sites in the structure). Its structure is made of corner-linked single chains of FeO₆ octahedra that are linked in turn by SO₄ tetrahedra.

Type-2 has the following composition: (Fe_{1.2-1.3}As_{0.6-0.8}S_{0.2-0.4}O₄(OH)_{2.6-3.5}). It is structurally similar to the As end-member of Phase-3. In accordance with the XAFS spectra shown on Figure 2, XAFS-derived short-ranges of Type-2 and As end-member of Phase-3 are also comparable.

Pressure oxidation residues from the autoclaves display similarities (i.e., XAFS and electron microprobe) to Type-2 and As-rich Phase-3 compounds (Fig.2).

Roasting

In the case of roasting, the pretreatment process destroys the sulfide matrix by driving off sulfur from the structure. This results in the formation of iron oxide particles that are made of concentrically zoned and porous hematite and maghemite (Paktunc *et al.* 2006). Arsenic is volatilized as As₂O₃ and oxidised to

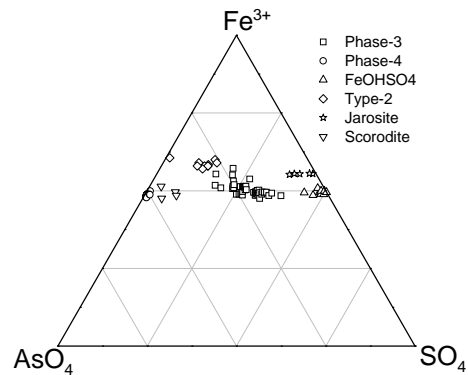


Fig. 1. Composition of ferric arsenate-sulfate compounds forming in the autoclaves treating refractory gold ores.

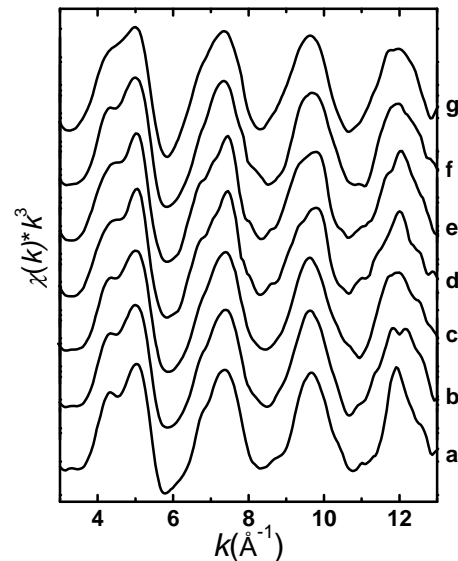


Fig. 2. As K-Edge XAFS spectra of Phase-3 (a, b), Type-2 (c), Phase-4 (d,e), autoclave residues (f,g).

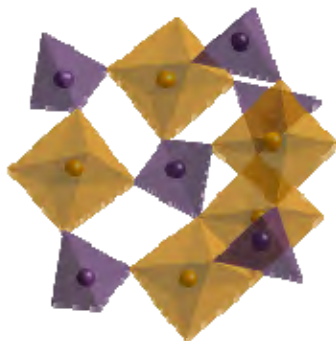


Fig. 3. Local structure of Phase-4 showing an arsenate tetrahedron (black) surrounded by 5 FeO₆ octahedra (grey) at 3.34±0.09 Å and 5 arsenate tetrahedra at 4.35±0.23 Å.

As₂O₅ under the highly oxidizing conditions of a roaster.

Micro-XANES spectra collected from maghemite-rich and hematite-rich domains within Fe-oxide particles indicate the presence of both As³⁺ and As⁵⁺ species. This observation is similar to that of Walker *et al.* (2005) in the Giant gold mine tailings. As³⁺ species appear to be more common in the maghemite-rich domains, indicating a clear relationship between retarded transformation of Fe-oxide compounds and incomplete oxidation of As species during roasting (Paktunc 2008). This finding is not only important for the recovery of gold (Paktunc *et al.* 2006), but also assessing the stability of the arsenic species in the tailings.

Arsenic in Smelter Emissions

Recent studies examining the distribution of smelter-derived elements around a copper smelter found that arsenic deposition rates in snow and concentrations in organic soils decrease gradually with distance from the smelter (Henderson *et al.* 2002; Knight & Henderson 2006; Telmer *et al.* 2003; Zdanowicz *et al.* 2006). In order to explore the nature and behaviour of arsenic, a limited number of samples (stack and impacted soil) were characterized.

The sample collected from the middle of a copper smelter stack representing emitted particles was highly complex.

XANES analyses indicated the presence of both As³⁺ and As⁵⁺ species in the stack sample and that about one-third of the total As is trivalent (Paktunc 2008). X-ray mapping supplemented by micro-XANES analyses indicated that As is localized along thin rims around spherical Cu particles. These rims have higher As³⁺ species ranging from 34 to 40% of the total As.

The soil samples impacted by the copper smelter were selected based on arsenic concentrations, location (i.e., proximity to the smelter) and depth within the soil horizon. XANES spectra of the soil samples collected from 2 to 10 km distances and depths of 0 to 95 cm are dominated by As⁵⁺ species. Least-square analysis of the spectra with the organic As species of Smith *et al.* (2005) indicated the presence of monomethylarsonic acid (CH₃AsO(OH)₂) and tetramethylarsonium iodide (C₄H₁₂AsI) in addition to arsenolite and goethite with adsorbed As (Paktunc 2008). Arsenolite (As³⁺) that forms 6 to 13 % of the arsenic species is found only in the near surface samples from 2 to 6 km away from the smelter whereas the samples 10 km away from the smelter are composed of goethite and monomethylarsonic acid (Fig. 4). Considering that monomethylarsonic acid is at least 600 times less toxic than arsenous acid (H₃AsO₃) and 60 times less toxic than arsenic acid (H₃AsO₄) (Andrewes *et al.* 2004), quantitative speciation of arsenic in the soil profile would have significant implications in risk assessment studies. Although it is premature to draw any conclusion, the preliminary results from this exploratory data set justify the need to undertake a systematic sampling and studies to determine the speciation of arsenic and its methylation within the soil profile and distance from the point source.

ACKNOWLEDGEMENTS

The XAFS experiments were carried out at the Pacific Northwest Consortium - Collaborative Access Team's (PNC/XOR) beamline at the Advanced Photon Source

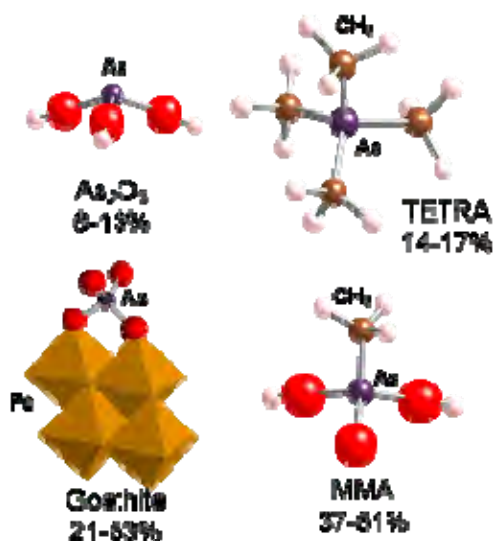


Fig. 4. Arsenic species present in the impacted soil. TETRA: $C_4H_{12}AsI$; MMA: $CH_3AsO(OH)_2$

(APS) under the user agreement to the author which is supported by the US Department of Energy under contracts W-31-109-Eng-38 (APS) and DE-FG03-97ER45628 (PNC-CAT). The XAFS experiments at PNC/XOR were also supported by the Natural Sciences and Engineering Research Council of Canada through a major facilities access grant.

REFERENCES

- ANDREWES, P., DEMARINI, D.M., FUNASAKA, K., WALLACE, K., LAI, V.W.M., SUN, H., CULLEN, W.R., & KITCHIN, K.T. 2004. Do arsenosugars pose a risk to human health? The comparative toxicities of a trivalent and pentavalent arsenosugar. *Environmental Science and Technology*, **38**, 4140-4148.
- HENDERSON, P.J., KNIGHT, R.D., & MCMARTIN, I. 2002. Geochemistry of soils within a 100 km radius of the Horne Cu smelter, Rouyn-Noranda, Quebec. *Geological Survey of Canada Open File* **4169**.
- KNIGHT, R.D. & HENDERSON, P.J. 2006. Smelter dust in humus around Rouyn-Noranda,

Québec. *Geochemistry: Exploration, Environment and Analysis*, **6**, 203-214.

- PAKTUNC, D. 2008. Speciation of arsenic in an anaerobic treatment system at a Pb-Zn smelter site, gold roaster products, Cu smelter stack dust and impacted soil. Proc. 9th Int. Cong. *Applied Mineralogy (ICAM2008)* 8-10 Sep 2008, Brisbane, Queensland, *The Australasian Institute of Mining and Metallurgy*, **8/2008**, 343-348.

- PAKTUNC, D. & DUTRIZAC, J. 2003.

Characterization of arsenate-for-sulfate substitution in synthetic jarosite using X-ray diffraction and X-ray absorption spectroscopy. *Canadian Mineralogist*, **41**, 905-919.

- PAKTUNC, D., KINGSTON, D., PRATT, A., & MCMULLEN, J. 2006. Distribution of gold in pyrite and in products of its transformation resulting from roasting of refractory gold ore. *Canadian Mineralogist*, **44**, 213-227.

- SMITH, P.G., KOCH, I., GORDON, R.A., MANDOLI, D.F., CHAPMAN, B.D., & REIMER, K.J. 2005. X-ray absorption near-edge structure analysis of arsenic species for application to biological environmental samples. *Environmental Science and Technology*, **39**, 248-254.

- TELMER, K., BONHAM-CARTER, G.F., KLIZA, D.A., & HALL, G.E.M. 2003. The atmospheric transport and deposition of smelter emissions: evidence from the multi-element geochemistry of snow, Quebec, Canada. *Geochimica et Cosmochimica Acta*, **68**, 2961-2980.

- WALKER, S.W., JAMIESON, H.E., LANZIROTTI, A., & ANDRADE, C.F. 2005. Determining arsenic speciation in iron oxides derived from a gold-roasting operation: Application of synchrotron micro-XRD and micro-XANES at the grain scale. *Canadian Mineralogist*, **43**, 1205-1224.

- ZDANOWICZ, C.M., BANIC, C.M., PAKTUNC, D. & KLIZA-PETELLE, D.A. 2006. Metal emissions from a Cu-smelter, Rouyn-Noranda, Quebec: Characterization of particles sampled in air and snow. *Geochemistry: Exploration, Environment and Analysis*, **6**, 147-162.

Importance of sorption in the geochemistry of nickel in waste rock

Benoît Plante¹, Mostafa Benzaazoua¹, Bruno Bussière¹, & Donald Laflamme²

¹Université du Québec en Abitibi-Témiscamingue (UQAT), 445 boul. de l'Université, Rouyn-Noranda, QC, J9X 5E4 CANADA (e-mail: benoit.plante@uqat.ca)

²Rio Tinto, Fer et Titane Inc., 1625, route Marie-Victorin, Sorel-Tracy, QC, J3R 1M6 CANADA

ABSTRACT: Humidity cell tests were used for contaminated neutral drainage (CND) prediction from waste rock piles of an ilmenite deposit known to occasionally release above-regulatory level nickel loadings. The influence of mineralogy and in-situ weathering degree of waste rock on its geochemical behaviour are investigated in this study, using samples of waste rocks having various mineral compositions and which underwent different alteration levels (fresh and approximately 25 years old waste samples). The rates of sulfide oxidation appear to be of the same order in fresh and weathered waste rock. However, the nickel ions produced by sulfide oxidation do not get leached in the fresh waste rocks while they are leached in the weathered waste rocks. The nickel sorption potential of the studied waste rocks appears to play a significant role on the nickel geochemical behaviour. Batch sorption tests followed by sequential extraction procedures suggest that the number and type of available sorption sites appear to vary between fresh and weathered mine waste rocks.

KEYWORDS: *Nickel geochemistry, contaminated neutral drainage*

INTRODUCTION

Acid mine drainage (AMD) is often characterized by low pH, high acidity, and high metal loadings. The phenomenon received much attention in the past decades in terms of prediction, control, and remediation (e.g., MEND 2001). However, many toxic metals such as Ni, Zn, Co, As, and Sb are soluble at near-neutral pH, and can potentially lead to the contamination of mine effluents without acidic conditions; this phenomenon is called Contaminated Neutral Drainage (hereinafter called CND) or simply Neutral drainage (Nicholson 2004). Since many Canadian mines can potentially face Ni release from waste rock, and Ni geochemistry received much less attention than other CND-related metals (ex. As) in the past years, this work focuses on Ni geochemistry at near-neutral conditions. The present study is performed on waste rock sampled from the Lac Tio mine, an ilmenite deposit near Havre-Saint-Pierre, Québec, Canada, exploited by an open pit operation by Rio Tinto, Fer et Titane Inc. (RTFT) since the early 1950's. The gangue material of the mine is mainly composed of a calcic

plagioclase mineral (approximate formulae $\text{Na}_{0.4}\text{Ca}_{0.6}\text{Al}_{1.6}\text{Si}_{2.4}\text{O}_8$). Water draining from the waste rock piles are near-neutral and sporadically show Ni concentrations slightly higher than those allowed by Quebec regulations. Preliminary studies on this waste rock showed that the material is not acid generating and that Ni is generated mainly from Ni-bearing pyrite (FeS_2) and pentlandite ($(\text{Fe,Ni})_9\text{S}_8$) that seem to be associated with ilmenite in the Lac Tio deposit, and the waste rock beneficiate from an important metal retention potential occurring most probably via surface sorption (Bussière *et al.* 2005; Plante *et al.* 2008; Pepin *et al.* 2008). This study aims to clarify the sorption importance on Ni geochemistry in mine waste rocks.

MATERIALS AND METHODS

In this work, 6 Lac Tio waste rock samples are investigated: 3 samples were freshly blasted waste rock and 3 were "weathered" samples from an old waste rock pile (approximately 25 years old) which underwent significant natural alteration. The ilmenite content varies from approximately 20 to 60 wt% in both

the fresh and weathered waste rock samples. The Ni content varies from 0.028 to 0.043 wt% and S content (mainly as sulfide) from 0.142 to 0.384 wt% in the waste rock samples studied. Weathered samples have significantly lower S values (<0.172 wt%) than fresh samples (>0.345 wt%), probably due to previous alteration. The Ni geochemistry was evaluated through the use of humidity cell tests (ASTM D5744-96), which consist of weekly drying-wetting cycles ending with flushing of the studied material (1 kg) with deionised water (1 L), and analysis for various geochemical parameters such as pH and metals (using ICP-AES) on the leachates. These cell tests were performed on the -¼ inch fraction of the mine wastes without grinding, since doing so would generate unwanted fresh surfaces in the weathered waste rock samples.

RESULTS AND INTERPRETATION

Kinetic cells

The pH values measured in the kinetic tests are shown in Figure 1. The pH of all waste rock samples remain stable between 7 and 8 after 200 days until the end of the test, suggesting conditions will remain near-neutral in the field.

As is often the case in CND generating materials (or in low-acid generating potential materials), the detected metal levels in leachates were generally low, in the order of thousandths to hundredths of mg/L. In fact, the Ni concentrations obtained from the fresh waste rocks are often under the detection limit of the ICP-AES employed (0.004 mg/L). For greater appreciation of the environmental behaviour of the different studied waste rocks, particularly to differentiate the geochemical behaviour of fresh and weathered waste rocks, the release rates were calculated.

The elemental release rates were determined as the slope of the linear regression of the cumulated (from each leachate) and normalized (with regards to total mass in the corresponding cell) metal loads over time (in mg/kg/day); they are summarized in Figure 2. The range of

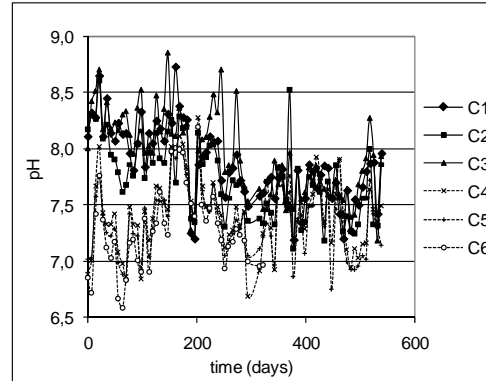


Fig. 1. pH evolution during kinetic cell tests.

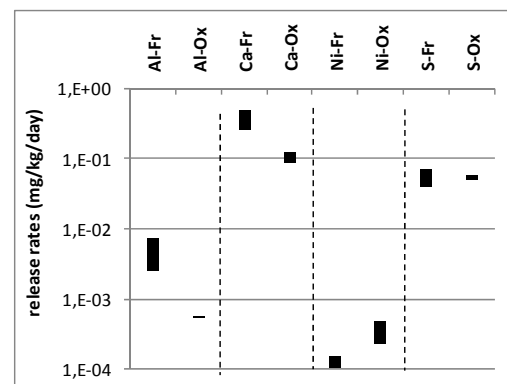


Fig. 2. Ranges of elemental release rates obtained with laboratory kinetic cell tests on fresh (-Fr) and weathered (-Ox). waste rocks.

obtained release rates is shown for Al, Ca, S and Ni for the fresh (labeled “-Fr”) and weathered materials (labeled “-Ox”). The S and Ni releases are associated with sulfides oxidation, while Al and Ca releases are associated with the neutralizing minerals contained in the waste rock (plagioclase).

Plagioclase dissolution is known to be incongruent, with Al and Ca being preferably dissolved at the surface (Blum & Stillings 1995). This dissolution generates an Al-Ca-poor thin layer at the surface, which is consistent with the lower Al-Ca release rates obtained in the leaching waters of the weathered waste rocks. The S release rates obtained from the fresh and weathered waste rocks are of the same order, suggesting that sulfide oxidation occurs at approximately the same rate in both, assuming that all the oxidation products do end up in the

leachates (an acceptable assumption at this pH range). Consequently, the Ni release rates of fresh and weathered waste rocks should be of the same order. However, the Ni release rates from the weathered waste rocks are about half an order of magnitude greater than those from the fresh waste rocks.

Geochemical simulations (not shown) of water quality suggest that Ni is soluble in the test conditions, eliminating secondary mineral precipitation as an explanation for the absence of Ni in leachates. These observations could be explained by the metal retention potential of the Lac Tio waste rock being still active in the humidity cell tests. Consequently, the Ni produced in the humidity cell tests will continue to be retained by the fresh waste rock until saturation of the retention sites.

Batch sorption and Sequential Extraction Procedure (or SEP)

In order to validate the hypothesis mentioned above, the Ni retention capacity of the Lac Tio waste rock was estimated using a batch sorption test performed on a fresh (C1) and weathered (C4) sample, followed by a 3-step Sequential Extraction Procedure (or SEP). The batch sorption test was done using a 10 mg/L Ni solution with an initial pH of 6, an ionic force adjusted to 0.05 M with NaNO₃ and with a liquid/solid ratio of 25. Some of the batch sorption results are presented in Figure 3.

Almost 100 % of the Ni was sorbed on the fresh waste rock after 400 minutes, while Ni retention reaches only 50 % after 1500 minutes on the weathered waste rock. The resulting Ni sorption capacities from these batch tests are 0.34 mg/g for the fresh and 0.19 mg/g for the weathered waste rock. However, the Ni sorption capacity of the fresh waste rock is probably greater, since all the Ni was retained in the batch test and the sorption sites were not fully saturated.

Despite strong criticisms on the interpretation of SEP's (Nirel & Morel 1990), they are still recognized as a valuable tool to evaluate metal partition in soils, tailings, and waste rocks. (Wasay *et*

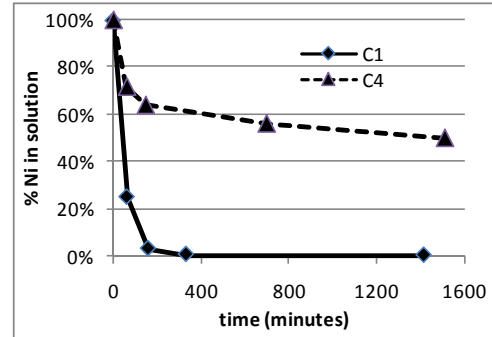


Fig. 3. Batch Ni sorption test.

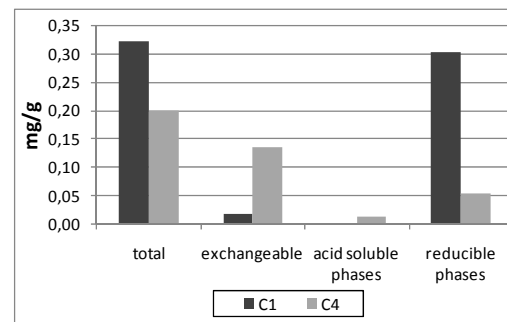


Fig. 4. Distribution of the Ni retention phases in fresh (C1) and weathered (C4) waste rock after a batch sorption test.

al. 1998; Zagury *et al.* 1999). The 3-step SEP employed in this study (see detailed procedure in Neculita *et al.* 2008) enabled the determination of the Ni fraction that is 1) soluble and exchangeable, 2) bound to acid-soluble phases and 3) reducible or bound to Fe-Mn oxides. The results are presented in Figure 4: most of the Ni is sorbed on reducible phases of the fresh waste rock (C1) with very few Ni that is easily exchangeable. For the weathered waste rock (C4), about 70 % of the Ni is easily exchangeable, about 25 % of the Ni occurs as reducible phases and the remaining Ni is on acid soluble phases.

CONCLUSIONS

This study allows a better understanding of the Ni geochemistry in near-neutral conditions. Kinetic cell tests run for 75 weeks on 6 waste rock samples suggest that the pH will remain near neutral in the waste rock piles. Sorption phenomena seem to drive Ni leaching in laboratory kinetic cells, and the sorption type and capacity vary between fresh and

weathered waste rocks. Applications of these findings to waste rock piles management and remediation are currently being studied.

ACKNOWLEDGEMENTS

The Authors would like to thank the NSERC Polytechnique-UQAT Chair in environment and mine wastes management for financial support, and are grateful to QIT-Fer et Titane Inc. for making this research possible and the URSTM personnel for their technical support. The Authors are also grateful to the NSERC Collaborative Research and Development (CRD) Grants.

REFERENCES

- BLUM, A.E. & STILLINGS, L.L. 1995. Feldspar dissolution kinetics. In: WHITE, A.F. & BRANTLEY, S.L. (ed.), *Reviews in mineralogy*, **31: Chemical weathering rates of silicate minerals, Mineralogical Society of America, USA, 291-352.**
- BUSSIÈRE, B., DAGENAIS, A.-M., VILLENEUVE, M., & PLANTE, B. 2005. Rapport final: Caractérisation environnementale d'un échantillon de stériles du Lac Tio. URSTM, Rouyn-Noranda.
- MEND, 2001. MEND Manual, Report 5.4.2 CD, CD-ROM: MEND Manual, Ottawa, ON.
- NECULITA, C.-M., ZAGURY, G.J., & BUSSIÈRE, B., 2008. Effectiveness of sulfate-reducing passive bioreactors for treating highly contaminated acid mine drainage: II. Metal removal mechanisms and potential mobility. *Applied Geochemistry*, **23**, 3545-3560.
- NICHOLSON, R.V. 2004. Overview of neutral pH drainage and its mitigation: results of a MEND study. *Proceedings of the MEND Ontario workshop*, Sudbury, 2003.
- NIREL, P.M.V. & MOREL, F.M.M. 1990. Pitfalls of sequential extractions. *Water Research*, **24**, 1055-1056.
- PEPIN G., BUSSIÈRE B., AUBERTIN M., BENZAAZOUA M., PLANTE B., LAFLAMME D., & ZAGURY G.J. 2008. Field experimental cells to evaluate the potential of contaminated neutral drainage generation at the Tio mine, Quebec, Canada. *Proceedings of the 10th IMWA Mine Water and the Environment*, Czech Republic, 309-312.
- PLANTE, B., BENZAAZOUA, B., BUSSIÈRE, B., PEPIN, G., & LAFLAMME, D. 2008. Geochemical behaviour of nickel contained in Tio mine waste rocks. *Proceedings of the 10th IMWA Mine Water and the Environment*, Czech Republic, 317-320.
- WASAY, S. A., BARRINGTON, S., & TOKUNAGA, S. 1998. Retention form of heavy metals in three polluted soils. *Journal of Soil Contamination*, **7**, 103-119.
- ZAGURY, G.J., DARTIGUENAVE, Y., & SETIER, J.-C. 1999. Ex situ electroreclamation of heavy metals contaminated sludge: pilot scale study. *Journal of Environmental Engineering*, **125**, 972-978.

Distribution of elements of concern in uranium mine tailings, Key Lake, Saskatchewan, Canada

Sean A. Shaw¹, M. Jim Hendry¹, Joseph Esselfie-Dughan¹,
Tom Kotzer², & Harm Maathuis²

¹Department of Geological Sciences, University of Saskatchewan, 114 Science Place, Saskatoon SK, S7N 5E2
CANADA (email: sean.shaw@usask.ca)

²Cameco Corporation, 2121-11th Street West, Saskatoon, SK, S7M 1J3 CANADA

ABSTRACT: Boreholes were drilled and detailed tailings samples collected through the entire depth profile (76 m) at three locations in the Deilmann Tailings Management Facility, located at the Key Lake Uranium mine in Saskatchewan, Canada. Pore waters and solid phases were separated using piston core squeezing. The concentrations of the elements of concern (EOC: As, Mo, Ni, and Se) as well as other elements were determined for all solid phase (n = 87) and pore water (n=83) samples. Additional analyses, including X-ray Diffraction and Scanning Electron Microprobe were conducted on the solid samples to provide characterization and spatial definition of mineral phases that could influence the distribution of the elements of concern. The pH, Eh and temperature were also measured on core samples and extracted pore waters. The mean concentrations for As, Mo, Ni, and Se were 2,918, 41.9, 3,178, and 9.84 $\mu\text{g g}^{-1}$ in the solid phase and 39.0, 139, 0.63, and 0.83 $\mu\text{mol L}^{-1}$ in the aqueous phase. Results indicated a strong correlation between solid phase As, Mo, Ni, and Se concentrations and aqueous phase As, Mo, and Se values. In addition, comparisons between whole-rock geochemical and micron-scale elemental concentrations suggest a strong correlation between As, Fe, and Ni in the solid phase.

KEYWORDS: uranium, mine tailings, geochemistry, mineralogy, Key Lake

INTRODUCTION

Uranium deposits of the Athabasca basin in northern Saskatchewan, Canada, produce about one-third of the world's uranium. The uranium ores associated with these deposits can contain variable and high concentrations of nickel (up to 5 wt %) and arsenic (up to 10 wt %). Consequently, elevated concentrations of As and Ni have been associated with the tailings facilities for these type of deposits (Donahue & Hendry 2000). The US EPA has set the drinking water limit for As at 0.010 mg L⁻¹, while the World Health Organization suggests a maximum Ni concentration of 0.070 mg L⁻¹. Elevated concentrations of additional elements of concern (EOC), including Mo and Se, have also been associated with uranium mine tailings (Morrison *et al.* 2002). At high concentrations, Se compounds are carcinogenic and teratogenic (Ohlendorf *et al.* 1986), while Mo may be toxic as it

leads to a secondary Cu deficiency (e.g., Vunkova-Radeva *et al.* 1988).

The Key Lake uranium mine is located at the southern rim of the Athabasca Basin in north central Saskatchewan, approximately 650 km north of Saskatoon, Saskatchewan (57°13'N, 105°38'W). The Deilmann tailings facility (DTMF) is located on site and has been in operation since 1996.

A 10 Ka criteria for uranium tailings facilities, including the DTMF, has been developed due to elevated concentrations of long-lived transuranic elements (Atomic & Energy Control Board 1987). This 10 Ka criteria is also applied to other elements of concern to prevent their long-term mobilization to the surrounding environment. In order to understand the long-term effects of uranium tailings on the surrounding environment, detailed information on the geochemical and mineralogical controls on the elements of concern are required.

The global objective of this study is to characterize the geochemical characteristics of tailings within the DTMF over the immediate and long term. The specific objective of this study is to quantify the solid and aqueous phase concentrations of the elements of concern within the DTMF and determine the geochemical and mineralogical controls on these observed elemental distributions. This study documents one aspect of a holistic, multi-year scientific program on uranium mine tailings within Cameco Operations, designed to better understand the long-term geochemical behaviour of mine tailings.

Tailings Management Facility

The Deilmann Tailings Management Facility (DTMF) was constructed in the mined out Deilmann pit. The DTMF is characterized by two depositional zones: the east and west cells. Tailings deposition began in the east cell in 1996 and commenced in the west cell once the Deilmann ore body was mined out in 1999. Prior to 1999, the only source of tailings for the DTMF was the Deilmann ore body (Ruhmann & von Pechmann 1989). Since 2000, the tailings have been derived from a mixture of MacArthur River (Delany *et al.* 1998) and low and high-grade wastes from both the Deilmann and McArthur River ore bodies. Therefore, the tailings body can be conceptualized as two separate tailings types, the lower Deilmann and upper McArthur tailings, which are separated at approximately 410 m elevation within the DTMF.

In 1998 the tailings in the DTMF were converted to subaqueous storage by disabling perimeter drains and allowing the facility to naturally flood. Since 2006, the water level has been maintained at approximately 50 m above the top of the tailings.

MATERIALS AND METHODS

Sample Collection & Analyses

Since 1999, boreholes have been drilled into the DTMF tailings for the sole purpose of collecting tailings cores for their geochemical and geotechnical

characterization. Drilling collection periods have previously taken place in 1999, and 2004/2005 with boreholes from all three campaigns proximally-located within several meters of one another.

In June, 2008, boreholes were drilled at three locations in the DTMF east cell using a sonic track mounted drill rig on a floating barge. Boreholes were cored to depths of between 75.3 m and 79.0 m and continuous core samples were collected using a 3.1 m long, 75 mm diameter, core barrel. Following core collection, samples were sealed in containers and stored at temperatures of 4°C. Pore waters were extracted from the tailings samples within 24 h of collection using both centrifugation and piston squeezing techniques. Tailings (n = 87) and pore water (n = 83) samples were analysed for pH, Eh, alkalinity, organic/inorganic C, major cations, major anions, trace metals, and radionuclides.

Geochemical speciation modelling was conducted for all extracted pore waters using PHREEQC (Parkhurst & Appelo 1999). Preliminary mineralogical analysis of selected tailings samples collected in 2004 was conducted using a Philips PW1830 X-ray powder diffractometer and a JEOL JXA-8600 electron microprobe microanalyzer (EPMA). Samples were analyzed by EPMA using electron backscatter imaging, energy dispersive spectrometry, and wavelength dispersive spectrometry.

RESULTS AND DISCUSSION

Tailings Solid Phase

The stratigraphy of the DTMF mainly consists of tailings layers with varying water contents. The water content ranged between 10.3 and 172 %, while the tailings with a particle size < 75 µm ranged between 4.10 and 98.6 %, throughout all three boreholes. The average water content and particle size < 75 µm was 55.6 wt % and 58.8 % in the Deilmann tailings and 49.0 wt% and 42.9 %, in the McArthur tailings. The lower water content and larger grain size observed in the McArthur tailings was mainly attributed to a sand wedge deposited by sloughing events in 2001.

In all boreholes the average concentrations of As, Ni, Mo, and Se were greater in the Deilmann, relative to the McArthur tailings (Table 1). This can be attributed to differences in solid phase compositions of the original Ni-As rich Deilmann ores versus relatively Ni-As poor McArthur River ores.

Mineralogical Analyses

Major mineral phases identified in the DTMF included several aluminosilicates, quartz, gypsum and hydrobasaluminite. Minor mineral phases identified included ferrihydrite, gersdoffite (NiCoAsS), sulfide phases, and several carbonates.

Preliminary EPMA analyses indicated the formation of As, Fe, and Ni-rich coatings surrounding Ca-SO₄-rich particles (Fig. 1). A comparison of solid phase As and Ni concentrations demonstrated a good correlation between samples from all three boreholes, which was previously observed by EPMA analyses conducted by Donahue and Hendry (2000) on tailings from a similar facility. This relationship potentially resulted during the neutralization portion of the milling process where a strong pH gradient developed around un-reacted lime particles forming FeO(OH)-AsO₄ complexes along with theophrastite (Ni[OH]₂).

Tailings Pore Water

The pH of pore waters, collected by piston squeezing, ranged between 8.0 and 10.7, with an average pH value of 9.9. Measured Eh values ranged between 50 and 525 mV, with an average of 200 mV. Aqueous concentrations for As, Mo, and Se were greater in the Deilmann relative to the McArthur tailings. However, no difference was observed between Ca, Fe, Ni, and SO₄ concentrations between the two tailings types (Table 2) which is largely due to crystallization of gypsum, iron oxy-hydroxides and theophrastite.

Geochemical speciation modelling indicated saturation with respect to gypsum and several carbonates, slight under-saturation with respect to calcium arsenate (Ca₃[AsO₄]₂) and ferrihydrite.

Table 1. DTMF tailings average solid phase concentrations for 2008 boreholes.

EOC	Mean ($\mu\text{g g}^{-1}$)	Min. ($\mu\text{g g}^{-1}$)	Max. ($\mu\text{g g}^{-1}$)
McArthur Tailings (n = 42)			
As	406	0.70	1,440
Ni	531	1.60	2,000
Mo	14.0	0.60	32.0
Se	3.20	0.00	8.30
Deilmann Tailings (n = 45)			
As	5,374	165	13,700
Ni	5,764	243	14,300
Mo	69.7	9.00	183
Se	16.3	1.40	27.0

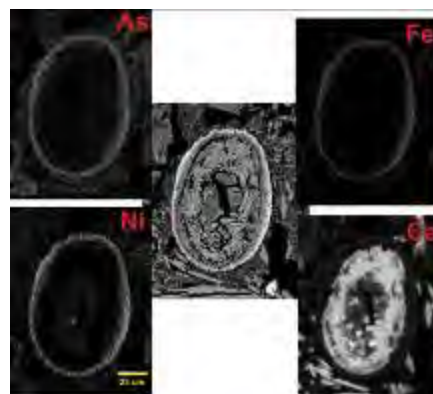


Fig. 1. Electron backscatter image of a Ca-SO₄-rich grain showing a secondary precipitate ring (centre) and individual backscatter images for As, Fe, Ni, and Ca of the same grain.

Additionally, both calcium arsenate and ferrihydrite approached equilibrium with increased depth in each borehole, which was well correlated to the observed increased As aqueous concentrations.

SUMMARY AND CONCLUSIONS

Solid and aqueous phase geochemical results indicate that tailings derived from the Deilmann ore are different from tailings originating from the McArthur ore body. Significantly greater concentrations of solid phase As, Ni, Mo, and increased aqueous concentrations of As, Mo, and Se are associated with tailings derived from Deilmann ore.

Mineralogical analyses suggest that gypsum and hydrobasaluminite are major secondary precipitates found within the DTMF, with trace amounts of gersdoffite and ferrihydrite also present. Electron microprobe analyses indicates a strong co-location between As, Ni, and Fe, which

Table 2. DTMF tailings average pore water concentrations for 2008 boreholes.

EOC	Mean ($\mu\text{mol L}^{-1}$)	Min. ($\mu\text{mol L}^{-1}$)	Max. ($\mu\text{mol L}^{-1}$)
McArthur Tailings (n = 39)			
As	10.8	0.19	33.2
Ni	0.73	0.00	4.38
Mo	50.9	0.00	92.2
Se	0.56	0.00	1.42
Fe	0.18	0.00	0.82
Ca	15,500	6,740	16,700
SO ₄	16,200	11,500	17,700
Deilmann Tailings (n = 44)			
As	67.5	7.34	147
Ni	0.52	0.00	1.45
Mo	227	38.3	433
Se	1.11	0.31	1.85
Fe	0.15	0.00	0.57
Ca	15,700	15,000	16,500
SO ₄	18,400	15,600	21,900

is supported by the linear relationship observed between the solid phase As, Ni and Fe concentrations in bulk tailings.

ACKNOWLEDGEMENTS

We would like to thank Andrew Jansen and Virginia Chostner for their assistance with the collection of samples. We would also like to thank Tom Bonli for assistance with the EPMA analyses. This project was jointly funded by Cameco Corporation and NSERC.

REFERENCES

ATOMIC ENERGY CONTROL BOARD. 1987. GRegulatory objectives, requirements and guidelines for the disposal of radioactive wastes – long-term aspects. Ottawa, Canada.

DELANY, T.A., HOCKLEY, D.E., CHAMPMAN, J.T., & HOLL, N.C. 1998. Geochemical characterization of tailings at the McArthur River Mine, Saskatchewan. *Tailings and Mine Waste '98*, Balkema, Rotterdam.

DONAHUE, R., HENDRY, M.J., & LANDINE, P. 2000. Distribution of arsenic and nickel in uranium mill tailings, Rabbit Lake, Saskatchewan, Canada. *Applied Geochemistry*, **15**, 1097-1119.

DONAHUE, R. & HENDRY, M.J. 2003. Geochemistry of arsenic in uranium mine mill tailings, Saskatchewan, Canada. *Applied Geochemistry*, **18**, 1733-1750.

OHLENDORF, H. M., HOFFMAN, D. J., SAIKI, M. K., & ALDRICH, T. W. 1986. Embryonic mortality and abnormalities of aquatic birds: Apparent impacts of selenium from irrigation drainwater. *Science of the Total Environment*, **52**, 533-535.

PARKHURST, D.L. & APPELO, C.A.J. 1999. User's guide to PHREEQC (version 2) A computer program for speciation, batch reaction, one dimensional transport, and inverse geochemical calculations. *USGS Survey Water Resources Investigations Report 99-4259*, 310 p.

RUHRMANN, G. & VON PECHMANN, E. 1989. Structural and hydrothermal modification of the Gaertner uranium deposit, Key Lake, Saskatchewan, Canada. *IAEA TECDOC-500*, 363-377.

VUNKOVA-RADEVA, R., SCHIEMANN, J., MENDEL, R.R., SALCHEVA, G., & GEORGIEVA, D. 1988. Stress and activity of molybdenum containing complex in winter wheat seeds. *Plant Physiology*, **87**, 533-535.

Source, attenuation and potential mobility of arsenic at New Britannia Mine, Snow Lake, Manitoba

Stephanie Simpson¹, Barbara L. Sherriff¹,
Nikolay Sidenko^{1,2}, & Jamie Van Gulck³

¹ Department of Geological Sciences, University of Manitoba, Winnipeg, MB, R3T 2N2 CANADA
(email: jared.etccherry@gmail.com)

² TetreES Consultants Inc., Winnipeg, MB, R3C 3R6 CANADA

³ Arktis Solutions Inc. 186 Steepleridge St., Kitchener, ON, N2P 2V1 CANADA

ABSTRACT: High concentrations of arsenic (As) (~17 ppm) in a groundwater monitoring well at the gold mine site in Snow Lake Manitoba are either emanating from a Residue Stockpile (ARS) containing arsenopyrite concentrate and/or from an old emergency discharge area used for Nor Acme tailings. Hydrological modelling suggests that As is transported into the aquifer from the ARS by advection and diffusion. The concentration of As in the Nor Acme tailings is <0.1 mg/L, and in the pore water of the tailings <5 mg/L, making the tailings an unlikely source of the contamination. Attenuation of As in surface waters appears to be adsorption of As(V) on Fe-oxyhydroxides such as ferrihydrite, but in the aquifer, the majority of the As is in the more soluble As(III) phase. Arsenic is also attenuated by adsorption on plants either alone or with FeOOH. The objectives of this research were to determine the potential for contamination of Snow Lake, the source of drinking water for the town of Snow Lake, and the local environment. At the time the study was conducted, water quality in Snow Lake met the Canadian Drinking Water Standard of 0.010 mg/L As.

KEYWORDS: arsenic, mobility, attenuation, geochemistry, hydrologic modelling

INTRODUCTION

High concentrations of arsenic are present in the ground water at New Britannia Gold Mine, Snow Lake, Manitoba, Canada. Between 1995 and 2005, ground water samples from a monitoring well (MW 17) had <20 ppm arsenic. This well is installed into an aquifer below a low-lying former Nor Acme Mine emergency tailings disposal area (NATA) (Fig. 1). MW17 is also 100 m down gradient from an arsenopyrite residue stockpile (ARS) that contains pore water concentrations of up to 100 ppm arsenic (Salzsauler *et al.*, 2005).

The objectives of this research were to determine the potential for contamination of Snow Lake which provides drinking water for the town of Snow Lake, and the local environment by identifying the source of arsenic in the ground water at MW17 and the mechanisms by which arsenic is being transported and attenuated.

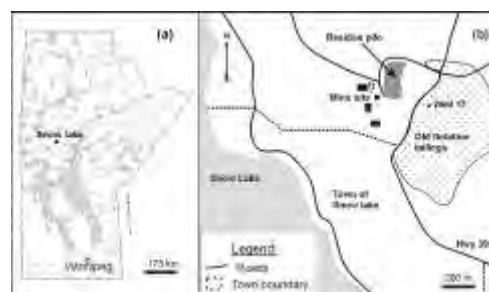


Fig.1. (a) map of Manitoba showing the location of Snow Lake (b) diagram of the mine site showing the ARS, MW17 and the emergency tailings.

SITE DESCRIPTION

From 1949 to 1958, Nor-Acme Gold Mine piped 227,000 tonnes of refractory gold-bearing sulfide concentrate into a rock-walled impoundment (Richardson & Ostry 1996, Salzsauler *et al.* 2005) in hope of finding a means to extract the gold. The ARS remained uncovered until 2000 when a cover was placed to inhibit sulfide oxidation and prevent further contaminated surface runoff. Arsenic is

now suspected to be leaching through the base of the ARS into the local underlying aquifer, which is monitored at MW17. Prior to capping, drainage water from the ARS flowed north into a marshy runoff area (RA) that empties via Canada Creek into Snow Lake. Surface water in the RA has <13 ppm arsenic (Salzsauler 2004). This contamination is suspected to be the result of 50 years of drainage emanating from the ARS and the mine site.

METHODOLOGY

Cores were collected from the NATA and adjacent wetland. Solid material was obtained from the aquifer beneath the NATA by filtering water samples from MW17. Pore water was squeezed from cores in a hydraulic press. Groundwater, surface and lake water samples were filtered (0.2 µm) in the field. Sub-samples were acidified to preserve cations. Arsenic species were separated on site by passing filtrate through SAX cartridges (Le *et al.* 2000).

Solid and solution samples were analyzed using a combination of induced neutron activation analysis, infrared spectroscopy and inductively coupled plasma, optical emission and mass spectroscopy. Phases controlling water composition were assessed with the geochemical program WATEQ4F (Ball & Nordstrom 1991). Piezometers were installed into the NATA to determine static water table elevations and hydraulic conductivity of the tailings. The hydrology of the site was modelled using the Ogata-Banks analytical solution to assess transport of As. Local water flow directions were approximated using water table data from piezometers in the watershed.

Shoots and roots of the common cattail (*Typha latifolia*) and water sedge (*Carex aquatilis*) were collected and analyzed to examine the passage of arsenic into the plants.

Polished thin sections were made in the absence of water to prevent dissolution of soluble phases. Mineral composition was determined using a combination of X-ray diffraction, electron microprobe analysis, and scanning electron microscopy with

energy dispersive X-ray spectrometry.

RESULTS

Hydrology

The NATA site consists of tailings overlying relatively low permeability clay soil, gravel-sand, and bedrock units. There are two aquifers: one is confined between the bedrock and clay, and another unconfined aquifer which developed within the NATA tailings. Vertical exchange between aquifers is limited due to the clay separation. This is demonstrated by the higher piezometric levels of the unconfined aquifer compared to the confined one.

The surface of the ARS drains NW, however, the base of the ARS dips south (Fig. 2). The ARS is underlain by red-brown clayey soil, which overlies a sand-gravel aquifer.

The water table in the ARS is elevated compared with the aquifer hydraulic heads. This would promote the transport of As from the ARS into the aquifer by advection. Given the higher concentration of As in the ARS compared to the aquifer, As transport could also occur by diffusion through the clayey soil.

Surface and groundwater flow within the Canada Creek watershed is SE from the high level of the mill and ARS to the low lying NATA then north through the wetlands (Fig 3). This path is based on local topography, core log data, and hydraulic head values for the confined aquifer. Hydraulic heads show groundwater in the Canada Creek watershed flowing in the general direction as surface water.

Solid phase Geochemistry

The Nor Acme tailings are composed of 97% quartz and 3% sulfides, which contain <1.5 wt. % As. The clay horizon, 3m below the NATA contains <0.005 ppm As, while the sediments isolated from the aquifer at MW17 have 0.2 ppm As.

Aqueous Geochemistry

The NATA groundwater has a neutral pH, but the surface water varies from 3 to 8. Arsenic concentration at MW17 appears

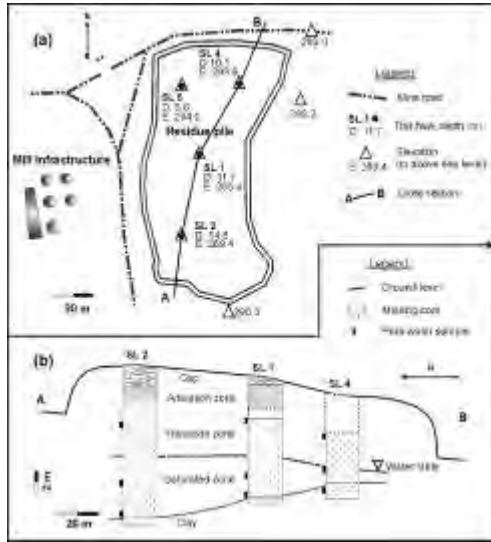


Fig. 2. (a) Elevation and location of drill holes in the ARS (b) Cross section of the ARS from S (drill hole SL2) to N (SL4)

to have decreased from 2004 to 2006 (Fig. 4). New Britannia Mines' (NBM) values are consistently <10 mg/L lower than those reported by Salzsauler *et al.* (2005) and Simpson (2007). This may be related to different sampling methods or variation in data incorporated in averages presented per year. Arsenite (As(III)) is the predominant species in groundwater at MW17.

Concentrations of As in surface water range from 1mg/L at the NATA to 11 mg/L in the ARS surface runoff area (RA). Overall, As concentration in the wetlands decreases from the NATA towards Snow Lake (Fig. 3). The lake water contains <0.005 mg/L As, which is well below the Canadian Drinking Water Standards of 0.010 mg/L, however up to 0.016 mg/L was measured at the water-sediment interface.

Wetland Accumulators

Concentrations of As are significantly greater in roots of cattails (<1200 mg/L dry weight (dw)) and sedges (<3000 mg/L dw) than in shoots, probably due to adhering soils and sediments, which contain <6800 mg/L As. Both cattails and sedge plants contain significant As in live (<138 mg/L) and dead (<235 mg/L) shoots.

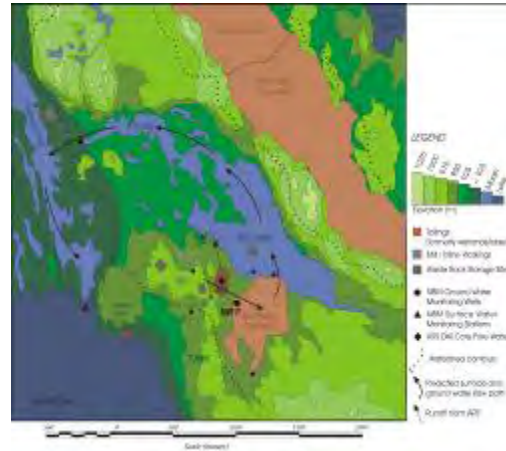


Fig. 3. Topographic map of mine site showing the drainage path.

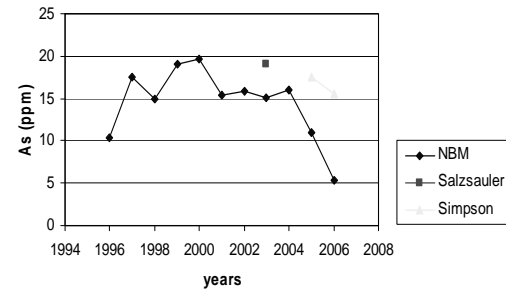


Fig. 4. Graph showing total concentrations of As in the groundwater at MW17. Data points represent annual averages.

DISCUSSION

The source of As in the ARS and NATA is arsenopyrite, a phase that is stable in low Eh, high pH conditions of unoxidized residue. Oxidation would have been initiated during deposition of the residue and would have progressed in the ARS during the 50 years of exposure. During this time, As rich runoff would have flowed into the runoff area (RA) where As was concentrated by plant material.

With the emplacement of the cover, the atmospheric oxygen that fuelled the precipitation of secondary As phases was essentially eliminated. Secondary phases such as jarosite, scorodite and amorphous iron sulfo-arsenates became unstable in the present conditions in the ARS (Salzsauler *et al.* 2005). Reductive dissolution of the secondary phases and residual arsenopyrite gives rise to 100 mg/L As in pore water at the base of the residue pile (Salzsauler *et al.* 2005).

Arsenic leaches from the base of the ARS, transports through the underlying clayey soil, and into the underlying aquifer producing the high concentration in MW17.

From MW17, the ground water flows initially SE beneath the NATA but due to rock outcrops veers N to combine with surface water in the RA. The sediment in this area has been contaminated with As from the surficial runoff from the ARS as well as earlier mining operations. The As in the surface water is then attenuated by ferric (Fe(III)) oxyhydroxides (HFO) so that by the time it reaches Snow Lake level of As are significantly reduced to <0.005 mg/L.

Aquatic plants can sequester As from soils, sediments and directly from water. Temperature, pH, redox potential and nutrient availability affect this sequestration (Robinson *et al.* 2006), but aquatic plants can control the local conditions. Arsenic is adsorbed to the surface of plant roots via physiochemical reactions. A positive correlation between As and Fe concentrations is consistent with As being incorporated into HFO on the surface of plants. Plant roots at NBM generally have >1000 mg/kg dw As. Plant roots contain 4-5 orders of magnitude more As than surface water or sediments at the same location.

Although the sequestration by plants immobilizes As, it may also facilitate its entry into the food chain and provide an exposure pathway to animals.

CONCLUSIONS

Covering the ARS at Snow Lake prevented further oxidation and resulting As-rich surface runoff into the environment. However, secondary As

phases are now soluble in the reduced environment of the ARS, resulting in 100 mg/L As in pore water at its base and subsequent transport of dissolved As species into the ground water at MW17. The Nor Acme tailings do not significantly contribute to this contamination. Arsenic may have been mobilized from an earlier runoff from the ARS. Arsenic is absorbed by HFO in soils and plants prior to discharge to Snow Lake.

ACKNOWLEDGEMENTS

This project was funded by the Manitoba Government through its Sustainable Development Innovation Fund as well as by an NSERC DG to BLS.

REFERENCES

- BALL, J.W. & NORDSTROM, D.K. 1991. User's manual for WATEQ4f, with revised thermodynamic data base and test cases for calculating speciation of major, trace, and redox elements in natural waters. *US Geological Survey Open-File Report 91-183*.
- LE, X.C, YALCIN, S., & MA, M. 2000. Speciation of sub microgram per liter levels of As in water: On-site species separation integrated with sample collection. *Environmental Science and Technology*, **34**, 2342-2347.
- RICHARDSON, D. & OSTRY, G. 1996. Gold deposits of Manitoba. Manitoba Energy and Mines, Geological Services. *Economic Geology Report ER86 – 1* (2nd edition), 114 p.
- SALZSAULER, K. A., SHERRIFF, B.L., & SIDENKO, N.V. 2005. As mobility in alteration products of sulfide-rich, arsenopyrite-bearing mine wastes, Snow Lake, Manitoba, Canada. *Applied Geochemistry*, **20**, 2303-2314.
- SIMPSON, S. 2007 *The Source, Attenuation and Potential Mobility of As at New Britannia Gold Mine, Snow Lake, Manitoba*. M.Sc Thesis, University of Manitoba.

Geochemistry and mineralogy of ochre precipitates formed as waste products of passive mine water treatment

Teresa M. Valente¹, Marcel D. Antunes,
Maria Amália S. Braga, & Jorge M. Pamplona

¹CIG-R - Centro de Investigação Geológica, Ordenamento e Valorização de Recursos, Universidade do Minho, Campus de Gualtar, 4710-057, Braga PORTUGAL (email: teresav@dct.uminho.pt)

ABSTRACT: Passive systems with constructed wetlands are designed to simulate natural attenuation processes in order to treat mine water in a long-term and cost-effective manner. In this way, they are especially appropriate to treat mine water discharging from abandoned mines. This paper presents geochemical and mineralogical data obtained from a recently constructed passive system (from Jales abandoned mine, North Portugal). It shows the role of fresh ochre-precipitates, formed as waste products from the neutralization process, in the retention of trace elements. Chemical analysis revealed strong enrichment factors for metals and arsenic, relative to the water from which they precipitate. The mineralogical study shows that ochre-precipitates are poorly ordered iron-rich material, such as ferrihydrites, that occur as small spherical aggregates that are less than 0,1 µm in diameter. Firing experiments on these precipitates gave rise to hematite and to a crystalline arsenate. This provides evidence for the scavenging of arsenic by means of a precursor arsenic-rich amorphous compound. The results revealed that ochre-precipitates are wastes of environmental concern, which should be taken into account when considering the possibilities for reuse or disposal.

KEYWORDS: ochre-precipitates, mine water, metals, arsenic, concentration factors.

INTRODUCTION

The best compromise between regulatory compliance and costs of mine water treatment has being, world-wide, the use of passive systems such as limestone channels and wetlands. There are numerous bibliographic references highlighting the advantages of these approaches (e.g., Skousen *et al.* 1998; Younger *et al.* 2002). Among the advantages, low cost and infrequent maintenance are crucial issues in the cases of abandoned mines. In these passive systems, the production of sludge, although in lesser amounts than in active systems, where chemicals are constantly added, is a major problem.

Sludge formed during initial steps of the treatment process (passive oxidation and neutralization) may affect the overall performance of the plant, especially when they are leached through the biological cells. Therefore, their disposal, or their recovery, as they may have economic value (Hedin 2003), is an issue of concern in the management of the treatment plant.

This paper presents data from a passive system implemented to treat the mine water from the abandoned mining site of Jales, in North Portugal. The layout of the plant comprises initial oxidation and neutralization in a limestone channel. The present work is focused on the resulting products that are generically named ochre-precipitates.

The geochemical and mineralogical properties of the ochre-precipitates are provided in order to demonstrate their ability to concentrate arsenic and metals from the mine water. Additionally, data may support management decisions, regarding disposal or recovery of the wastes, taking into account of their environmental behaviour.

SITE DESCRIPTION

Jales mine is located near Vila Pouca de Aguiar, North Portugal (Fig.1). It has been exploited since Roman times, in a relatively sulfide-rich deposit. In modern times it was mined for gold and silver between 1933 and 1992.

The mine water to be treated flows from an old adit into the nearby watercourse (Peliteira Creek). Water properties are rather variable, dependent on seasonal variations (Loureiro 2007). Nevertheless, it can be generically described as an acid (pH<4), sulfate and metal-rich solution, especially in iron, arsenic, zinc and manganese.

Figure 1 represents the layout of the treatment plant, which had a start up in 2006. It includes two wetlands, planted with *typha*, and an initial inorganic stage with a reception basin (of which the bottom is filled with limestone), a cascade aeration facility and a limestone channel.

SAMPLING AND ANALYTICAL METHODS

The ochre precipitates were taken at the end of the limestone channel (Fig. 1). In order to represent diverse seasonal conditions, samples were collected in three sampling campaigns, between 2007 and 2008. At each time, a water sample was collected at the same site.

The samples were air-dried at room temperature, sieved to < 63 µm and analysed by x-ray diffraction (XRD) and scanning electron microscopy combined with an energy dispersive system (SEM-EDS). For chemical analysis, samples were submitted to an extraction with Aqua Regia and analysed by inductively coupled plasma-optical emission spectrometry (ICP/OES). Firing experiments were performed following the procedure described by Brindley & Brown (1980).

Water analysis parameters such as pH, electric conductivity, oxidation-reduction potential and temperature were measured in the field. Ionic chromatography, turbidimetry and ICP-OES were used for anions and metals.

RESULTS AND DISCUSSION

XRD Pattern and Morphology

Figure 2 presents the properties of the ochre-precipitates and the respective firing products, concerning crystallinity pattern, morphology and chemical composition by

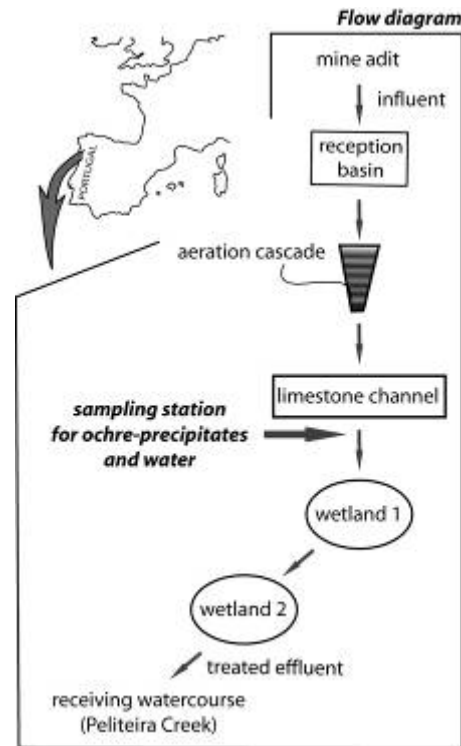


Fig. 1. Location and layout of the mine water treatment plant.

SEM-EDS. All the samples of fresh ochre-precipitates exhibit XRD patterns typical of poorly crystalline material, such as ferrihydrite (Schwertmann & Cornell 2000). They present the strongest band centred at 2.56Å, corresponding to the (110) reflection of 6-line ferrihydrite, as well as the characteristic poorly resolved reflections at *d* spacings 1.47 - 1.73 - 1.98 and 2.24Å.

Firing experiments induced thermal transformations on the ochre-precipitates. From these experiments, hematite and a well crystalline arsenate resulted. This indicates that arsenic may be scavenged by an arsenic-rich compound, freshly formed during the initial stages of the water treatment. This is in agreement with the results obtained by Jia & Demopoulos (2008), when performing aging tests on solids precipitated from As(V)-Fe(III) solutions.

SEM-EDS shows that ochre-precipitates are iron-rich particles, with other elements, such as As, Ca, Si and Cu (Fig. 2b). They

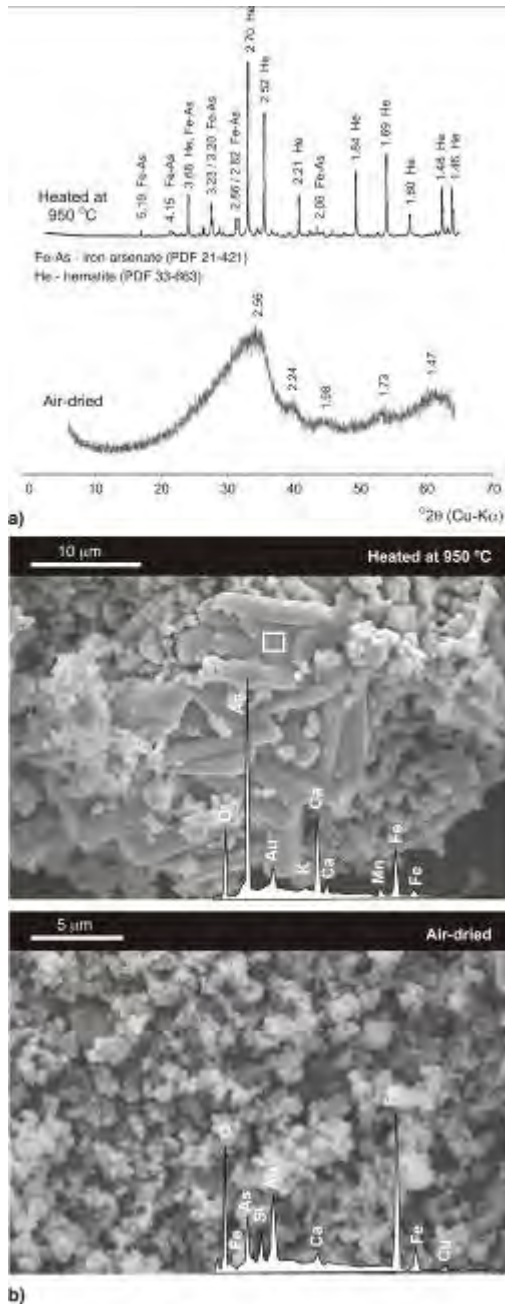


Fig. 2. Characteristics of the ochre-precipitates and thermal evolution. a) XRD patterns; b) SEM – SE images, showing the morphology of the aggregates and respective EDS spectra.

occur as aggregates of poorly developed spheres of less than 0.1 µm in diameter. After heating at 950°C, the material transforms to hematite (tabular and

prismatic crystals, often hexagonal dipramids) and an As-rich phase (elongated prismatic grains), that may be corresponding to the arsenic compound detected by XRD (Fig. 2a).

Chemical Composition and Partitioning

Chemical analysis shows that iron and arsenic are the major elements, with concentrations around 30% and 5% (average values), respectively.

Combined results on ochre-precipitates and water from which they precipitate indicate strong enrichment regarding several relevant metals (Fig. 3). The concentration factor was estimated using the formulation by Munk *et al.* (2002), which calculates the ratio between the concentration of the elements in the solid and the concentration in the water.

The partitioning of trace elements between the precipitates and the associated water suggests the following trend of affinities for some significant toxic elements: Pb>Cu>As>Cd>Zn>Ni>Mn.

Although there are no universal rules for metal selectivity as it depends on numerous factors, the obtained sequence is in agreement with the results reported in literature for the *Kd* sorption values on fresh precipitates of hydrous ferric oxide (Dzombak & Morel 1990; Munk *et al.* 2002). The lowest factor observed for Mn comes in agreement with the well-known difficulty to remove this metal from mine waters due to its high solubility over a wide pH range (*e.g.*, Hedin *et al.* 1994).

CONCLUSIONS

This study, focused on ochre-precipitates from a passive system, can be summarized in the following items:

- (1) the waste-products are iron-rich aggregates that denominated ochre-precipitates;
- (2) the ochre-precipitates are poorly crystalline materials, with XRD patterns typical of ferrihydrite;
- (3) firing experiments confirm this mineralogical precursor, promoting its evolution to hematite;
- (4) Upon heating initial phases transform to hematite and to a well-crystalline

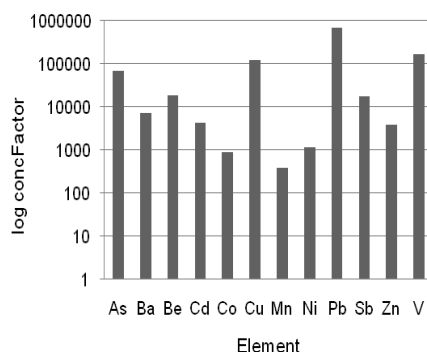


Fig. 3. Affinities of metals for ochre-precipitates, estimated by the relation between concentration in the solid and in the water.

arsenate, suggesting that arsenic is retained in the water treatment plant as an amorphous ancestor, co-precipitated with the iron oxy-hydroxide;

(5) the hazardous potential of ochre-precipitates is highlighted by the high enrichment in metals, and especially in arsenic (5%);

(6) Metal contents, as well as the influence of the firing products (thermal behaviour) on the industrial re-use are worthy of further research, as these are environmentally and economically relevant issues.

ACKNOWLEDGEMENTS

We thank to EDM (Empresa de Desenvolvimento Mineiro, S.A) for providing access to the water treatment plant. We are also grateful to Lucia Guise and A. Azevedo for assistance with chemical analysis and XRD analysis.

Authors would like to thank Dr Dogan Paktunc for the valuable comments and suggestions.

References

- BRINDLEY, G. & BROWN, G. 1980. Crystal structures of clay minerals and their X - ray identification. *London: Mineralogical Society.*
- DZOMBAK, A. & MOREL, M. 1990. *Surface complexation modeling: hydrous ferric oxide.* Wiley-Interscience, New York.
- HEDIN, R. 2003. Recovery of marketable iron oxide from mine drainage in the USA. *Land Contamination & Reclamation*, **11**, 93-97.
- HEDIN, S.; WATZLAF, G., & NARIN, R. 1994. Passive treatment of acid mine drainage with limestone. *Journal of Environmental Quality*, **23**, 1338-1345.
- JIA, Y. & DEMOPOULOS, G. 2008. Coprecipitation of arsenate with iron(III) in aqueous sulfate media: Effect of time, lime as base and co-ions on arsenic retention. *Water Research*, **42**, 661-668.
- LOUREIRO, C. 2007. *Sítios mineiros abandonados – monitorização de efluentes e acompanhamento de uma obra de reabilitação.* BSc Thesis, Universidade do Minho, Braga.
- MUNK, L.; FAURE, G.; PRIDE, D., & BIGHAM, J. 2002. Sorption of trace metals to an aluminum precipitate in a stream receiving acid rock-drainage; Snake River, Summit County, Colorado. *Applied Geochemistry*, **17**, 421-430.
- SCHWERTMANN, U. & CORNELL, R. 2000. *Iron oxides in the laboratory – preparation and characterization.* Wiley-VCH, Weinheim.
- SKOUSEN, J.; ROSE, A.; GEIDEL, G.; FOREMAN, J.; EVANS, R., & HELLER, W. 1998. A handbook of technologies for avoidance and remediation of acid mine drainage. *Natl. Mine Land Reclamation Center*, Morgantown, WV.
- YOUNGER, P.; BANWART, S., & HEDIN, R. 2002. *Mine Water: Hydrology, Pollution, Remediation.* Springer.

Instability of AMD samples and evolution of ochre-precipitates in laboratory conditions

Teresa M. Valente¹ Lúcia M. Guise, & Carlos A. Leal Gomes

¹CIG-R - Centro de Investigação Geológica, Ordenamento e Valorização de Recursos, Universidade do Minho, Campus de Gualtar, 4710-057, Braga PORTUGAL (email: teresav@dct.uminho.pt)

ABSTRACT: Acid mine drainage is a peculiar focus of environmental impact, due to a combination of the presence of many pollutants and their reactivity. These aspects demand special attention for an accurate characterization of AMD samples in field and in laboratory. The samples are unstable due to the presence of colloidal material such as iron-oxyhydroxides. They induce physical and chemical transformations, even during the transport to the laboratory, which may affect the analytical results. Variations in pH were recorded within the first several hours following their collection as an indicator of the changes in their evolution. The present work presents evidences of the instability of AMD samples, through the results of monitoring experiments performed in different laboratory conditions. Expedient indicators, like pH and electrical conductivity, combined with the analysis of crystallinity, composition and morphology of the resulting precipitates, allow monitoring of the evolution of the samples. The results also provide information about the origin and transformations of the typical ochre-products that precipitate from AMD.

KEYWORDS: Acid mine drainage (AMD), chemical instability, ochre-precipitates, schwertmannite, goethite.

INTRODUCTION

Effluents emerging from sulfide-rich waste-dumps have special characteristics, such as very low pH (< 4), high metal solubility and presence of iron colloids, which provokes water turbidity and precipitation of ochre-products. These effluents are generically named acid mine drainage (AMD), since they result, primarily, from mineral-water interactions involving some sulfide minerals that typically produce acidity upon oxidative dissolution.

AMD are often very heterogeneous and reactive systems. Therefore, to describe their properties is often an issue of analytical concern as it is difficult to obtain representative samples of the affected watercourses. The instability of AMD is related to the formation and transformations of ochre-products, such as jarosite, schwertmannite and goethite (Bigham *et al.* 1996). Mineralogical transformations involving these ochre-precipitates have been the subject of intensive research (Kawano & Tomita 2001; Kim *et al.* 2002; Knorr & Blodau

2006). However, geochemical controls as well as contribution of microorganisms to their evolution still need to be investigated.

This work provides information about the instability of AMD and of AMD-precipitates obtained in a set of experiments carried out with natural and synthetic samples, in different laboratory conditions.

AMD AT VALDARCAS MINING SITE

The samples are from the abandoned mine of Valdarcas, Northern Portugal (Fig. 1). This mine was exploited for tungsten in a skarn ore deposit rich in sulfides, mainly pyrrhotite, pyrite and minor chalcopyrite and sphalerite. AMD emerges at the base of the enriched-sulfide waste-dumps. It is naturally drained into a small permanent stream (Poço Negro Creek), and, then discharged in the Coura River. Table I presents the pH range at different sites along the system, obtained by monthly monitoring over a two-year period. A complete characterization of the samples is provided by Valente & Leal Gomes (2008).

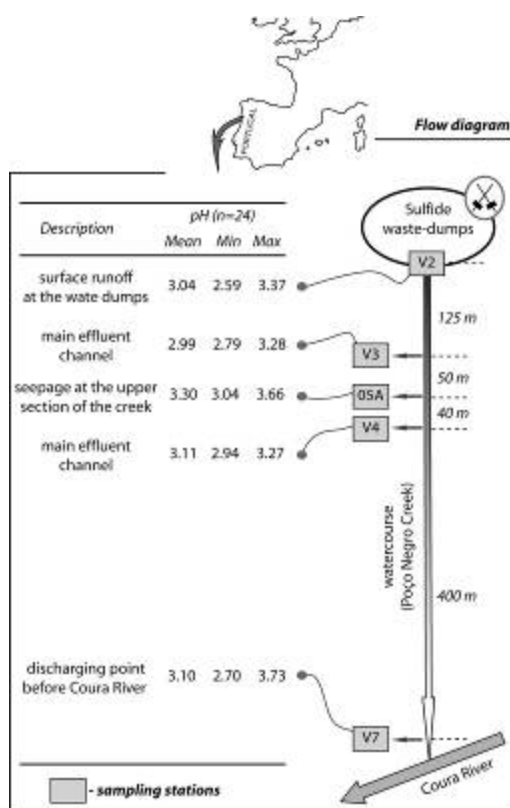


Fig. 1. Location of Valdearcas mine in Northern Portugal and sampling stations for AMD.

METHODS

Water Sampling

In order to represent the heterogeneity of AMD, sampling stations included acidic seepages and surface runoff at the waste-dumps, as well as points along the main effluent channel (Poço Negro creek) (Fig. 1).

EXPERIMENTS

The following experiments were performed: (1) – monitoring of pH of natural AMD, with and without refrigeration, during the first week after collection; (2) – monitoring of water parameters and of the resulted precipitate, for the most instable samples (pH 3.1), over a period of 8 months, with refrigeration (T = 4 °C); (3) - monitoring of water parameters and of the resulted precipitate, at 30°C, in three distinctive reactors: Reactor A – using the same AMD sample as in the experiment (2); Reactor B – using a synthetic AMD solution (prepared accordingly with

Kawano & Tomita 2001); Reactor C – using the synthetic solution, but inoculated with two small fragments of natural schwertmannite (0.05 g).

The pH, EC and Fe³⁺ were used as control parameters. The first two were measured with an Orion probe combined pH/ATC electrode Triode and a conductivity cell DuraProbe ref. 0133030. Fe³⁺ was determined by molecular absorption (thiocyanate method). Mineralogical composition of the precipitates was determined by X-ray powder diffraction (XRD). Scanning electron microscopy, combined with an energy dispersive system (SEM-EDS), allowed the observation of morphological and compositional aspects of the precipitates.

RESULTS AND DISCUSSION

Fig. 2 represents the variation of pH in refrigeration conditions (4°C) and at 20°C (average regional temperature). The samples had initial pH in the range 2.7-3.2. For both situations, the samples reported a decrease in pH. Nevertheless, pH was more stable with refrigeration, except for samples with initial pH between 3.0 and 3.1. In fact these were the more unstable samples in both conditions.

This is in agreement with the observations of Valente & Leal Gomes (2008), regarding the precipitation of AMD-precipitates in the Poço Negro creek. They verified that neutralization around pH 3.1 favours the precipitation of schwertmannite, which is also in accordance with the paragenetic relations proposed by Bigham *et al.* (1996) for jarosite, schwertmannite and goethite in AMD systems. For these reasons, samples with pH 3.1 were selected to evaluate their behaviour in a long term base, and especially to monitoring the precipitation of ochre-products. In that context, Fig. 3 shows the pH variations in the experiment performed with refrigeration along 8 months.

This temperature (4 °C) was intended to analyse the transformations in unfavourable kinetic conditions. It is also an adverse temperature to biologic

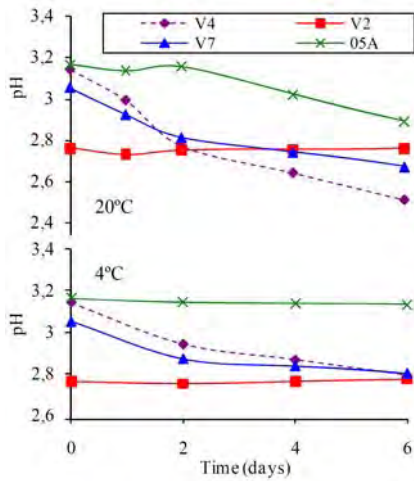


Fig. 2. Variation of pH in natural AMD samples.

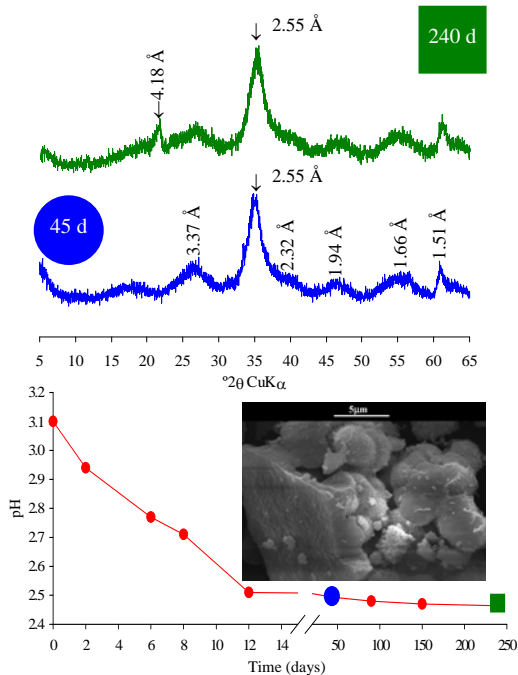
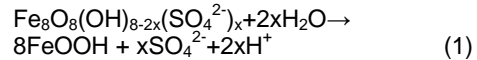


Fig. 3. Evolution of AMD at 4°C (sample collected at V4). The moments of withdrawal of precipitate are marked and the respective XRD patterns are presented. SEM-ES image corresponds to the precipitate at 45 days.

reactions that could be inducing precipitation of ochre-precipitates. However, even in these circumstances, pH decreased continuously until the end of the experiment. Such decline was especially sudden during the first 12 days, and can be related to the oxidation of

ferrous iron and subsequent hydrolysis and precipitation of ferric iron. The formation of an ochre deposit on the walls of the reactor was visible during the first week.

After 45 days of experiment, the precipitate showed an XRD pattern typical of a poorly ordered mineral, such as schwertmannite. Identification of this AMD mineral was confirmed by its distinctive spike morphology, observed by SEM-SE (Fig. 3). After 240 days, XRD detected the resolved reflection at d spacing of 4.18 Å, which is characteristic of goethite. Therefore, the maintenance of the precipitate in contact with the solution enabled its evolution to a more crystalline state. The trend of decrease in pH that is observed by the end of the experiment reflects the production of acidity, associated with the transformation of schwertmannite into goethite as it was observed by Bigham *et al.* (1996) (eq. 1).



It is expected that schwertmannite would be stable at this low temperature (Kumpulainen *et al.* 2008). Furthermore, Jonsson *et al.* (2005) referred to periods of time of > 514 or even several years to promote transformation at pH 3.0. This experiment confirms that mineralogical evolution may be highly variable in AMD systems and still requires further research.

The effect of temperature and of eventual biological contributions was investigated in the experiment. Observations during the experiment as well as the analysis of the Fig. 4 can be summarized as follows:

- the reactors A and C display similar behavior for pH, EC and Fe^{3+} , although initially lagged in time;
- Fe^{3+} increases initially rapidly, followed by pH decrease, indicating oxidation and hydrolysis of iron;
- After 45 days, XRD indicated the formation of schwertmannite in reactors A and C. There were no significant chemical changes in the reactor B.

These experiments suggest that the addition of schwertmannite to the

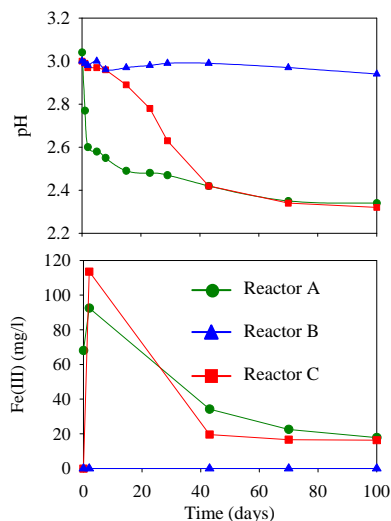


Fig. 4. Variation of pH and ferric iron for the experiment at 30°C.

synthetic system promotes oxidation and hydrolysis of iron, which were not detected in the non-inoculated system (reactor B). This can be a strictly inorganic effect, providing nuclei for precipitation, or may be representing an inoculum of acidophilic microorganisms that contribute to the observed changes.

CONCLUSIONS

The work can be summarized as follows:

- (1) Monitoring of the solution as well as of the ochre-precipitates confirm the instability of AMD from Valdarca;
- (2) Higher instability was detected for samples with pH around 3.0-3.1;
- (3) Ochre-products precipitate from the solution even when samples are preserved at $T < 4^{\circ}\text{C}$;
- (4) Ochre-precipitates displayed the typical XRD patterns of schwertmannite 45 days after collection;
- (5) With time, schwertmannite progressed to a more crystalline mineral (low crystalline goethite), even under unfavourable kinetic conditions ($T < 4^{\circ}\text{C}$);
- (6) Addition of natural schwertmannite to a synthetic AMD solution induced similar changes to that observed in the natural

AMD;

(7) These results should be taken into account in the laboratory and field routines for characterizing AMD samples; for instance they demonstrate the need to filtrate samples in the field, since refrigeration does not necessarily preserve this kind of water samples during transport to the lab.

ACKNOWLEDGEMENT

Authors would like to thank Dr Dogan Paktunc for the valuable comments and suggestions.

REFERENCES

- BIGHAM, J.; SCHWERTMANN, U.; TRAINA, S.; WINLAND, R., & WOLF, M. 1996. Schwertmannite and the chemical modeling of iron in acid sulfate waters. *Geochimica et Cosmochimica Acta*, **60**, 2111-2121.
- JONSSON, J.; PERSSON, P., SJOBERG, S., & LOVGREN, L. 2005. Schwertmannite precipitated from acid mine drainage: phase transformation, sulphate release and surface properties. *Applied Geochemistry*, **20**, 179-191.
- KAWANO, M. & TOMOTA, K. 2001. Geochemical modeling of bacterially induced mineralization of schwertmannite and jarosite in sulfuric acid spring water. *American Mineralogist*, **86**, 1156-1165.
- KIM, J.; KIM, S.; & TAZAKI, K. 2002. Mineralogical characterization of microbial ferrihydrite and schwertmannite and non-biogenic Al-sulfate precipitates from acid mine drainage in the Donghae mine area, Korea. *Environmental Geology*, **42**, 19-31.
- KNORR, K. & BLODAU, C. 2007. Controls on schwertmannite transformation rates and products. *Applied Geochemistry*, **22**, 2006-2015.
- KUMPULAINEN, S.; RAISANEN, M.-L.; VON DER KAMMER, F.; & HOFMANN, T. 2008. Ageing of synthetic and natural schwertmannite at pH 2-8. *Clay Minerals*, **43**, 437-448.
- VALENTE, T. & LEAL GOMES, C. 2009. Occurrence, properties and pollution potential of environmental minerals in acid mine drainage. *Science of the Total Environment*, **407**, 1135-1152.

Arsenic mineralogy and potential for bioaccessibility in weathered gold mine tailings from Nova Scotia

Stephen R. Walker¹, Michael B. Parsons², & Heather E. Jamieson¹

¹Geological Sciences and Geological Engineering, Queen's University, Kingston, ON, K7L 3N6 CANADA
(e-mail: jamieson@geol.queensu.ca)

²Natural Resources Canada, Geological Survey of Canada (Atlantic), Challenger Drive, Dartmouth, NS, B2Y 4A2
CANADA

ABSTRACT: Detailed mineralogical characterization of arsenic (As) in near-surface samples of tailings and soil from four Nova Scotia gold mines has revealed a diversity and complexity in both the mineral species within a given sample, and the mineral form and texture at the grain and sub-grain scale. Samples range from arsenopyrite-rich mill concentrates (one of which has almost completely weathered to very fine grey-green aggregates of scorodite), to As-rich tailings containing from four to nine different amorphous to crystalline As host phases, including, but not limited to hydrous ferric arsenate (HFA), hydrous ferric oxyhydroxide (HFO), Ca-Fe arsenate and yukonite. The long-term stability and solubility of these As-bearing phases is critical for understanding the potential human health risk associated with exposure to As-rich mine waste. The variety of As weathering products can be explained by the processing and disposal history of tailings, and subsequent weathering conditions (i.e., carbonate-buffered pH neutral, post-neutral, and acidic). Secondary As forms are all micro- to nano-particulate or crystalline aggregate grains or grain coatings, suggesting that in addition to mineral solubility and grain-size, the grain texture (massive vs. grain coatings) and sub-grain porosity and permeability may control dissolution processes and rates.

KEYWORDS: arsenic, tailings, weathering, scorodite, yukonite

INTRODUCTION

Mining of arsenopyrite-rich gold ores in Nova Scotia in the late 1800s and early 1900s has left a legacy of weathered, As-rich tailings deposits in more than 60 gold districts across the province. Many of these tailings areas are now located close to residential areas and are publicly accessible. The goal of this research was to examine the As mineralogy in a range of near-surface materials collected from several Nova Scotia gold mine sites frequented by the public, and to use the detailed mineralogical characterization to help explain the geochemical fate, mobility and bioaccessibility of As in weathered mine wastes.

Fourteen near-surface tailings samples and one soil from several former gold mines were sieved to <150 µm and mineralogically characterized using conventional techniques (XRD, microscopy and EPMA) and synchrotron micro-analysis (µ-X-ray diffraction, µ-X-ray

fluorescence and µ-X-ray absorption spectroscopy).

GEOLOGY, PROCESSING, AND SOURCE OF ARSENIC

The Meguma Terrane that covers most of the southern mainland of Nova Scotia (Fig.1) consists of a wedge of folded, greenschist to amphibolite grade, Cambro-Ordovician age, meta-greywacke to slate and meta-siltstone rocks of the Goldenville and Halifax groups (Ryan & Smith 1998). Most of the gold production was from bedding-concordant auriferous quartz veins in the interstratified slate and meta-siltstone sequences.

Tailings were generally deposited close to the mills in low-lying areas and along creeks. Prolonged breaks in production, erosion and reprocessing of tailings have significantly complicated weathering patterns within tailings areas. Changes in ore character and milling processes (especially concentration) over time led to

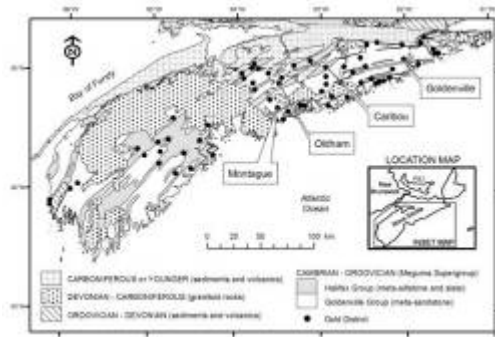


Fig. 1. Generalized geological map of southern Nova Scotia showing the location of historical gold districts within rocks of the Meguma Supergroup (after Ryan & Smith 1998; bedrock geology simplified from Keppie (2000)).

heterogeneity in the distribution of arsenopyrite and other sulfides in the tailings. Tailings for the present study were collected from the Goldenville (GD), Caribou (CAR), Montague (MG) and Oldham (OLD) gold districts (Fig. 1).

SAMPLING AND ANALYTICAL METHODS

All tailings samples except two were visibly oxidized and were selected based on distinct visual characteristics thought to be indicative of different mineralogy. Of the two unoxidized samples, one was distinctly arsenopyrite rich (CAR02) and another was from saturated tailings beneath a thin organic layer (MG04).

Analyses of major and trace elements were accomplished by digesting the samples using modified *aqua regia* and ICP-MS. Total C and organic C were measured using combustion analysis. Petrographic examination indicated that distinct Fe-As phases could be identified using colour (transmitted and reflected light), transparency, reflectivity, optical relief and texture but in most cases (due to fine-grain size, poor crystallinity or amorphous nature), they could not be uniquely identified by petrography alone. Synchrotron micro-probe and EPMA data when combined with the petrographic observations were able to unambiguously identify a range of As mineralogy in each section. Conventional X-ray powder diffraction analyses were carried out using

a Siemens D-500 X-ray diffractometer with a Co lamp (18 mA, 20 keV). Polished thin-section samples were characterized at Beamline X26A, National Synchrotron Light Source using methods similar to those described by Walker *et al.* (2005). Techniques included micro X-ray Fluorescence (μ -XRF), transmission mode micro-X-ray Diffraction (μ -XRD) and fluorescence mode micro-X-ray Absorption Near Edge Structure (μ -XANES) at a beam spot size of < 10 μ m.

RESULTS AND DISCUSSION

The As content of the sieved (<150 μ m) tailings ranges from 0.07 wt. % As to over 30 wt. %. The Fe/As ratios of all tailings samples are low on a molar basis (range 1.3 to 5.3) and lower As content samples generally have higher Fe/As ratios (Table 1). These data are consistent with the arsenopyrite-rich source material in relatively Fe-poor gangue. The S/As ratio is usually significantly less than 1 (Table 1), which suggests the preferential leaching of S over As during oxidative weathering of these tailings samples.

Arsenic, Fe, S and Ca are indicative of the underlying geochemical conditions in the Nova Scotia tailings, because of the strong As source influence of arsenopyrite (with near stoichiometric equivalents of Fe, As and S) and the importance of carbonates as the main source of Ca in the tailings (Kontak & Smith 1988). The presence of excess carbonate leads to neutral drainage conditions, while its absence may lead to acid rock drainage in the tailings.

Micro-scale characterization (μ -XRF, μ -XANES, μ -XRD, petrography, and EPMA) was able to confirm As forms identified by bulk XRD and in all cases identify additional As forms. Grain-scale mineralogical analysis unambiguously identified a minimum of two and typically four or more As-bearing phases in each tailings sample (Fig. 2, Table 2).

Micro-XRD confirms that secondary phases are generally aggregates of micro- or nano-scale crystallites, or in some cases amorphous or short-range ordered. Arsenic-mineral associations within

Table 1. Grain Size and Element Concentrations in Tailings and Soil Samples

Sample		% <150 µm	Element Concentrations (mg/kg)				Ratios (mol/mol)				Carbon (% dry wt.)		
ID	Type		As	Fe	S	Ca	Fe/As	S/As	Ca/As	Ca/S	Total	Organic	Inorganic
CAR01	tailings	18.3	76,500	75,200	1,900	<100	1.3	0.06	0.00	0.00	0.12	0.11	0.01
CAR02	mill concentrate	13.7	313,400	364,300	168,200	200	1.6	1.3	0.00	0.00	6.47 ^a	6.47 ^a	0
CAR03	tailings	12.1	21,300	31,900	1,100	700	2.0	0.12	0.06	0.51	0.19	0.13	0.06
CAR04	tailings	12.5	15,200	40,800	10,700	11,300	3.6	1.6	1.4	0.84	0.64	0.09	0.55
GD01	mill concentrate	30.4	210,300	200,400	34,200	<100	1.3	0.38	0.00	0.00	0.17	0.17	0
GD02	tailings	28.6	19,200	36,000	700	1,200	2.5	0.09	0.12	1.4	0.23	0.22	0.01
GD03	tailings	17.7	38,900	48,800	900	900	1.7	0.05	0.04	0.80	0.23	0.23	0
GD04	tailings	7.4	48,700	77,600	2,900	900	2.1	0.14	0.03	0.25	0.25	0.17	0.08
GD05	tailings	61.4	7,209	28,500	1,400	8,400	5.3	0.45	2.18	4.8	0.30	0.09	0.21
MG01	tailings	11.0	62,100	81,800	2,900	600	1.8	0.11	0.02	0.17	0.13	0.11	0.02
MG02	tailings	9.4	24,000	54,800	1,100	1,200	3.1	0.11	0.09	0.87	0.13	0.12	0.01
MG03	tailings	21.4	23,700	58,800	2,100	4,500	3.3	0.21	0.35	1.7	0.55	0.49	0.06
MG04	tailings	18.4	21,400	52,500	16,800	1,400	3.3	1.8	0.12	0.07	0.83	0.81	0.02
MG06 ^b	soil	16.0	318	59,200	1,100	200	250	8.1	1.18	0.15	4.93	3.11	1.82
OLD04	tailings	18.5	33,900	80,100	5,200	600	3.2	0.4	0.03	0.09	2.23	1.89	0.34

^a Carbon analyses for CAR05-T02 may contain interference from high sulfide content of sample.

^b B-horizon soil sample collected beneath an up-rooted tree over mineralized bedrock.

individual grains are often complex with up to three As forms associated within an individual grain (10 to 100 µm). The only macro-crystalline (e.g. > 2µm) As-bearing phases identified are the primary arsenopyrite and pyrite, although the spotty nature of diffraction from pharmacosiderite and jarosite suggests the presence of discrete crystallites (> 0.1 µm) for these phases.

CONCLUSIONS

Detailed mineralogical characterization of near-surface tailings and soil samples from As-rich Nova Scotia Au mine sites has revealed a diversity and complexity in both the mineral species within a given sample and the mineral form and texture at the grain scale. Gravity concentration of during milling seems to have been a major factor in determining the geochemical fate of As in the Nova Scotia tailings, by altering the ratio of carbonate to arsenopyrite in the tailings.

Secondary As forms are all micro- to nano-particulate aggregate grains or grain coatings. This suggests that in addition to mineral solubility and grain-size, the grain texture (massive or coatings) and sub-grain porosity and permeability may be important in controlling dissolution rates, especially for short reaction times (e.g. dissolution in gastro intestinal fluids by accidental ingestion of tailings). Results from this study are being used by the Province of Nova Scotia to help assess the potential health

risks associated with these high-As mine wastes.

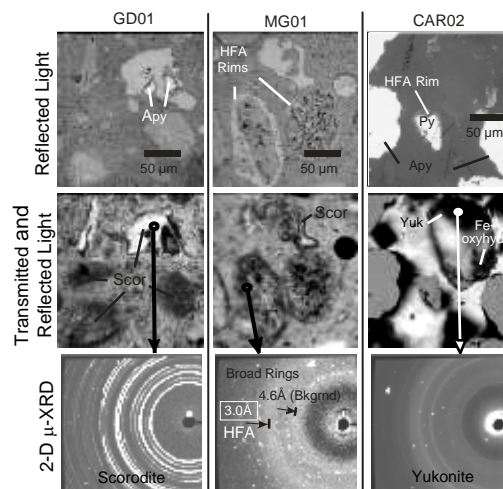


Fig. 2. A variety of As phases occur in weathered Nova Scotia gold mine tailings with mixtures of different forms varying from sample to sample. A combination of optical microscopy and µ-XRD allows definitive identification of a range of mineral forms and textures at the micron scale. These As-bearing mineral forms range from finely crystalline transparent to translucent aggregates of scorodite (Scor) (e.g., GD01 and MG01), to amorphous forms that sometimes coat or cement other grains (e.g. MG01 and CAR02). Note the broad diffraction ring at ca. 3 Å (MG01) indicative of amorphous hydrous ferric arsenate (HFA). Yukonite, a Ca-Fe arsenate, occurs most commonly in carbonate-rich samples. In CAR02, it is present in an arsenopyrite(Apy) rich mill concentrate along with other trace oxidized As forms.

Table 2. Mineralogy in Tailings and Soil Samples

Sample	Depth interval (cm)	Minerals		
		Major Gangue ¹	As-bearing Major ²	As-bearing Minor to Trace ²
CAR01	0 to 5	Qtz, Ms, Pl, Chl	Scor, Kank	HFA, HFO
CAR02	0 to 4	Qtz, Pl, Ms, Chl	Apy, Py	HFO, Yuk, HFO
CAR03	0 to 8	Qtz, Ms, Pl, Chl	HFA, HFO	Yuk, Gt, Lpc, Akg, Apy, Py
CAR04	0 to 4	Qtz, Ms, Pl, Chl, Ank	Apy, Py	Yuk, HFO
GD01	0 to 5	Ms, Qtz	Scor	Apy, Py
GD02	0 to 5	Qtz, Pl, Ms, Chl	Scor, HFA	HFO, Yk, Apy, Py, Jrs
GD03	0 to 5	Qtz, Ms, Pl, Chl	Scor, HFA	Kank, HFO, Apy, Py
GD04	0 to 5	Qtz, Ms, Pl, Chl	HFA	Gt, Lpc, HFO, Apy, Py
GD05	0 to 5	Qtz, Ms, Chl, Pl, Cal	Ca-FA, Yuk, Apy	Py, HFO
MG01	0 to 6	Qtz, Ms, Pl, Chl	Scor, HFA	Gt, Lpc, HFO, Apy, Py, Tooel
MG02	0 to 5	Qtz, Ms, Chl, Vrm, Pl	HFA	HFO, Apy, Scor, Py, Yk, Phar, Akg, Hm*
MG03	0 to 15	Qtz, Vrm, Ms, Chl, Pl	Phar, Yuk	HFA, Ca-FA, Gt, Lpc, HFO, Apy, Py
MG04	15 to 20	Qtz, Vrm, Ms, Chl, Pl	Apy	HFA, HFO, Py, Rgr
MG06	0 to 5	Qtz, Ms, Pl, Chl	HFO	Gt**
OLD04	0 to 5	Qtz, Ms, Pl, Chl	HFA, Jrs	Gt, HFO, Schw, Tooel

Bold and Underlined – indicates As-bearing phase that dominates the sample.

Bold indicates detected in bulk XRD.

Ank=ankerite, Cal=calcite, Chl=chlorite, Ms= muscovite, Pl=plagioclase, Qtz=quartz, Vrm=vermiculite

Akg=akaganeite, Apy=arsenopyrite, Ca-FA=amorphous Ca ferric arsenate, Gt=goethite, HFA=hydrous ferric arsenate, HFO=hydrous ferric oxyhydroxide, Hm=hematite,

Jrs=jarosite, Kank=kankite, Lpc=lepidocrocite, Phar=pharmacosiderite, Rgr=realgar,

Schw=schwertmannite, Tooel=tooeleite, Yuk=yukonite

¹ In decreasing order of abundance based on semi-quantitative fitting of XRD patterns.

² Estimated decreasing order of abundance.

* Single more reflective Fe-oxyhydroxide identified appears to be mixture of nano-crystalline hematite and ferrihydrite with relatively low arsenic content (6.7% As₂O₃).

** EPMA analysis for As in a single grain was just above detection (0.08%). As was

confirmed by synchrotron μ -XRF, but not quantified.

Note: Py was confirmed to contain trace As (<0.1%) in some cases, but was not systematically analysed in each sample where present.

assistance during fieldwork for this project. We also thank Karina Lange and Lori Wrye for their assistance in conducting analysis at the synchrotron, and Tony Lanzirrotti at beamline X26A for his continued support and assistance. The authors gratefully acknowledge the support of the NSERC MITHE Strategic Network. A full list of sponsors is available at: www.mithe-sn.org. This study was also funded in part through the Environment and Health Program, Earth Sciences Sector, Natural Resources Canada.

REFERENCES

- KEPPIE, J.D. (compiler) 2000. Geological Map of the Province of Nova Scotia. Nova Scotia Department of Natural Resources, *Map ME 2000-1*, Scale: 1:500 000.
- KONTAK, D.J. & SMITH, P.K. 1988. Meguma gold studies IV: Chemistry of vein mineralogy. In Mines and Minerals Branch Report of Activities 1987, Part B, Nova Scotia Department of Mines and Energy, *Report 88-1*, Halifax, Nova Scotia. 85-100.
- RYAN, R.J. & SMITH, P.K. 1998. A review of the mesothermal gold deposits of the Meguma Group, Nova Scotia, Canada. *Ore Geology Reviews*, **13**, 153-183.
- WALKER, S.R., JAMIESON, H.E., LANZIROTTI, A., ANDRADE, C.F., & HALL, G.E.M. 2005. The speciation of arsenic in iron oxides in mine wastes from the Giant gold mine, N.W.T. Application of synchrotron micro-XRD and micro-XANES at the grain scale. *Canadian Mineralogist*, **43**, 1205-1224.

ACKNOWLEDGEMENTS

We are grateful to Paul Smith and Terry Goodwin from the Nova Scotia Dept. of Natural Resources for their capable



Sponsors



Symposium bags sponsor



Platinum sponsors



**ANGLO
AMERICAN**

Gold sponsors



Silver sponsors



Bronze sponsors

